SAPIENZA
UNIVERSITÀ DI ROMA

Dottorato di Ricerca in Scienze Immunologiche - XXII ciclo

PhD Thesis

Function of Ena/VASP proteins in cancer cell migration and epithelial morphology

CANDIDATE: MICHELE BALSAMO

Host Lab: Prof. **Frank B. Gertler**, David H. Koch Institute for Integrative Cancer Research, Massachusetts Institute of Technology, Cambridge, Massachusetts, USA

Advisors: Prof. **Angela Santoni**, "Sapienza" Università di Roma
Dr. **Paola Nisticò**, Istituto Nazionale Tumori Regina Elena, Roma

Anno Accademico 2009 – 2010

Chapter 1 - Introduction

Cell migration in physiology and disease

Cell migration during embryogenesis

Cell migration plays a central and pivotal role in a wide variety of biological phenomena. During embryogenesis, cellular migrations are a recurring theme in important morphogenic events, ranging from gastrulation to tissues formation. During gastrulation, for example, large groups of cells migrate collectively as sheets to form the resulting three-layers embryo. Subsequently, cells migrate from various epithelial layers to target locations, where they then differentiate to form the specialized cells that make up different tissues and organs. Among several, a well-studied example comes from the neuronal development. The correct positioning of neurons during development, achieved through directed migration, is the basis for proper brain function. After closure of the neural tube at an early embryonic stage, the most anterior part of the tube becomes an enlarged vesicle called the prosencephalon. The wall of this structure is composed of one continuous sheet of neuroepithelial cells that will give rise to all of the structures in the forebrain including the cerebrum, hippocampus, and thalamus. Cortical neurons arise from the proliferative pseudostratified epithelium at the margin of the embryonic cerebral ventricles. During each cell cycle, the progenitor cells undergo a distinctive pattern of oscillation in the ventricular zone, termed interkinetic nuclear migration. Cells undergo S phase at the basal surface of the ventricular zone and mitosis at the apical surface. Concurrently, cells begin to undergo asymmetric cell division, and the fraction of cells that begin to differentiate into neurons increases, whereas the proportion of cells remaining as progenitors decreases. Toward the end of cortical development, the majority of

neural progenitors give rise to two daughter cells that differentiate into neurons, leading to the eventual depletion of neural precursors. Once a cell has exited the cell cycle, it must migrate out of the ventricular zone toward its final resting place in the developing neocortex (Ayala et al., 2007). Other examples of migration during embryonic development are the movements and fusions of epithelial cells, essential morphogenetic events in both vertebrate and invertebrate systems. Many of these processes, such as ventral enclosure in *Caenorhabditis elegans* (Williams-Masson et al., 1997), embryonic dorsal closure (Jacinto et al., 2000) and imaginal disc fusion in *Drosophila melanogaster* (Martín-Blanco et al., 2000), neural tube (Jean-FranÁois and Gary, 2001) and palate closure in vertebrates, involve extensive and directed movements of two epithelial faces. During the later stages of mouse embryonic and post-natal development, the eyelid closure is another important model of epithelial migration. The development of mouse eyelid starts at E13.5 (embryonic, days post coitum) with eyelid folds that extend over the cornea and move towards the center of the eye; eyelid closure is accomplished at E15.5-E16.5. This process is followed by the fusion of the eyelid epidermis to form a closed eyelid that covers the ocular surface and serves as a protective barrier crucial for normal eye development (Findlater et al., 1993) (Figure 1). Although the initial eyelid formation and growth requires the proliferation of epithelial cells, its closure depends on the movements of the epithelial sheets rather than on cell proliferation and death. As will be discuss later, the underlying cellular and molecular mechanism involved in the epithelial sheets fusion relies on the dynamics of the actin cytoskeleton.

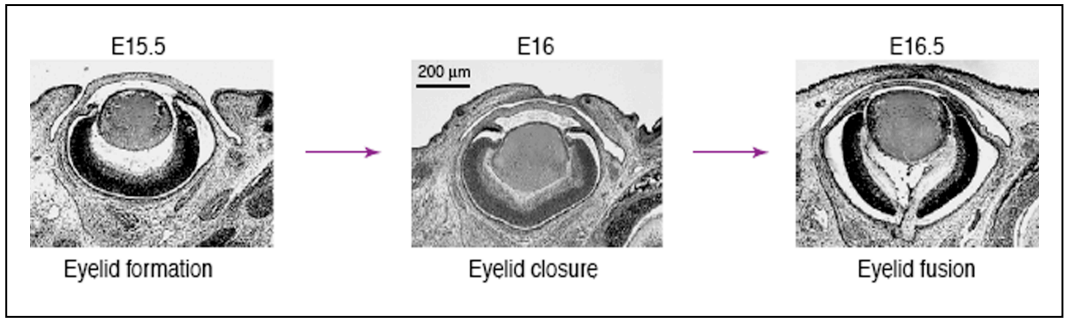

Figure 1. Eyelid formation and fusion during mouse development.

Cell migration in the adult life: the example of cutaneous wound healing

Migration remains prominent in the adult life, in normal physiology as well as during pathological conditions. In the inflammatory response, for example, leukocytes migrate into areas of insult, where they mediate phagocytic and immune functions. Migration of keratinocytes, fibroblasts and vascular endothelial cells is essential for wound healing. Re-epithelialization of wounds begins within hours after injury. Epidermal cells from skin appendages such as hair follicles quickly remove clotted blood and damaged stroma from the wound space. At the same time, the cells undergo marked phenotypic alterations that include retraction of intracellular keratins, dissolution of inter-cellular desmosomes, which provide physical connections between the cells and formation of peripheral cytoplasmic actin filaments, which allow cell movement (Paladini et al., 1996). Furthermore, epidermal and dermal cells no longer adhere to one another, because of the dissolution of hemidesmosomal links between the epidermis and the basement membrane, which allows the lateral movement of epidermal cells (Gabbiani et al., 1978; Goliger and Paul, 1995). The expression of integrin receptors on epidermal cells allows them to interact with a variety of

extracellular-matrix proteins (e.g., fibronectin and vitronectin) that are interspersed with stromal type I collagen at the margin of the wound and interwoven with the fibrin clot in the wound space (Larjava H et al., 1993). The migrating epidermal cells dissect the wound, separating desiccated eschar from viable tissue. The path of dissection appears to be determined by the array of integrins that the migrating epidermal cells express on their cell membranes. The degradation of the extracellular matrix, which is required if the epidermal cells need to migrate between the collagenous dermis and the fibrin eschar, depends on the production of collagenase by epidermal cells, as well as on the activation of plasmin by plasminogen activator produced by the epidermal cells in order to facilitate the degradation of collagen and extracellular-matrix proteins (Pilcher et al., 1997). One to two days after injury, epidermal cells at the wound margin begin to proliferate behind the actively migrating cells. The stimuli for the migration and proliferation of epidermal cells during re-epithelialization are several. The absence of neighbor cells at the margin of the wound (the "free edge" effect) may signal both migration and proliferation of epidermal cells. Local release of growth factors and increase expression of growth-factor receptors may also stimulate these processes. Known growth factors are epidermal growth factor (EGF), transforming growth factor alpha (TGF-α) (Nanney and King, 1996), and keratinocyte growth factor (KGF) (Werner et al., 1994). As re-epithelialization proceeds, basement membrane proteins reappear in a very ordered sequence from the margin of the wound inward, in a zipper-like fashion. Epidermal cells revert to their normal phenotype, once again firmly attaching to the re-established basement membrane and underlying dermis.

Cancer metastasis

In the early phases of multi-step progression of solid tumors, cancer cells multiply around the site where the initial cancer cell originated and first began the uncontrolled proliferation. Such primary tumor eventually increases in size and may locally infiltrate and invade. This uncontrolled proliferation in the primary site is ultimately responsible for only 10% of the deaths from cancers. The remaining approximately 90% of the deaths originate by cancerous growth far away from the primary tumor site, these cancers in secondary sites are called metastases. Metastases are formed by cancer cells that acquire a migratory and invasive phenotype and are capable of leaving the primary tumor mass and disseminate through blood and lymphatic vessels in secondary organs or lymph nodes. The so called "invasion-metastasis cascade" ascribes six different steps to the overall process (Figure 2). It starts with tumor cell proliferation and localized invasion in the surrounding stroma. For breast cancers, this localized invasion enables *in situ* carcinoma cells to breach and disrupt the basement membrane. Thereafter, the invasive cells may intravasate in lymphatic or blood microvessels, allowing the transportation through circulation and the dissemination of cancer cells to distant anatomical sites. The migrated cancer cells may extravasate and form a micrometastasis in the secondary site. Eventually, some of them may acquire the ability to colonize and grow in the secondary site and form a macrometastasis (Fidler, 2003). The metastatic cascade is thought to be a very inefficient process. Tens of thousands of cancer cells can be shed into the circulation every day, yet less than 0.01% of these will survive to produce metastases (Chambers et al., 2002). It is intuitive that cell motility and deregulation of it is the (or one of the) fundamental process that allows the

formation of metastases. The capacity to disseminate could be intrinsic to certain pre-malignant cell lineages. It has long been recognized that many normal cell types are involved in complex migratory and invasive behaviors during development and adulthood. For example, normal epithelial cells are motile. In the mammary gland, the invasive and migratory mechanisms that underlie the branching morphogenesis of normal epithelial cells also regulate the formation of mammary hyperplasia (Ewald et al., 2008). Together with the long standing notion that the phenotype of cancer cells is dictated by their genome and that the tumorigenesis is essentially a cell-autonomous phenomenon, the other component that plays a significant role in the induction of cell growth and metastasis is the tumor microenvironment. As it will be discussed in greater detail later, the tumor microenvironment shapes and is a potent inductor of cancer metastasis (Joyce and Pollard, 2009a).

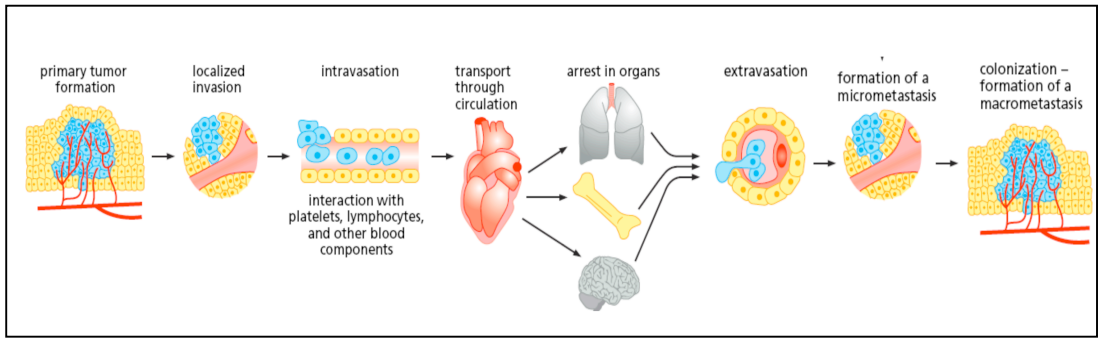

Figure 2. The invasion-metastasis cascade The invasion-metastasis cascade ascribes six distinct steps to the overall process. The initial step of localized invasiveness enables *in situ* carcinom cells to invade the surrounding stroma. Thereafter, they may intravasate into either lymphatic or blood microvessels. The latter may then transport these cancer cells to distant anatomical sites, where they may extravasate and form dormant micrometastases. Eventually some of the micrometastases may acquire the ability to colonize the tissue in which they have landed, enabling them to form a macroscopic metastasis. The last step, colonization, seems to be the most inefficient of all. The small probability of successfully completing all steps of this cascade explains the low likelihood that any single cancer cell leaving a primary tumor will succeed in becoming the founder of a distant, macroscopic metastasis. *Adapted from I.J. Fidler, Nat. Rev. Cancer 3:453–458, 2003*

Mechanisms of cell migration

With a major focus on cell motility in a 2D substrate, the present understanding of cell migration is a composite derived from studies of different cell types and environments. In general, cell migration can be usefully conceptualized as a cyclic process (Lauffenburger and Horwitz, 1996). The initial response of a cells plated on matrix-coated surfaces to a migration-promoting agent is the polarization of the cell body and the extension of protrusions in the direction of migration. These protrusions can be branched filaments leading to sheet-like protrusions (lamellipodia) or long parallel or bundled finger-like protrusions (filopodia), and are usually driven by actin polymerization and are stabilized by adhering to the extracellular matrix (ECM) or adjacent cells via transmembrane receptors linked to the actin cytoskeleton. These adhesions serve as traction sites for migration as the cell moves forward over them, and they are disassembled at the cell rear, allowing it to detach. Carcinoma cells cultured on top of dense ECM form invadopodia, specialized actin-rich structures that protrude into the matrix and secrete proteases focally that degrade the matrix.

Cell polarization

The first step of cell migration is a morphological polarization that the cell must acquire in order to generate intracellular forces that produce a net body translocation. This means that the molecular process that acts at the front of the cell is different compared to the one on the back. A master regulator of cell polarity in eukaryotic organisms, ranging from yeast to humans, is Cdc42 (Heasman and Ridley, 2008). Cdc42 is a member of the Rho GTPases family

proteins, which switch between an active GTP-bound form and an inactive GDP-bound form. The cycle is regulated by guanine nucleotide-exchange factors (GEFs), which activates Rho GTPases by promoting the release of GDP and the binding of GTP and GTPase-activating proteins (GAPs), which inactivate Rho GTPase by increasing the intrinsic GTPase activity of Rho proteins. Cdc42 is activated toward the front of migrating cells and, together with Rac and RhoG, is the main activator of the WASP/WAVE-Arp2/3 complex pathway, leading to the formation of a branched actin network and extension of lamellipodia. Another important role of Cdc42 for cell polarity is the active localization of the microtubule-organizing center (MTOC) and Golgi apparatus in front of the nucleus, toward the leading edge. The MTOC and Golgi polarization may be needed for the microtubule-mediated delivery of vesicles to the leading edge, providing proteins important for cell protrusion (Etienne-Manneville and Hall, 2002).

Membrane protrusion and the protrusive machinery

The extension of both lamellipodia or filopodia in response to migratory stimuli is almost universally found to be associated with local actin polymerization (Condeelis, 1993). Actin filaments are intrinsically polarized with fast-growing "barbed" ends and slow-growing "pointed" ends, and this inherent polarity is used to drive membrane protrusion. The presence of free barbed ends act as template for new polymerization. To initiate actin assembly, free barbed ends can be created by three general mechanisms: uncapping of pre-existing filaments, severing of filaments (Condeelis, 2001) or *de novo* nucleation (Welch and Mullins, 2002a). Studies with permeabilized platelets indicate that uncapping

of barbed ends capped by capping protein (CP) is the primary mechanism for the production of free barbed ends in response to thrombin stimulation (Hartwig et al., 1995). Polyphosphoinositides, including PIP2, can bind to CP and inhibit its capping activity also causing rapid uncapping. One attractive hypothesis is that PIP2 generated in the membrane helps to inhibit capping by CP near the membrane, at the site of protrusion. A second mechanism for the generation of free barbed ends *in vivo* is the severing of pre-existing filaments. The two proteins that have been studied most extensively in this regard are gelsolin and cofilin. Gelsolin severs filaments in a Ca^{++} dependent step and caps the barbed end of the filament fragment at the severed site. To generate free barbed ends, gelsolin must be released from the barbed end in a subsequent uncapping step, which can be accomplished *in vitro* by removal of Ca^{++} from, and the binding of phosphoinositides to, gelsolin (Hartwig et al., 1995). The ADF/Cofilin family of proteins nucleates actin polymerization by severing filaments to generate free barbed ends. As cofilin does not remain bound to the barbed end of the filament at the severed site, severing produces free barbed ends directly. As long as monomeric actin (G-actin) is present and unsequestered at concentrations sufficient to support polymerization (1 μM), severing will result in nucleation. When the concentration of G-actin is limiting, the net result of severing by cofilin is depolymerization, not nucleation. When cofilin and actin are present in near-equimolar concentrations, severing, increased off-rate and sequestering can cause the treadmilling of the actin filaments population (Carlier et al., 1997). Because cofilin is essential for cell viability and can increase the rate of actin polymerization, depolymerization and barbed ends number, it has been proposed as a potential dominant player in generating actin polymerization transients *in vivo* (Bamburg, 1999).

Another general model of generation of free barbed ends is *de novo* nucleation by the Arp2/3 complex as the nucleation template. As discussed before, the organization of filaments depends on the type of protrusion (lamellipodia vs filopodia). Actin polymerization in lamellipodia is mediated by the Arp2/3 complex, which binds to the sides or tip of a preexisting actin filament and induces the formation of a new daughter filament that branches off the mother filament (Welch and Mullins, 2002b). Activation of the Arp2/3 complex is localized by WASP/WAVE family members, which are themselves activated at the cell membrane. Pushing of the membrane, the actual protrusive event is believed to occur not by elongation of the actin filament per se but by an "elastic Brownian ratchet" mechanism, in which thermal energy bends the nascent short filaments, storing elastic energy. Unbending of an elongated filament against the leading edge would then provide the driving force for protrusion (Pollard and Borisy, 2003). As mentioned before, small Rho GTPases are central regulators of protrusions. Cdc42 and Rac can both activate N-WASP/WAVE proteins and in turn regulate Arp2/3 activity. Extracellular chemotactic stimuli can activate through receptors and the ras signaling the phosphoinositide 3-kinase (PI3K) and the phosphatase PTEN (phosphatase and tensin homolog), key signaling proteins supposed to work as gradient amplifiers. PI3K and PTEN catalyze the production and degradation of phosphatidylinositol (3,4,5)-trisphosphate (PtdIns(3,4,5)P3; referred as PIP3) at the plasma membrane, resulting in a net accumulation of PIP3 at the leading edge (Kolsch et al., 2008). The accumulation of PI3K and PIP3 at the leading edge activates several molecules important for cell migration. PI3K products activate Rac GEFs, once Rac is active it activates several feedback loops that are aimed to potentiate the directional protrusion. First, Rac itself stimulate the recruitment of PI3K at the plasma membrane (Srinivasan et al., 2003); second

Rac may stabilize microtubule and in turn be activated by microtubule polymerization (Rodriguez et al., 2003); third Rac is activated and localizes at plasma membrane after integrin engagements, so new adhesions formed at the leading edge will stimulate Rac (Kiosses et al., 2001). Several actin-binding proteins regulate the rate and organization of actin polymerization in protrusions by affecting the pool of available monomers and free ends. For example, profilin prevents self-nucleation by binding to actin monomers and also serves to selectively target monomers to barbed ends. Filament elongation is terminated by capping proteins, thereby restricting polymerization to new filaments close to the plasma membrane. In addition, disassembly of older filaments, which is needed to generate actin monomers for polymerization at the front end, is assisted by proteins of the ADF/cofilin family, which sever filaments and promote actin dissociation from the pointed end. Other proteins play supporting roles in the dendritic network: cortactin stabilizes branches, whereas filamin A and α-actinin stabilize the entire network by cross-linking filaments (Welch and Mullins, 2002a). Filopodial protrusion is thought to occur by a filament treadmilling mechanism, in which actin filaments within a bundle elongate at their barbed ends and release actin monomers from their pointed ends (Welch and Mullins, 2002a). The long and unbranched filament organization is consistent with assembly occurring by elongation rather than by branched nucleation. Many proteins are enriched at filopodial tips, including Ena/VASP proteins, which bind barbed ends of actin filaments and antagonize both capping and branching, thereby allowing continuous elongation of filaments, and fascin, which bundles actin filaments and might thereby generate the stiffness needed to allow efficient pushing of the plasma membrane in filopodia (Welch and Mullins, 2002a). The geometric design of lamellipodia and filopodia endows them with the capacity to perform distinct

functions. Through localized activation of the Arp2/3 complex, the lamellipodium could be induced to grow in a particular direction, providing the basis for directional migration. In contrast, filopodia, with their parallel bundle organization, are particularly well designed to serve as sensors and explorers the local environment, acting as sites of signal transduction, and attaching to extracellular matrix (Davenport et al., 1993). Contained within filopodia are receptors that detect cues from the microenvironment (Lidke et al., 2005), and initiate downstream signaling pathways leading to cellular responses. Filopodia in neuronal growth cones orient toward gradients of guidance cues, an event that precedes the extension, turning or branching of the growth cone neurite towards chemoattractants (Bentley and Toroian-Raymond, 1986). Filopodia appear to be essential for neurite initiation and filopodia function may be needed for the establishment of neural circuitry (Smith, 1994). Similarly, filopodia are central in the proper alignment and attachments of cell during the dorsal closure in *Drosophila* embyo (Jacinto et al., 2000) and in a process known as "adhesion zippering" which occurs in epithelial sheet fusion in *Caenorhabditis Elegans* (Raich et al., 1999) and in cultured cells (Vasioukhin et al., 2000). Two mechanisms that use actin-nucleating proteins have been proposed for filopodia formation. In the "convergent elongation" model (Svitkina et al., 2003) filopodia are initiated by F-actin regulators including Arp2/3 complex-mediated nucleation downstream of Cdc42, Ena/VASP at filopodial tips, and fascin along the shafts, whereas the opposing model proposes that mDia2 performs most of these functions (Pellegrin and Mellor, 2005).

Formation and stabilization of attachments

For a migration to occur, a protrusion must form and then stabilize by attaching to the surrounding matrix. Integrins are the major family of migration-promoting receptors and may act as "feet" of a migrating cell supporting adhesion on ECM. Integrins link ECM to the actin cytoskeleton and may activate signaling cascades, so integrins are molecules that allow an "inside-out signaling". Integrins are heterodimeric receptors with large ligand-binding extracellular domains and short cytoplasmic domains. The binding of ligands confers conformational changes in the receptor that leads to receptor clustering, that initiate intracellular signaling such as protein phosphorylation, activation of small GTPases, change in phospholipids biosynthesis. This is linked to formation and strenghting of adhesion sites and organization and dynamics of the actin cytoskeleton (Geiger et al., 2001). Integrins affinity is regulated by alterations in the conformations of the extracellular domains that result from interactions at the integrin cytoplasmic tail. Talin is a component of adhesion plaques and interacts with integrin cytoplasmic tails (Horwitz et al., 1986), modulating the receptor affinity. The mechanism by which adhesions assemble in migrating cells is still not well understood. It may starts with little focal contacts, dependent on Cdc42 and Rac that stabilize the lamellipodium by mediating attachments to ECM.

Tractional forces

A migrating cell must be able to protrude and then detach from the older adhesions in order to move. By connecting the ECM to the intracellular cytoskeleton, integrins serve as both traction sites over which the cell moves and

as mechanosensors, transmitting information about the physical state of the ECM into the cell and altering cytoskeletal dynamics (Galbraith et al., 2002). The force transmitted to sites of adhesion derives from the interaction of myosin II with actin filaments that attach to these sites. Myosin II activity is regulated by myosin light-chain (MLC) phosphorylation, which is either directly positively regulated by MLC kinase (MLCK) or Rho kinase (ROCK) or negatively regulated by MLC phosphatase, which is itself phosphorylated and inhibited by ROCK. Whereas MLCK is regulated by intracellular calcium concentration as well as by phosphorylation by a number of kinases, ROCK is regulated by binding Rho-GTP (Riento and Ridley, 2003). MLC phosphorylation activates myosin, resulting in increased contractility and transmission of tension to sites of adhesion.

Retraction at the rear

At the rear of migrating cells, adhesions must also disassemble. The cell rear is a region where integrin-cytoskeletal linkages tend not to form and the membrane is not well supported by the cytoskeleton network. Rho GTP-ases are more active in the cell rear than in the front and it regulates negatively Rac activity. The Rho/ROCK/MLC/Myosin II pathway is implicated in the high tension exerted on the rear adhesions and contributes to the detachments (Lauffenburger and Horwitz, 1996; Riento and Ridley, 2003).

How does a cancer cell migrate *in vivo*?

Although our current understanding of cell migration and movements comes from studies performed in 2D environments, when we consider a migrating cell in

3D environments, such in a tissue, an additional component is the proteolitic remodeling of the extracellular matrix (ECM) and in other cases, the ability of a cell to change in shape in order to squeeze through the gaps in the ECM. Advances in intravital imaging techniques, together with fluorescent proteins technology are shedding the light on the mode of motility of cancer cell in their microenvironment. Intravital multiphoton microscopy combines the advanced optical techniques of laser-scanning microscopy with long-wavelength multiphoton fluorescence excitation to capture high-resolution, three-dimensional images of living tissues that have been tagged with highly specific fluorophores and now make it possible to directly observe cell behavior in primary tumors in live animals (Condeelis and Segall, 2003). These advances in the ability to image cells in primary tumors have stimulated hypotheses about the mechanisms of cell migration during invasion and intravasation, and provided new insights about the microenvironment that is required for these key steps in metastasis. Tumor cells can infiltrate neighboring tissue matrices in diverse patterns. They can disseminate as individual cells, adopting a mesenchymal motility or expand in solid cells strands, sheets, files or clusters, adopting a collective cell migration. Some carcinoma cells move with an amoeboid morphology, a kind of motility similar to the one that *Dictyosteliun discoideum* adopts (Friedl and Wolf, 2003). The speed and character of cell motility *in vivo* is quite different from that normally observed on two-dimensional substrates *in vitro* (Condeelis and Segall, 2003). *In vivo*, cancer cells move at high speeds (up to 15 μm a minute) and can change shape and direction rapidly in a manner similar to some leukocytes. This type of motility is usually termed amoeboid motility and uses preferentially cycles of actin polymerizations, cell adhesion and acto-myosin contraction. The Arp 2/3 complex and cofilin pathways are up-regulated in mammary tumor cells *in vivo*

(Wang et al., 2004; Wang et al., 2006) and are key players for the starting of productive migrations. Following the extension of a protrusion by a motile cell, adhesions are formed to the ECM and a dense network of collagen fibers around the margin of most tumors can be visualized. Moving tumor cells make contacts with collagen fibers and frequently move along fibers (Wyckoff et al., 2000). However, the large focal adhesions characteristic of cell-matrix interactions *in vitro* are not observed as motile cells contact collagen fibers *in vivo*. Focal adhesions usually take many minutes to mature, and this length of time is not compatible with fast moving cells that can travel their entire length in 2-3 minutes. Once new attachments to the ECM have been formed, acto-myosin interactions cause contractile forces that result in movement of the rest of the cell body. *In vivo* multiphoton confocal imaging of motile tumor cells expressing myosin light chain fused to GFP revealed that the acto-myosin network is largely cortical and not organized in 'stress-fibers' as seen in two-dimensional environments *in vitro* (Wyckoff et al., 2006). This cortical acto-myosin is largely controlled by the Rho-associated coiled-coil containing kinases (ROCK). Contraction of cortical acto-myosin can also generate points of constriction in the cell body that enable cells to squeeze between and around collagen fibers. These constrictions are typically around 5 μm in diameter. Squeezing between collagen fibers abrogates the requirement to cleave the fibers (Wolf et al., 2003). Correspondingly, inhibition of matrix metalloproteinases (MMPs) does not stop amoeboid cancer cell movement *in vivo*, demonstrating how the plasticity of cancer cell movement (from mesenchymal to amoeboidal) can negate the efficacy of anti-invasion drugs. Mammary tumor cells often migrate in a common direction consistent with the existence of chemotactic gradients, presumably EGF secreted by tumor-associated macrophages (Wyckoff et al., 2004). The ability of

cells to orient themselves with respect to blood vessels may be specific to metastatic cells. Two studies have shown that even when non-metastatic cells began to intravasate, they frequently became fragmented by shear stress (Wyckoff et al., 2000) and conversion of cells that normally move with an elongated morphology to a more rounded morphology increased both their ability to move and to enter vessels (Sahai et al., 2007). Together, these studies suggest that tumor cells with an elongated morphology may need to adopt a more rounded shape to efficiently intravasate and withstand shear stresses within blood vessels. It is tempting to speculate that the increased cortical acto-myosin contraction that promotes the rounded morphology may also enable the cortical cytoskeleton to withstand greater mechanical stress.

Role and Ena/VASP proteins in cell migration

Ena/VASP proteins have emerged as important regulators of actin assembly and cell motility in a variety of organisms and cell types. Drosophila Enabled (Ena), was discovered in a genetic screen for dominant suppressors of Drosophila Abelson tyrosine kinase (D-Abl) mutants (Gertler et al., 1990). VASP was discovered as protein substrate for cAMP and cGMP-activated kinases in platelets (Haffner et al., 1995), while EVL was identified together with Ena using a probe from Drosophila Ena used to isolate the Ena murine cDNAs (Gertler et al., 1996). Ena/VASP proteins are a structurally conserved family found in vertebrates, invertebrates and *Dictyostelium discoideum*. It consists of *Drosophila* Ena, *C. elegans* Unc-34, *Dictyostelium* VASP, and the three mammalian family members VASP, Mena, and EVL. All Ena/VASP family members share a conserved tripartite domain structure (Figure 3): an amino-terminal Ena/VASP homology 1

(EVH1) domain followed by a proline-rich central region and a carboxy-terminal Ena/VASP homology 2 (EVH2) domain. Mena is the only member of the family to have a long stretch of highly charged basic and acid amino acids (LERER). This insertion might adopt an extended helical structure and confer a further binding-binding interface and flexibility to the molecule.

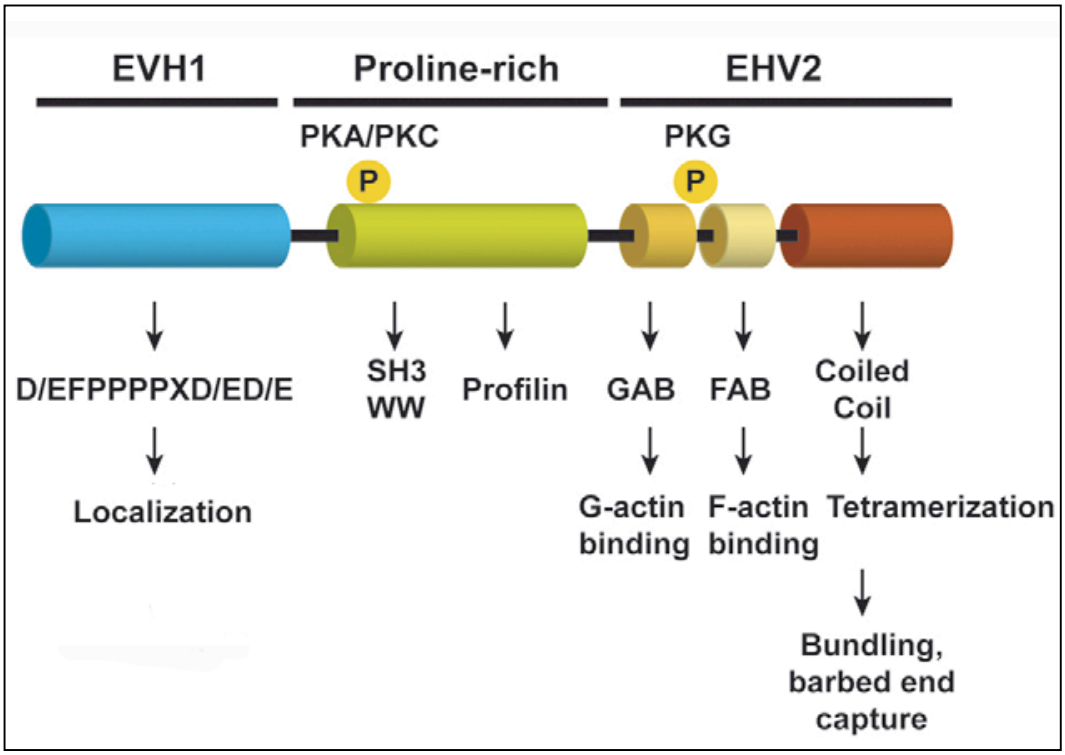

Figure 3. Organization of Ena/VASP proteins. The domains and protein interaction sites are shown in the schematic. Phosphorylation sites are also indicated. *Adapted from Drees & Gertler, Curr Opin Neurobiol. 2008 Feb;18(1):53-9*

Domains and functional organization

The EVH1 domain belongs to the pleckstrin-homology (PH) domain superfamily but unlike PH domains, EVH1 domains do not appear to bind to phosphatidylinositol lipids. Instead, the EVH1 domain, similar to PTB domains (another branch of the PH domain superfamily), binds to peptide ligands with high affinity. The EVH1 domains appear to bind to peptides containing a poly-

proline II helix, a left-handed helix with three residues per turn (Prehoda et al., 1999). EVH1 domains use a conserved hydrophobic cleft to bind a four-residue motif containing 2-4 prolines. Conserved aromatic residues, including an invariant tryptophan, create a wedge-shaped groove on the EVH1 surface that matches the triangular profile of a polyproline type II helix. Hydrophobic residues adjacent to the polyproline motif dock into complementary sites on the EVH1 domain to enhance ligand-binding specificity. Flanking residues in the vicinity of the PPII helix confer specificity of binding to SH3, WW, and EVH1 domains. The EVH1 domain in Ena/VASP proteins binds to the consensus site (F/W/Y/L)PPPPX(D/E)(D/E)(D/E) ϕ (X=any amino acid, ϕ=hydrophobic amino acid). Functional binding sites for EVH1 domains are found in zyxin (Drees et al., 2000), vinculin (Brindle et al., 1996), Fyb/SLAP (Krause et al., 2000), the *Drosophila* and *C. elegans* axon guidance receptor Robo/Sax-3 (Bashaw et al., 2000), and in the ActA protein of *Listeria monocytogenes* (Niebuhr et al., 1997). EVH1 domain recruits Ena/VASP proteins to specific sites within the cell. Ena/VASP proteins are recruited to focal adhesions by zyxin and vinculin, to phagocytic cups of macrophages and the contact site of T cells with antigen-presenting cells by Fyb/SLAP, and to *Listeria* tail by ActA. Other proteins such as palladin (Mykkanen et al., 2001), migfilin (Tu et al., 2003), human FAT (Moeller et al., 2004), RIAM (Lafuente et al., 2004) and Lamellipodin (Krause et al., 2004) also harbor putative EVH1-binding sites. In particular, Lamellipodin has a PH domain that binds specifically to PIP2 and is sufficient for plasma membrane recruitment upon treatment with PDGF. Since often phosphatidylinositol lipid products of PI-3 kinase, PI(3,4,5)P3 and its metabolite PI(3,4)P2 are downstream mediators of chemotactic receptors, Lamellipodin can be the link between extracellular chemotactic stimuli and Ena/VASP, since it was shown to be

responsible for Ena/VASP recruitment to the leading edge (Krause et al., 2004). Recently, a new EVH1 binding-protein as been identified by Michael Way lab. TES is a putative human tumor suppressor gene at 7q31.2, a chromosomal region that is frequently deleted in hematopoietic malignancies and epithelial tumors (Tobias et al., 2001). Although Tes doesn't contain any FPPPP motifs, it is shown to bind specifically Mena and not EVL or VASP. The LIM3 domain of Tes binds to the residues A12 adjacent to F32, and residues such as I53 in the ß3- ß4 loop of Mena's EVH1 domain. Moreover, Tes regulates Mena-dependent but not EVL or VASP-dependent cell migration (Boeda et al., 2007). This is an intriguingly finding, since in mammary tumor cells, Tes is downregulated while Mena is upregulated (Di Modugno et al., 2004; Di Modugno et al., 2006; Wang et al., 2004; Wang et al., 2007) and one could envisage that Tes may somehow regulate Mena and its lost may also contribute to a Mena-dependent tumor invasion.

The proline-rich domain harbors binding sites for SH3 and WW domain-containing proteins and the actin monomer-binding protein profilin. This region is the most divergent within the family and therefore may have different binding partners and mechanisms of regulation. Ena binds to the SH3 domains of Abl, Src, and the carboxy-terminal SH3 domain of Drk (Ahern-Djamali et al., 1999; Gertler et al., 1995). Similarly, EVL binds to the SH3 domains of Lyn, N-Src, Abl, and the WW domain of FE-65 (Lambrechts et al., 2000). In contrast, Mena does not bind to the SH3 domain of N-Src, but is bound by the SH3 domain of IRSp53 (Krugmann et al., 2001), Abl, Arg, Src (Gertler et al., 1996), and the WW domain of FE65 (Ermekova et al., 1997). So far, it is not clear which is the fisiological role of the interaction of Ena/VASP with several or proline-rich binding partners. All Ena/VASP family members contain proline-rich-binding sites for the small G-actin-binding protein profilin, and this binding is

independent of their phosphorylation status (Ahern-Djamali et al., 1999; Gertler et al., 1996; Lambrechts et al., 2000). Since the majority of actin is complexed to profilin in the cell (this is needed to avoid spontaneous nucleation of actin), the binding of profilin-actin complexes by Ena/VASP can explain, at least in part, the contribution of this protein family to actin-dependent processes. A model for binding of profilin-actin has been shown recently. Ena/VASP binds to profilin-G-actin complexes through two interfaces simultaneously, a profilin:Ena/VASP interface and a G-actin:Ena/VASP interface. The G-actin in the profilin-G-actin-Ena/VASP complex is oriented towards the F-actin binding motif of Ena/VASP; it is presumably positioned in this way to facilitate its addition to growing filaments. In fact, the poly-proline region of VASP contains three different modules: a regulatory site, a recruiting site and a loading site for profilin:actin (Ferron et al., 2007). The model for the elongation machinery shows three steps of the elongation mechanism: 1) recruitment of profilin–actin to the poly-Pro regions, 2) loading of profilin–actin from the last poly-Pro site onto the G-actin binding domain in the EVH2 domain and 3) filament elongation resulting from the addition of the actin subunit at the barbed end and the release of profilin (Figure 4).

The EVH2 is the “business” domain of Ena/VASP. It contains the necessary for the regulation of actin dynamics: starting from the amino terminus, a G-actin-binding site, an F-actin-binding site, and a coiled-coil motif required for oligomerization (Bachmann et al., 1999; Gertler et al., 1996). The G-actin-binding site resembles a motif in the small actin-monomer-binding protein ß-thymosin (Gertler et al., 1996) and is required for the *in vitro* actin nucleation activity of VASP (Birgit et al., 2002). The second conserved block in the EVH2 domain of VASP can co-sediment and bundle F-actin at low salt conditions (Bachmann et

al., 1999; Huttelmaier et al., 1999). The third conserved block consists of a coiled-coil structure that mediates oligomerization of Ena/VASP proteins (Bachmann et al., 1999; Zimmermann et al., 2002). VASP behaves as a tetramer, and the coiled-coil motif is sufficient to mediate tetramer formation. Furthermore, co-immunoprecipitation and yeast two-hybrid analysis indicate that homo- and hetero tetramerization among the members of the Ena/VASP family can also be observed *in vivo* (Ahern-Djamali et al., 1999). The coiled-coil sequence of VASP has been analyzed by crystalloghraphy (Kuhnel et al., 2004). It tetramerizes in parallel with an unusual right-handed coil raising the interesting possibility that this forms a structural interface for binding to barbed ends of F-actin (which also forms a right-handed coil). The EVH2 domain alone is sufficient to fully complement the function of full-length Ena/VASP in Ena/VASP deficient cells. Interestingly, tetramers formation is very important for Ena/VASP in order to exploit the function, since deletion of the coiled-coil domain doesn't rescue the phenotype in the deficient cells (Loureiro et al., 2002). Recently, the sequence between the F-actin binding domain and the tetramerization domain as been found to be important for the capture of barbed ends of growing actin filaments (Pasic et al., 2008).

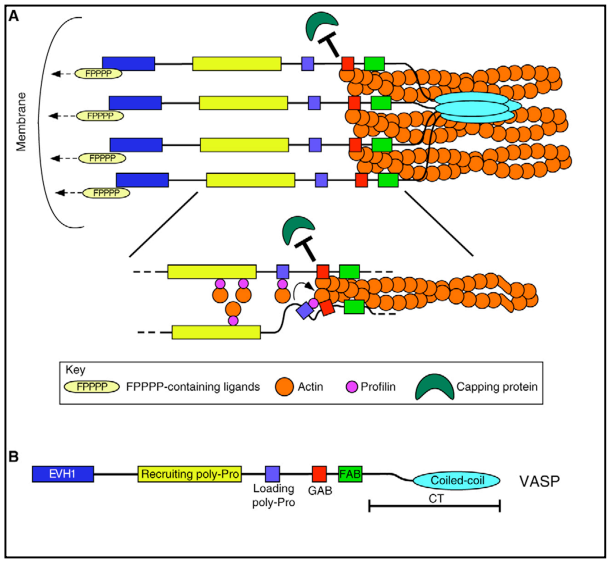

Figure 4. Mechanism of anti capping by Ena/VASP proteins.
(A) Tetramer of VASP in association with a bundle of actin filaments. Interactions between the EVH1 domain of Ena/VASP and FPPPP-motif-containing proteins help to position the Ena/VASP tetramer near the plasma membrane. (B) The profilin–G-actin loading mechanism by which Ena/VASP is thought to supply actin monomers to the barbed ends of filaments while antagonizing the ability of capping proteins to terminate filament elongation. *Adapted from Bear & Gertler, J Cell Sci. 2009 Jun 1;122(Pt 11):1882-94.*

The role of Ena/VASP proteins in cell migration was first studied in mouse embryonic fibroblasts derived from the mouse double knock-out for Mena and VASP and selected for low expression of EVL. When this cell line (MV^{D7}) is rescued with a physiological level of Mena, EVL or VASP, the cells moved more slowly than the parental null line. Conversely, the overexpression of Ena/VASP proteins in normal fibroblasts led to slower movement (Bear et al., 2000). Rescues experiments, using deletion mutants of Mena, have shown the structural requirements for the fibroblasts motility (Loureiro et al., 2002). Re-expression of a mutant lacking the proline-rich region slowed cells down to the same extent as the wild-type protein, indicating that profilin and other ligand recruitment mediated by this region are dispensable for random cell migration. However, the proline-rich region is required for other Ena/VASP-dependent processes. The F-actin-binding site is essential for proper fibroblast motility and for the ability of Ena/VASP proteins to be recruited effectively to the leading edge. An alternate approach to block Ena/VASP function is to remove the proteins from their normal localization within cells. To sequester Ena/VASP proteins on the surface of mitochondria, Frank Gertler group engineered the FPPPP repeats from ActA protein in a plasmid bearing four copies of FPPPP linked to a mitochondrial anchoring sequence. FPPPP-Mito blocks the function of all Ena/VASP family members by deleting them from their normal sites of function and replicates the phenotypes observed in Ena/VASP deficient cells (Bear et al., 2000). These observations using the null cells and re-localization strategies led to the conclusion that Ena/VASP proteins negatively regulate fibroblast migration speed. Despite the localization in focal adhesions, when Ena/VASP proteins are

selectively de-localized from focal adhesions, but not from the leading edge, using FPPPP-Cyto, random fibroblast migration speed on a fibronectin substrate is not affected, indicating that Ena/VASP proteins do not have a critical function in focal adhesions in this type of migration assay. At a gross level, the composition, number, and morphology of focal adhesions is unaffected by loss of Ena/VASP. At present, the function of Ena/VASP proteins within focal adhesions is unclear. A siRNA screening in MCF10A cells for genes that regulates epithelial cell migration show no phenotype when VASP is knock-down and an accelerated phenotype when Mena is knock-down, even if with 50% consistency among different siRNA and different experiments (Simpson et al., 2008). Another group, using a siRNA approach to knock-down genes important for focal adhesions formations and adhesions and quantitative microscopy, shows a slight changes in focal adhesion morphology and an increase in cell elongation when Mena is knock-down in HeLa cells (Winograd-Katz et al., 2009). However, both studies don't look at complete knock-down of Ena/VASP family members, so no definitive conclusions on the role of Ena/VASP in epithelial cell lines and focal adhesions formation can be made

The function of Ena/VASP proteins as negative regulators of fibroblast motility seemed paradoxical given that lamellipodial protrusion rate positively correlates with the intensity of GFP-VASP at the leading edge (Rottner et al., 1999). A careful examination of the dynamics of lamellipodia lacking Ena/VASP proteins resolved this apparent conflict and indicated that such lamellipodia protrude more slowly, but the protrusion persists longer. Conversely, cells overexpressing Ena/VASP proteins have lamellipodia that protrude faster than controls, but these protrusions are rapidly withdrawn in the form of ruffles. Therefore, Ena/VASP proteins increase lamellipodial protrusion velocity but have

a global negative effect on cell motility. These observations have led to a more general conclusion that whole-cell motility rates correlate better with persistence of protrusion than with instantaneous protrusion rate (Bear et al., 2002). Interestingly, deletion or re-localization of Ena/VASP proteins from the leading edge causes reorganization of actin filament architecture in lamellipodia. Lamellipodia lacking Ena/VASP function contain actin filament networks with shorter and more highly branched actin filaments. Excess Ena/VASP leads to longer but less-branched filaments. These changes in actin network geometry are responsible for the changes in lamellipodial behavior and, ultimately, changes in cell migration rate (Bear et al., 2002). It needs to be taken into account that the output of Mena activity is cell type specific and can be affected by the other components of the protrusion machinery.

VASP was the first molecule identified to bind ActA protein of the intracellular bacterium *Listeria monocytogenes* and this was also the first indication that Ena/VASP might directly regulate actin dynamics (Chakraborty et al., 1995; Pistor et al., 1995). *Listeria* is a master of mimicry that uses the host cell actin system both to move within the cytoplasm of infected cells and for cell-to-cell spread. ActA binds directly to Ena/VASP through the FPPPP repeats, moreover the same protein binds Arp 2/3 and G-actin. Ena/VASP binds directly to profilin, suggesting that the recruitment of profilin by Ena/VASP proteins may be one function of this protein family important for *Listeria* motility. *Listeria* speed is reduced after depletion experiments of either Ena/VASP proteins or profilin from cell extracts and by the restoration of *Listeria* movement in both rescue experiments and from reconstitution of pure proteins (Laurent et al., 1999; Theriot et al., 1994). Ena/VASP proteins also facilitate ActA-induced Arp2/3-mediated actin nucleation, possibly by increasing the amount of actin monomer available on

the bacterial surface. Finally, Ena/VASP proteins decrease the number of F-actin branches induced by ActA and the Arp2/3 complex *in vitro*, suggesting that they might regulate the geometry of the actin filament network in the tails of motile bacteria (Skoble et al., 2000). Within living cells, *Listeria* speeds are reduced an order of magnitude in the absence of Ena/VASP proteins. Expression of Ena/VASP deletion mutants lacking either profilin or the G-actin-binding site in Ena/VASP null cells provided only a modest increase in bacterial speed relative to wild-type protein, indicating that both domains are important for *Listeria* motility. In contrast, deletion of the F-actin-binding site increased the *Listeria* speed to higher than wild-type levels, whereas deletion of the coiled-coil domain had no effect (Geese et al., 2002).

Ena/VASP proteins co-localize with the hematopoietic-specific adaptor protein Fyb/SLAP; the adaptor molecules SLP-76, Nck, Vav, WASP; and the F-actin nucleator Arp2/3 complex in phagocytic cups of macrophages. They also co-localize at the interface between T cells and anti-CD3 coated beads (Coppolino et al., 2001; Krause et al., 2000). This localization of Ena/VASP is mediated by direct binding of the EVH1 domain to Fyb/SLAP. Ena/VASP proteins are also detected in a protein complex with Fyb/SLAP, SLP-76, Nck, Vav, and the Arp2/3 activator WASP upon ligation of the T cell receptor or the Fcγ receptor of macrophages, indicating that two key modulators of the actin dynamics, Ena/VASP and WASP, can be linked in regulated, physiological processes. Importantly, properly localized Ena/VASP proteins and Arp2/3 are each required for effective Jurkat T cell polarization and for phagocytosis suggesting that Ena/VASP-WASP-Arp2/3 networks may function together to promote these processes (Coppolino et al., 2001; Krause et al., 2000; May et al., 2000).

Role in Neuronal Migration and Axon Guidance

One of the most important and studied role of Ena/VASP regards neuronal migration and axon guidance. The development of the nervous system involves extensive migration of neurons. One of the first study of the role of Ena/VASP proteins in neuronal migration was performed using the FPPPP-Mito approach to block Ena/VASP function in cortical neurons (Goh et al., 2002). Neutralization of Ena/VASP function within neurons that normally migrate radially from their birthplace to the deep layers of the cortex resulted in frequent misplacement of these neurons to more superficial layers. Analysis of early stages of neuronal migration indicated that neurons expressing the FPPPP-Mito construct were already present in more superficial structures and therefore moved farther than control cells. During development the growth cones, the motile tips of growing processes, must traverse great distances and continually integrate a plethora of extracellular guidance signals into appropriate changes in cytoskeletal dynamics for proper movement. There are several reasons to believe that Ena/VASP proteins play important roles in intracellular signaling cascades that transduce extracellular guidance signals into actin dynamics within growth cone filopodia and lamellipodia. First, Ena/VASP proteins are concentrated at the tips of growth cone filopodia and lamellipodia in primary cultured neurons (Lanier et al., 1999). Second, all three vertebrate family members are regulated by protein kinase A (PKA), and at least VASP is known to be phosphorylated by protein kinase G (PKG) (Aszodi et al., 1999), two important kinases that modulate signaling downstream of many axon guidance molecules. Third, genetic studies in worms and flies implicate their Ena/VASP homologs in response to specific axonal guidance signals. In worms, unc-34 is required for proper response to netrin, a

guidance factor that can act either as an attractant or a repellent depending on the receptor repertoire and signaling context present within responding neurons (Colavita and Culotti, 1998; Gitai et al., 2003). In both flies and worms, Ena/VASP appears to function downstream of the repulsive guidance receptor Robo/Sax3, a molecule that binds directly to Ena/VASP through an EVH1-binding site found on its cytoplasmic tail (Bashaw et al., 2000). In mice, deletion of Mena caused axonal guidance defects in the formation of the corpus callosum, hippocampal commissure, and pontocerebellar fiber bundles (Lanier et al., 1999). However, the presence of the other two members of the family with similar functions and overlapping expression patterns in the neocortex precluded complete analysis of Ena/VASP function during cortical development. To overcome this, Frank Gertler lab engineered a transgenic mouse triple null for Mena, VASP and EVL (MVE). They show that loss of Ena/VASP causes two defects in neuronal migration during corticogenesis: a defect in cortical positioning and a non-cell-autonomous defect in pial membrane integrity that causes neuronal ectopias. Unexpectedly, they find that loss of Ena/VASP blocks axon fiber tract formation in the cortex, and they demonstrate that this defect results from the failure of cortical neurons to produce neurites. Of mechanistic note, evidences suggest that the defect in neurite formation results from the inability of Ena/VASP-deficient neurons to make filopodia and the neurite formation can be uncoupled from neuronal migration (Kwiatkowski et al., 2007). The majority of MVE embryos were exencephalic and with a cobblestone cortex. Interestingly, if Ena/VASP-deficient neurons are plated on laminin, or are transfected with MyosinX or mDia2, a rescue of the phenotype and filopodia formation is observed, suggesting different extrinsic and intrinsic pathways of filopodia formation and neuritogenesis (Dent et al., 2007).

Role in endothelia and epithelia

Endothelial cells line blood vessels and provide both a barrier function between blood and other tissue while still allowing immune cells access to the surrounding tissue. Barrier function requires cell-cell interactions, mediated in large part by adherens and tight junctions, which act to restrict the passage of material between cells in the endothelial lining. Both adherens and tight junctions use transmembrane proteins that interact with homotypic receptors on neighboring cells. Ligation of these receptors stimulates the cytoplasmic recruitment of multiprotein complexes that are involved in signal transduction and interaction with the cytoskeleton. The generation of the MVE mouse gave insights in the role of Ena/VASP in the endothelial barrier function. MVE mice exhibit edema and the vessel pattern and integrity are very compromised in these mice. This phenotype correlates in HUVEC cells, transfected with the FPPPP-mito construct, with an unperturbated assembly of cell-cell junctions but a reduced actin incorporation in the barbed end (Furman et al., 2007). Similarly to endothelial cells, epithelial cells form a physical boundary capable of regulating the transfer of molecules across the epithelial sheet. In these systems Ena/VASP proteins localize to adherens junctions, and disruption of their function affects epithelial dynamics (Grevengoed et al., 2001; Lawrence et al., 2002). Studies in *Drosophila* have demonstrated that reduction of either D-Abl or Ena affects epithelial morphology and epithelial sheet migration. Genetic interactions suggest that Ena functions in concert with components of the cadherin-catenin complex and D-Abl in epithelial sheets at the adherens junctions (Grevengoed et al., 2001). A more recent report shows that in flies Ena modulates filopodial number and length, thus influencing the speed of epithelial zippering and the ability of cells to match with

correct neighbors during dorsal closure (Gates et al., 2007). In mammals, Ena/VASP proteins are found in epithelial contacts that are revealed as a double row of dot-like structures also containing F-actin, E-cadherin, zyxin, and vinculin. These cell-cell contacts have been suggested to represent an early stage in junctions formation and have been termed the adhesion zipper (Vasioukhin et al., 2000). In this paper the authors adopt as strategy an overexpression a fragment of Ena/VASP responsible for oligomerization to disrupt epithelial sheet formation. However, the specificity of this approach for Ena/VASP proteins has not been demonstrated.

Molecular functions of Ena/VASP proteins

Several different molecular mechanisms as been proposed to explain the Ena/VASP dependent phenotypes in fibroblast migration, *Listeria* motility and the others actin-dependent phenotypes underlying fisiological processes in mice. The first model suggested a role in *de novo* nucleation of actin filaments. Purified Ena/VASP proteins can shorten the lag phase of actin polymerization in *in vitro* assays (Bachmann et al., 1999; Huttelmaier et al., 1999; Lambrechts et al., 2000). However, these investigators used low salt conditions (non fisiological) to polymerize actin, and moreover no convincing evidence supports this mechanism as a physiological for Ena/VASP function *in vivo*, since no F-actin is recruited when Ena/VASP proteins were relocalized to mitochondria in intact cells (Bear et al., 2000). Furthermore, *Listeria* that exhibit defective Arp2/3 activation but still recruit normal levels of Ena/VASP proteins fail to assemble or recruit any detectable F-actin (Skoble et al., 2000). More recent experiments both *in vivo* and *in vitro* point to three likely molecular mechanisms of Ena/VASP function: anti

capping, anti-branching, and profilin recruitment. These three different mechanisms may work together in order to give the final output of Ena/VASP function, the F-actin filament growth.

Ena/VASP proteins act to prevent or delay capping of barbed ends of actin filaments by capping proteins, CapZ and gelsolin, the three major barbed-end cappers in cells. Multiple lines of evidence support this anti capping mechanism. Ena/VASP proteins are localized to the leading edge of lamellipodia and the tips of filopodia. These locations contain a high density of actin filament barbed ends, and Ena/VASP localization to these places can be displaced by treatment with low concentrations of cytochalasin D (CD), a drug that binds with high affinity to the barbed ends of actin filaments and presumably displaces Ena/VASP proteins by competition. This observation is supported by *in vitro* assays in which Ena/VASP-coated beads can capture uncapped, but not capped, actin filaments (Bear et al., 2000). In addition, purified VASP antagonizes the activity of capping proteins and gelsolin in actin filament elongation assays (Barzik et al., 2005). Perhaps the most compelling evidence for this model comes from studies of fibroblasts with modified Ena/VASP function. Depletion of Ena/VASP leads to shorter actin filaments at the leading edge relative to controls. Conversely, overexpression of Ena/VASP leads to longer filaments than control cells at the leading edge (Bear et al., 2000). These data suggest a mechanism in which Ena/VASP proteins associate with actin filaments at or near their barbed ends to prevent capping by capping proteins. This model is supported by experiments *in vivo* in which low doses of CD were used to reverse Ena/VASP-dependent motility phenotypes in fibroblasts. This CD treatment mimics capping proteins overexpression and reduced the filament length to wild-type levels, indicating that a balance between capping proteins levels and Ena/VASP activity regulates actin filament geometry

in lamellipodia (Bear et al., 2002). Recent findings reinforce the anti capping activity of Ena/VASP. Using Total Internal Reflection Fluorescence Microscopy (TIRF) and VASP immobilized on a coverslip, Dorothy Schafer lab has shown that purified VASP delayed termination of filament growth by heterodimeric capping protein. The filament elongation rate was enhanced by addition of profilin along with VASP (Pasic et al., 2008). The Jan Faix group has also shown anti capping activity of VASP. In these studies, VASP immobilized on beads was capable of supporting continuous elongation of filaments even in the presence of a very high concentration of capping proteins (Breitsprecher et al., 2008). This study did not find anti capping activity for VASP when it was in solution, as others have; however, this may be due to differences in specific assay conditions or protein preparation or storage conditions.

Several groups have noted that Ena/VASP proteins reduce the frequency of actin-filament branching by the Arp2/3 complex (Bear et al., 2002; Samarin et al., 2003; Skoble et al., 2000). Skoble and colleagues observed that VASP reduced the branching induced by ActA-activated Arp2/3 complex in visual assays. These reactions did not contain capping proteins and the observed anti-branching activity must be independent of its anticapping function. Nothing more is know about the mechanisms of anti-branching mediated by Ena/VASP.

Recent structural and biochemical analyses indicate that VASP harbors a high-affinity profilin-binding “actin-loading site” adjacent to its actin-monomer-binding motif (Chereau and Dominguez, 2006; Ferron et al., 2007). The structural studies suggest a model in which profilin-G-actin binds to the Ena/VASP loading site in a manner that allows the actin monomer to bind to the Ena/VASP G-actin binding site (which is adjacent to the F-actin-binding motif). Such a model would explain how actin monomers could be transferred efficiently from profilin to the

barbed ends of actin filaments while bound to Ena/VASP; the model is consistent with the ability of profilin to increase Ena/VASP anti capping activity by increasing filament-elongation rates, however, profilin is not required for VASP anti capping activity *in vitro* (Barzik et al., 2005). Profilin recruitment by Ena/VASP plays an important role in supporting *Listeria* motility within living cells. EGFP-Profilin co-localizes only with moving *Listeria*, and its intensity correlates positively with the speed of the bacteria and Ena/VASP deficient cells that are complemented with forms of Mena or VASP that cannot bind profilin (the proline-rich deletion) do not support *Listeria* movement as effectively as wild-type protein (Geese et al., 2002).

Regulation of Ena/VASP proteins

The mammalian Ena/VASP proteins are known substrates of cAMP and cGMP- dependent serine and threonine kinases PKA and PKG (Gertler et al., 1996; Lambrechts et al., 2000). VASP harbors three phosphorylation sites (Ser-157, Ser-239, and Thr-278), whereas Mena contains the first two, and EVL only the first site (Butt et al., 1994; Gertler et al., 1996; Lambrechts et al., 2000). Studies of mutant mice revealed that VASP is required for the PKA-mediated inhibition of platelet aggregation (Aszodi et al., 1999) suggesting that VASP is the critical PKA substrate required for this process, and that Ser-157 may be the key site of regulation. In random fibroblast migration, phosphorylation of Mena at its first phosphorylation site (S-236, the equivalent of VASP Ser-157) is essential for its function. A non-phosphorylatable S-236-A Mena mutant localizes normally when expressed in Ena/VASP-deficient cells, yet fails to rescue the hypermotile phenotype of Ena/VASP null cells (Loureiro et al., 2002). Conversely, a

phosphomimetic S-236-D Mena mutant complements the fibroblast phenotype. Therefore, it seems likely that phosphorylation is not essential for Ena/VASP subcellular targeting but is probably required to regulate Ena/VASP function in lamellipodia. Phosphorylation of wild-type VASP (in particular S235) by PKA *in vitro* abolished VASP anti capping activity in the presence and absence of profilin and bundling formation (Barzik et al., 2005), probably because of an negative charge over phosphates that can interfere with F-actin binding. Ena/VASP can be phosphorylated in tyrosine as well. In fact, Enabled was identified as target of Abl kinase in *Drosophila* (Gertler et al., 1995). However, at present it is unclear whether tyrosine phosphorylation of Ena is important for its function.

Ena/VASP alternative splicing and splicing regulation

Human and mouse Mena contain at least 4 published isoforms (Figure 5) and other isoforms currently under investigation in the Frank Gertler and the Paola Nisticò laboratories. The larger isoform of Mena, called +, contains an extra 246 additional amino acids after the LERER repeats (Gertler et al., 1996), and is express in developing and adult brain tissues (Lanier et al., 1999). The + exon is proline rich and can be tyrosine phosphorylated *in vivo* (Gertler et al., 1996). Some cDNA containing the + exon may also contain two other small exons that introduce 4 and 19 aminoacids, right after the EVH1 domain, called ++ or +++ (INV) (Gertler et al., 1996). The EVH2 of Mena can contain a 21 aminoacids insertion between the F-actin and the coiled-coil domain. This isoform is called Mena11a, is expressed in epithelial tissues (Di Modugno et al., 2007; Pino et al., 2008; Balsamo et al., manuscript in preparation) and is the main focus of this thesis. Another isoform of Mena, identified by Tani and colleagues, is mainly

express in the spleen and in lymphoid cell lines. This isoform, called MenaS (short) lacks the aminoacids 300-333 in mouse Mena (Tani et al., 2003), so it should be incapable of binding profilin. Russ Carstens group identified two splice factor proteins ESRP1 and ESRP2 as regulators of the epithelial splicing. Among several other genes analyzed, the splicing of Mena11a seems to be regulated by these two splicing factors (Warzecha et al., 2009a; Warzecha et al., 2009b).

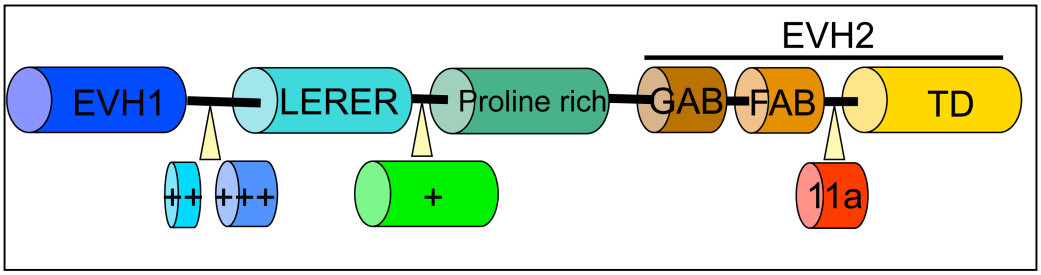

Figure 5. Mena isoforms scheme.

EVL is expressed in two isoforms, the larger one is called EVL-I and similarly to Mena11a, has a 21 aminoacids insertion right before the tetramerization domain (Lambrechts et al., 2000). We have shown that EVL-I can be phosphorylated by Protein Kinase D and like Mena11a, is also enriched in basal keratinocytes in mouse skin (Janssens et al., 2009).

Ena/VASP in cancer

The first indication of a role for Mena in cancer came from Paola Nisticò's group. With the goal of identifying new tumor-associated antigens in breast cancer, the screening of a cDNA library from a primary breast tumor with the autologous patient serum led to the isolation of a cDNA that encoded the Mena gene. The majority of the human sera screened showed anti Mena specific IgG and further analyses have shown overexpression of Mena in cancer cell lines and

in breast cancer patients (Di Modugno et al., 2004). The same year, two other reports showed that Mena mRNA was upregulated in invasive and metastatic cells. John Condeelis laboratory found that Mena is part of the "minimum motility machinery" genes that are upregulated in the subpopulation of mammary cancer cells chemoactratted by Epidermal Growth Factor (EGF) *in vivo*, compared to the primary tumor cells (Wang et al., 2004). Robert Weinberg's group found Mena upregulated in metastatic cells that also upregulated the transcription factor Twist (Yang et al., 2004).

A better characterization of Mena overexpression in human breast cancer patients was published in 2006 by Di Modugno et al. Mena was progressively overexpressed during breast cancer progression and this overexpression correlated with the proliferation index, the downregulation of Estrogen Receptor (ER) and Progesteron Receptor (PgR) and upregulation of Human Epidermal Growth Factor Receptor 2 (HER-2) (Di Modugno et al., 2006). The same group did further characterization of Mena function in cancer. We cloned and characterized Mena coding sequence and identified Mena11a, an alternative splicing isoform. We showed that Mena overexpression characterizes the transformed phenotypes and that treatment of breast cancer cells with EGF further upregulates Mena expression. The importance of this finding is due to the fact that EGF has a central role in the mammary gland biology and breast cancer progression. Interestingly, a shift versus more acidic pH (and a reversion of the shift in samples treated with phosphatase) of Mena11a was observed in protein extracts of EGF-treated cell lines. The overexpression of Mena11a was associated with an increase in cell proliferation and phosphorylation of Mitogen Associated Protein Kinase (MAPK) (Di Modugno et al., 2007). The functional role of Mena overexpression by EGF, the role of the putative Mena11a phosphorylation and the modulation of breast

cancer cells proliferation by Mena11a are still open questions that need to be further addressed and explored.

To extend our findings to other epithelial cancers, we looked into the role of Mena isoforms in human ductal pancreatic cancer cells. Interestingly, we found that Mena11a is expressed in pancreatic cancer cell lines with an epithelial phenotype, while downregulated in cells that express mesenchymal markers, addressing for the first time a role for Mena11a during the Epithelial to Mesenchymal Transition (EMT) (Pino et al., 2008). Of great interest for pancreatic cancer, we found that Mena11a may serve as a marker of sensitivity for EGFR targeted therapy since its expression is able to distinguish between Erlotinib (an EGFR tyrosine kinase inhibitor) sensitive versus resistant cell lines. We have also shown for the first time Mena expression in human pancreatic cancer tissues and metastasis (Pino et al., 2008).

Mena has also been shown to be overexpressed in colorectal cancer (Gurzu et al., 2008; Toyoda et al., 2009) and cervical cancer (Gurzu et al., 2009) lesions, even though these studies are performed on a very small number of patients.

A step forward for the understanding of the contribution of Mena in cancer came from Frank Gertler laboratory. The authors have found that Mena, and a splice isoform in particular (MenaINV/+++) plays a major role during mammary cancer invasion and metastasis (Philippar et al., 2008). MenaINV localizes to the leading edge of motile carcinoma cells *in vivo* and its overexpression promotes metastasis dissemination in the lungs. MenaINV promotes 3D invasion and matrix degradation *in vitro*, acting on stabilization of invadopodia, actin-rich structures that are need to invade 3D matrices. Interestingly, MenaINV overexpressing cells respond to low concentration of EGF, forming lamellipodia with an area bigger than control cells. This is associated with a promotion of actin incorporation at the

barbed ends in a cofilin-dependent manner (Philippar et al., 2008). The molecular mechanisms of the MenaINV-dependent EGF sensitivity in mammary cancer cells is still unclear.

EVL gene seems to be methylated in colorectal carcinomas (Grady et al., 2008) while upregulated in breast cancer patients, and this correlates with clinical stages (Hu et al., 2008). We have shown that EVL and EVL-I are highly expressed in breast cancer cell lines an in a B-cell lymphoma cell line as well (Janssens et al., 2009). Of note, in MCF7 human breast cancer cells, EVL unexpectedly binds to the RAD51 and RAD51B proteins, central players in homologous DNA recombination repair and stimulates the RAD51-mediated homologous pairing and strand exchange, adding a new role to this molecule (Takaku et al., 2009a). Moreover the same group also found that the DNA-binding activity of EVL resides in the EVH2 (Takaku et al., 2009b). The contribution of VASP in cancer is still unknown.

Epithelial to Mesenchymal Transition

The Epithelial to Mesenchymal Transition (EMT) is a biological process that allows a polarized epithelial cell, which normally interacts with a basement membrane via its basal surface, to undergo multiple biochemical and morphological changes that enable it to assume a fibroblastic-like, mesenchymal phenotype, which includes enhanced migratory capacity, invasiveness, elevated resistance to apoptosis and greatly increased of extracellular matrix (ECM) compounds. The completion of an EMT is signaled by degradation of ECM by a mesenchymal cell that migrates away from epithelial layer in which it originated (Thiery and Sleeman, 2006). The EMT program is activated at multiple steps of

embryonic development to enable the conversion of various types of epithelial cells into mesenchymal cells. Passage through an EMT, however, does not necessarily represent an irreversible commitment to switch differentiation lineages. Thus, the reverse program, termed the Mesenchymal to Epithelial Transition (MET), also occurs both during embryonic development and during several pathological processes. The reversibility of this process underscores the enormous plasticity of certain embryonic and adult cells that participate in processes of disease pathogenesis. Since EMTs are encountered in three distinct biological context that carry different functional consequences, a recent classification of the EMT processes has been proposed (Kalluri and Weinberg, 2009). Type I EMT is associated with implantation (Vicovac and Aplin, 1996), embryo formation, and organ development, such as cardiac valve formation (Bolender and Markwald, 1979) and secondary palate formation (Fitchett and Hay, 1989). These type I EMTs are the implantation of the embryo and the initiation of placenta formation (Vicovac and Aplin, 1996), cardiac valve formation (Bolender and Markwald, 1979) and secondary palate formation (Fitchett and Hay, 1989). Type II ETMs are associated with tissue regeneration and organ fibrosis. Inflammatory cells and fibroblasts that release inflammatory signals and ECM often mediate fibrosis. EMT has been found to be associated with fibrosis of kidney, liver, lung, heart and intestine (Kim et al., 2006; Zeisberg et al., 2007a; Zeisberg et al., 2007b). Type III EMT is associated with cancer progression and metastasis. The genetic control and biochemical mechanisms underlying the acquisition of an invasive phenotype and the subsequent systemic spread of cancer cell have been extensively studied areas and in many studies, the activation of an EMT program has been proposed to be the underlying mechanisms for the acquisition of malignant phenotypes by epithelial cancer cells

(Thiery, 2002). The full spectrum of signaling agents that contribute to EMTs of carcinoma cells remains unclear. One suggestion is that the genetic and epigenetic alterations undergone by cancer cells during the course of primary tumor formation render them especially responsive to EMT-inducing heterotypic signals originating in the tumor-associated stroma. Oncogenes induce senescence, and recent studies suggest that EMT may also play a role in preventing senescence induced by oncogenes, thereby facilitating subsequent aggressive dissemination (Ansieau et al., 2008). In the case of many carcinomas, EMT-inducing signals emanating from the tumor-associated stroma, notably HGF, EGF, PDGF, and TGF- ß, appear to be responsible for the induction or functional activation in cancer cells of a series of EMT-inducing transcription factors (Joyce and Raghu, 2007). The actual implementation by these cells of their EMT program depends on a series of intracellular signaling networks involving, among other signal-transducing proteins, ERK, MAPK, PI3K, Akt, Smads, RhoB, ß-catenin, lymphoid enhancer binding factor (LEF), Ras, and c-Fos as well as cell surface proteins such as α4 integrins, α5ß1 integrin, and αVß6 integrin. Activation of EMT programs is also facilitated by the disruption of cell-cell adherens junctions and the cell-ECM adhesions mediated by integrins. TGF-ß is an important suppressor of epithelial cell proliferation and thus primary tumorigenesis. However, it is now clear that in certain contexts it can also serve as a positive regulator of tumor progression and metastasis (Massague, 2008). Thus, *in vitro* studies have demonstrated that TGF-ß can induce an EMT in certain types of cancer cells (Vincent et al., 2009). Some data indicate that p38 MAPK and RhoA mediate an autocrine TGF-ß–induced EMT in NuMG mouse mammary epithelial cells (Bhowmick et al., 2001). TGF-ß can induce an EMT in Ras-transformed hepatocytes, mammary epithelial cells (via MAPK), and MDCK cells; at the same

time, Ras-activated PI3K inhibits TGF-ß–induced apoptosis to facilitate this transition (Janda et al., 2002). Typical hallmarks of EMT in cancer are the changes of differentiation markers from cell-cell junction proteins and cytokeratin intermediates filaments to vimentin filaments and fαibronectin. E-cadherin loss has been associated with carcinoma progression and poor prognosis in various epithelial cancers (Vincent-Salomon and Thiery, 2003). The best demonstration of this process is familiar gastric cancers in which the E-cadherin germline mutations play a causal role (Guilford et al., 1998). Activation of tyrosine kinase receptors in tumor cells can lead to disruptions of cell-cell junctions, with degradation of E-cadherin and ß-catenin (Fujita et al., 2002). In the majority of human carcinoma cell populations, the loss of E-cadherin appears to be heterogeneous, with foci of E-cadherin-positive carcinoma cells scattered among E-cadherin-negative areas. Moreover, E-cadherin is often detected in distant metastases, which may derive from cells that have previously passed through an EMT (Bukholm et al., 2000; Bukholm et al., 1998). This suggests that after their initial dissemination, some metastatic cells may revert to an epithelial state, and it indicates that other, non genetic mechanisms controlling transcription of the E-cadherin gene or post-translational modification of the E-cadherin protein may be responsible for the lack of expression of this protein in some tumor cells. Indeed, many EMT-inducing transcription factors, including Snail, Slug, EF1, SIP1, Twist1, FOXC2, ZEB1-2 and Goosecoid, have been associated with tumor invasion and metastasis. Expression of almost all of these genes has been detected in certain invasive human and mouse tumor cell lines. Expression of Twist-1 has been shown to be essential for a mouse breast carcinoma cell line to metastasize from the mammary gland to the lung (Yang et al., 2004) and overexpression of FOXC2 or Goosecoid increases the ability of weakly metastatic human carcinoma cells to disseminate

(Hartwell et al., 2006; Mani et al., 2007). Mina Bissell laboratory has reported that matrix-degrading enzymes such as MMP-3 facilitate EMT by inducing genomic instability via Rac1b and ROS (Radisky et al., 2005). Noncoding microRNAs are also components of the cellular signaling circuitry that regulates the EMT program. For example, microRNA 200 (miR200) and miR205 inhibit the repressors of E-cadherin expression, ZEB1 and ZEB2, and thereby help in maintaining the epithelial cell phenotype (Gregory et al., 2008; Korpal et al., 2008). In breast carcinoma, a loss of miR200 correlates with increased expression of vimentin and a decrease in the levels of E-cadherin in cancer cells. Acting in the opposite direction, miR21 is upregulated in many cancers and facilitates TGF-ß induced EMT (Zavadil et al., 2007). Interestingly, $CD44^{hi}/CD20^{lo}$ cells purified from normal and malignant breast cancer tissue exhibit features of an EMT, and human cancer cells induced to undergo EMT exhibit stem cell-like properties and increased metastatic potential (Mani et al., 2008). One major difficulty in demonstrating the role of EMT in metastasis in human cancers is identifying carcinoma cells that have passed through an EMT in primary human tumor samples. Most of the EMT markers currently used are expressed in either epithelial or mesenchymal cells, and therefore are not specific for identifying tumor cells at the EMT stage that are scattered among the many stromal cells present within a primary tumor. A few studies have shed some light on the existence of such EMT carcinoma cells in primary human cancers. The EMT-inducing transcription factor Twist-1 is overexpressed in two human cancer types, lobular breast carcinoma and diffused-type gastric cancer. Over 90% of these tumors do not express E-cadherin and exhibit a permanent EMT phenotype (Yang et al., 2004). In colorectal cancers that contain APC or ß-catenin mutations, ß-catenin expression is predominantly observed in tumor cells localized at the

invasion front and scattered in the adjacent stromal compartment. More interestingly, tumor cells with nuclear ß-catenin accumulation appear to have undergone an EMT, as demonstrated by the progressive loss of E-cadherin expression and acquisition of mesenchymal markers such as fibronectin (Fodde and Brabletz, 2007). Despite these various observations, the involvement of EMT in human cancer metastasis is still highly debated, due in part to clinical observations showing that the majority of human breast carcinoma metastases express E-cadherin and maintain their epithelial morphology, suggesting that they have disseminated without switching to a mesenchymal phenotype (Tarin et al., 2005). Several studies in mouse tumor models have also suggested that tumor invasion and metastasis can be achieved without an obvious EMT phenotype. In a TGF- ß1-induced mouse skin tumor model, blocking the EMT program with a dominant-negative TGF- ß type 1 receptor did not inhibit the occurrence of distant metastases (Han et al., 2005). Collective cell invasion (Wicki et al., 2006) and fibroblast-led collective invasion (Gaggioli et al., 2007) have also been responsible for carcinoma cell local invasion into the extracellular space. Indeed, cell migration during several developmental events does not require a complete EMT phenotype. However, partial EMT and collective cell migration are not sufficient to explain how individual tumor cells can intravasate into the blood circulation and travel to distant organs. Some of these controversies are due to the depiction of EMT as a permanent, irreversible process occurring during the course of tumor metastasis. Indeed, a reversible EMT model has been proposed to describe the transient activation of the EMT program that carcinoma cells undergo during tumor metastasis (Thiery, 2002). In this model, carcinoma cells activate the EMT program to achieve local invasion and dissemination to distant organs. Once they have reached those organs, these mesenchymal cells may revert via

MET to an epithelial identity and thereby regain proliferative ability and the ability to form epithelial growths in distant organ sites. Moreover, cancer cells may, more often than not, pass through a partial EMT program rather than a complete one; such cells may concomitantly express epithelial and mesenchymal markers. Better EMT mouse tumor models will be needed to test this hypothesis rigorously.

The tumor microenvironment

Tumors are complex ecologies of different cell types and the full manifestation of the malignant phenotype requires an appropriate microenvironment. The tumor-surrounding stroma contains a plethora of non-cancerous cells and different bone marrow-derived cells, embedded in the ECM. Among the stromal cell types that have been implicated in the tumor promotion are endothelial cells, pericytes, fibroblasts, macrophages, neutrophils, mast cells, myeloid cell-derived suppressor cells, lymphocytes, NK cells and mesenchymal stem cell (Joyce and Pollard, 2009b). Several cross talks between cancer cells and stromal cells have been reported as fundamental for tumor progression and metastasis. For example, cancer-associated fibroblasts secrete matrix metalloproteinases (MMPs) that are needed to degrade extracellular matrix and facilitate tumor cell stromal infiltration; fibroblast secreted protein-1 (FSP-1) which may inactivate p53 and interact with the cytoskeleton; CXCL-12 (SDF-1), which stimulates proliferation and chemoattraction of carcinoma cells through CXCR-4 and TGF-ß, which is a known tumor-promoting growth factor in the later stage of carcinoma progression (Egeblad et al., 2005). Fibroblasts are also responsible to secrete ECM proteins like collagens, fibronectin and laminin

(Kalluri and Zeisberg, 2006). The stroma is an innate anticancer mechanism, since it's needed to provide substratum and polarity to epithelia. Indeed, loss of polarity leads to increased cell proliferation and tumorigenesis (Bissell and Radisky, 2001). The inherent inflammation that is often associated with tumors may contribute to the so-called reactive stroma, a stroma with an increased number of fibroblasts, enhanced capillary density and type I collagen. The presence of leucocytes in tumors in the past was generally thought to be a consequence of a failed attempt at cancer cell destruction. However, tumors are not only effective in escaping from immune-mediated rejection, but they also modify certain inflammatory cell types to render them tumor promoting rather then tumor suppressive. For example, $CD4^+$ T cells, macrophages and NKT cells have either tumor-suppressive or tumor-promoting properties, depending on the tissue context and cellular stimuli (de Visser et al., 2006). The presence of macrophages infiltration correlates with poor patient prognosis (Bingle et al., 2002). An interesting cross talk between mammary cancer cells and macrophages as been shown by John Condeelis laboratory. A paracrine loop in which Epidermal Growth Factor (EGF) produced by tumor associated macrophages (TAM) increases the invasiveness and the invasion of neighboring breast cancer cells that express EGF receptor has been found. Cancer cells in turn express Colony Stimulating Factor 1 (CSF-1), which acts as potent chemoattractant and chemokinetic molecule for CSF1-R expressing TAMs (Goswami et al., 2005). Thus, a possible "invasive niche" exists within the primary tumor, in which the proximity of a triad of macrophage, cancer cell and endothelial cell establishes paracrine signaling loops that lead to enhanced intravasation and dissemination of cancer cells. Indeed, clusters of these three different cell types, termed the Tumor Microenvironment of the Metastasis (TMEM), are found in human breast cancer

and their increased density is associated with the development of distant organ metastasis (Robinson et al., 2009). Recently, a new player in this invasive niche has been found to be important for the formation of pulmonary metastasis from mammary cancer. Lisa Coussens group, employing elegant genetic experiments, has shown that Th2-polarized $CD4^+$ T lymphocytes express IL-4 and IL-13, these interleukins regulate TAMs to upregulate EGF mRNA and induction of mammary cancer cells to give raise to lung metastases (DeNardo et al., 2009).

Outline of the PhD thesis

My PhD thesis focuses in the understanding of the mechanisms of Mena-mediated cancer cell migration and Ena/VASP-dependent epithelial morphogenesis. In particular, my project aims to shed light on an alternatively spliced isoform of Mena, Mena11a, that we have previously isolated and identified in a luminal human breast cancer cell line (Di Modugno et al., 2007). We have indeed shown that Mena11a is exclusively expressed in human breast and pancreatic ductal adenocarcinoma cell lines with an epithelial phenotype (Pino et al., 2008). Intriguingly, in human pancreatic cancer cells Mena isoforms expression pattern was predictive of response to EGFR inhibition (Pino et al., 2008).

Based on these findings this thesis aims to evaluate whether Mena11a acts as a regulator of Mena activity in epithelial cells and whether Mena11a itself can have a specific role in epithelia. In order to investigate these hypotheses, we looked into the regulation of the actin cytoskeleton dynamics *in vitro*, *in vivo*, and in transgenic mice.

The finding that Mena11a expression correlates with EMT markers has prompted us to test whether Mena11a could also be downregulated in an established mammary EMT model. We show that the overexpression of the transcription factor Twist, a master regulator of EMT (Yang et al., 2004), in human mammary epithelial cells (HMLER) leads to downregulation of Mena11a at the mRNA and protein levels. To gain further insight into the regulation of Mena11a splicing during EMT, we engineered HLME cells with a splice reporter to follow Mena11a splicing; these cells are being injected in mice and we will

further look at the behavior of the splice reporter cells *in vivo* by multiphoton microscopy.

In addition, we found that Mena11a is highly expressed and co-localizes with Pan-Mena in the primary mammary tumors of MMTV-PyMT mouse model. Invasive cells collected by a 3D *in vivo* invasion assay, down-regulate Mena11a and up-regulate Mena and vimentin, a mesenchymal marker. Interestingly, Mena11a is re-expressed in the mammary lung metastases in this mouse model. We observed a more defined Mena11a staining to the cell-cell junctions of macrometastases compared to micrometastases, while Pan-Mena localizes to the junctions independently of the metastasis size, suggesting an important role for Mena11a in the Mesenchymal to Epithelial Transition (MET) process.

In mammary carcinoma cells Mena11a overexpression dampens the EGF-mediated lamellipodia protrusion. Moreover, in an *in vivo* 3D cell invasion model, Mena11a overexpression suppresses the EGF-mediated invasion of these carcinoma cells. Experiments looking at the contribution of barbed end formation and actin polymerization by Mena11a in cells are currently ongoing.

Since the 11a insertion falls in the EVH2 domain of Mena, the domain that is needed to exploit the function of Mena, we asked whether and how Mena11a affects the cytoskeleton dynamics. We found that Mena11a retains actin binding and bundling activity, typical of Ena/VASP, but lacks of F-actin barbed end capture activity *in vitro*. So we can hypothesize that the sequence between the F-actin and the tetramerization domain of Mena may be important for the initial F-actin barbed end binding. Moreover, Mena11a doesn't drive filopodia formation while Mena does, an activity highly related to the ability of binding barbed ends of growing actin cables in filopodia. Although the anti capping activity of Mena11a seems to be as potent as the one of Mena in pyrene actin assays, further

experiments where the population of actin filaments can be followed individually are required.

We investigated the role of Ena/VASP in the junction formation in mice triple-knock outs for Mena, VASP and EVL (MVE). MVE mice are essential to understand the physiology of Ena/VASP. We have found EVL-I, an isoform of EVL, to be highly expressed in the skin (Janssens et al., 2009). E16.5 MVE embryos show an open-eye phenotype and defects in the basal layer of the epidermis, suggesting an important role in the epithelial sheets migration and junctions formation. Since the lack of Ena/VASP is embryonic lethal, we started to generate Mena conditional, VASP and EVL null mice (MCVE) crossed with mice bearing CRE recombinase under the control of skin-specific promoters. Analysis of the epidermis in the adults and wound healing *in vivo* will be performed in the near future. Moreover, to investigate the molecular mechanisms of junction formation in these mice, epidermal keratinocytes from MCVE mice will be used as model and the junctions assembly will be monitored in the null keratinocytes or in the Mena single-isoform expressing reconstituted cells.

Chapter 2 - Experimental Procedures

Cell lines, mouse keratinocytes primary culture and tissue samples

All human cancer cell lines were mantained in DMEM supplemented with 10% Fetal Bovine Serum (Hyclone), L-glutamine, and antibiotics (penicillin/streptomycin; Invitrogen). MTLn3 cells were maintained in alpha-MEM supplemented with 5% Fetal Bovine Serum (Hyclone), L-glutamine, and antibiotics (penicillin/streptomycin; Invitrogen). Adherent monolayer cultures were incubated at 37°C in a mixture of 5% CO_2 and 95% air. MV^{D7}, Ena/VASP-deficient mouse embryonic fibroblastic cells, were isolated as described in Bear et al. 2000, and cultured at 32°C in Immorto medium [high-glucose Dulbecco's modified Eagle's with 15% FCS, penicillin/streptomycin, l-glutamine, and 50 U/mL recombinant mouse IFN-γ (Invitrogen)].

Mouse primary keratinocytes were isolated from the skin of neonatal mice. Skin were incubated over night at 4°C with 2 U/ml Dispase I and II solution (Roche). Next day, epidermis were separated from the dermis, minced and incubated for 10-20 minutes in 0.25% Trypsin solution (Gibco) at 37°C. Epidermis were passed through 45 μm cell strainers to obtain a single cell suspension of keratinocytes. Cells were maintained in S-MEM calcium free (Invitrogen), supplemented with 4% chelated FBS, 0.05 mM $CaCl_2$, 0.4 μg/ml hydrocortisone (Sigma Aldrich), 5 μg/ml bovine insulin (Sigma Aldrich), 10 ng/ml recombinant human epidermal growth factor (Invitrogen), 10^{-9} M cholera toxin (ICN), $2x10^{-9}$ M 3,3',5-triiodo-L-thyronine (T3) (Sigma Aldrich), 100units/ml penicillin and 100 μg/ml streptomycin, 2mM L-glutamine and 0,1 gr/l $MgSO_4$. For calcium switch experiments, calcium concentration in the culture

media was raised to 1.8 mM. Keratinocytes were incubated at 37°C in a mixture of 5% CO_2 and 95% air.

Mice were sacrificed at different embryonic and adult ages, and dissected immediately. MMTV-PyMT mice were sacrificed at 4 months. Tissues were then fixed in 3.7% buffered formalin, processed and embedded in paraffin.

Molecular cloning

EGFP-Ena/VASP family members and Mena splice isoforms were subcloned into retroviral vector packaging murine stem cell virus-EGFP using standard techniques. Plasmids to express N-terminal His6-tagged murine EVH2 domain proteins were constructed from PCR fragments cloned into pQE-80L (Qiagen).

Retroviral packaging, infection and fluorescence-activated cell sorting

Retroviral packaging, infection, and fluorescence-activated cell sorting were performed as previously described (Bear et al, 2000). Briefly, retroviral plasmids were transiently transfected into 293 Phoenix cells together with pCL-Eco helper plasmid, and supernatant was collected after 48 h. MV^{D7} cells were exposed to infectious supernatant for 24 h in the presence of 8 mg/mL polybrene (Invitrogen) and cultured to 90% confluence, trypsinized, and fluorescence-activated cell sorting sorted in PBS/5% FCS. MV^{D7} cells expressing EGFP-Mena isoforms were FACS sorted to a level of expression similar to the endogenous expression of Mena in mouse embryonic fibroblasts. MTLn3 EGFP-Mena cells were FACS sorted to as described in Philippar et al, 2008.

Western blotting and immunoprecipitation

Cells were lysed in NP-40 buffer (1% NP-40, 150 mM NaCl, and 50 mM Tris, pH 8.0) containing protease inhibitors (Complete tablets; Roche) and phosphatase inhibitors (1 mM sodium vanadate, 50 mM sodium fluoride, 40mM beta-glicerophosphate, 15mM sodium pyrophosphate). Protein extracts were run on 8% SDS-PAGE gels, transferred on PVDF membranes (Millipore), blocked in 5% milk in TTBS for 1h at RT and probed with the following antibodies: mouse monoclonal anti Mena (stock 1μg/μl; 1:5000), rabbit polyclonal anti Mena11a (stock 1μg/μl; 1:5000), mouse anti E-cadherin (1:2000), mouse anti N-cadherin (1:2000), mouse anti vimentin (1:2000), mouse anti tubulin (1:10000) (all from BD biosciences), mouse anti a.v.GFP (1:10000; Clontech), rabbit anti GFP (1:5000; BD biosciences). Mouse and rabbit affinity purified normal IgG and HRP secondaries (1:5000) were from Jackson Immunoresearch. PVDF membranes were developed with ECL reagents (GE).

For immunoprecipitation experiments, MTLn3 cells stably overexpressing EGFP-Mena isoforms or EGFP were lysed in IP buffer (1% NP-40, 200 mM NaCl, and 50 mM Tris, pH 8.0, 10% v/v glycerol and 2mM EDTA) containing protease inhibitors (Complete tablets; Roche) and phosphatase inhibitors (1 mM sodium vanadate, 50 mM sodium fluoride, 40mM beta-glicerophosphate, 15mM sodium pyrophosphate). 2 mg of cell lysates were incubated with Protein A/G Sepharose beads (Pierce) with rotation at 4°C for 1h (preclearing). The precleared lysates were incubated o.n. with 2 μg of anti GFP, anti Mena11a or the normal IgG at 4°C on rotation. The immune complexes were immobilized on Protein A/G

Sepharose beads for 1h (rotation, 4°C), washed on ice cold IP buffer and boiled in SDS sample buffer.

Immunofluorescence microscopy

Cells were plated on glass coverslips, fixed in buffered 4% paraformaldehyde for 15 min at RT, permeabilized in 0.2% Triton X-100 in PBS, blocked in 10% BSA for 30 minutes and incubated with the following antibodies: mouse anti Mena (stock 1μg/μl; 1:1000), rabbit polyclonal anti Mena11a (stock 1μg/μl; 1:1000), mouse anti E-cadherin (1:1000), mouse anti Vinculin (1:400; BD biosciences), mouse anti p34ARC (10 μg/ml; Upstate) for 1h at 37°C, washed 3 times in PBS and incubated with fluorescently labeled secondary antibodies and Phalloidin or Hoechst (Alexa Fluor, Molecular probes), to stain F-actin or DNA, respectively. For tissues staining, 5 μm sections were deparaffinized in xylene, treated with a graded series of alcohol, rehydrated in PBS and microwaved for 15 minutes at 96°C for antigen retrieval in 10 mM citrate buffer, pH 6.0. Sections were preincubated with 10% normal donkey serum in 0.5% Tween-20 for 2h at RT, incubated with primary antibodies in 1% donkey serum and 0.5% Tween-20 buffer o.n at 4°C, washed 3 times in PBS and incubated in fluorescently labeled secondaries antibodies (Alexa Fluor, Molecular probes) for 2h at RT and Hoechst to label the DNA.

Cells were imaged using a Deltavision microscope (Applied Precision, Olympus IX71, 60x/1.4NA Plan Apon Nikon objective), deconvolved and processed using Softworx software (SGI, Montain View, CA). Levels were adjusted with Adobe Photoshop.

Live cell imaging

For live cell imaging experiments, cells were plated on glass bottom dishes (MatTek Corporation), which had been treated with 1M HCl for 5 min, followed by 70% ethanol and PBS wash. Cells were imaged with an ORCA-ER camera (Hammamatsu) attached to a Nikon TE2000 microscope with dual Sutter filter wheels, a spinning disk confocal head (Yokagawa), a mercury light source and a Coherent 70C two watt multi-line laser using 40x/0.95NA Plan Apo Nikon or 60x/1.4NA Plan Apo Nikon objectives. During time lapse, MTLn3 cells were kept at 37°C with aid of a Solent Incubator chamber (Solent Inc.) fitted for the microscope. All images were collected, measured and compiled with the aid of Metamorph imaging software (Molecular Devices) and Adobe Photoshop.

Membrane protrusion assays

MTLn3 cells were starved for 3-4 hr in L15 medium (Gibco) supplemented with 0.35% BSA. For stimulation, cells were treated with a bath application of EGF (Invitrogen) at 37°C. Time-lapse movies were recorded for 10 min with a 10 s interval after the addition of EGF. Area fold change was quantified by cell tracing, and cell area was measured using Methamorph software. Area measurements of each cell were standardized over the area of the corresponding cell at time = 0, averaged and plotted over time after EGF stimulation. For kymography experiments, phase-contrast time-lapse sequences movies were 10-15 min long with frames taken every 3 s. Kymographs were produced and

analyzed using Metamorph software. Kymographs were generated along 1-pixel-wide line regions oriented in the direction of individual protrusions. For quantitative analysis, straight lines were drawn on kymographs from the beginning to the end of individual protrusion events, neglecting fluctuations <0.5 μm (2 pixels) in magnitude. Slopes of these lines were used to calculate the velocities, and projections of these lines along the x axis (time) were used to calculate the persistence of protrusions.

Animal models

Xenograft tumors were derived from subcutaneous injection of 1×10^6 MTLn3-EGFP, MTLn3-EGFP-Mena, MenaINV, Mena11a and HMLER-splice reporter cells into the right abdominal mammary gland (4th fat pad) of 5-7 wk-old female SCID mice. MTLn3 experiments were performed following 3-4 weeks of tumor growth, while HMLER-splice reporter tumor were harvested when was palpable, around 8-10 weeks post injection.

***In vivo* invasion assay**

The *in vivo* invasion assay was performed as previously described (Wyckoff et al., 2000). In brief, six catheterized microneedles containing Matrigel and EGF (concentrations varying from 0.0 to 250 nM) were inserted into the primary tumor and held in place by micromanipulators. Following 4 hr of cell collection, the total number of tumor cells that migrated into each needle was quantified as previously described (Wyckoff et al., 2004). At least five mice were used per condition.

Recombinant Protein Expression and Purification

All EVH2 proteins were recombinant, His6-tagged and purified from *Escherichia coli*. EVH2 proteins were expressed in *E. coli* strain BL21 (DE3) CodonPlus and purified by chromatography on TALON resin (BD Biosciences) and Superdex 200 in MKEI-200 buffer (20 mM imidazole, pH 7.0, 200 mM KCl, 1 mM EGTA, 2 mM $MgCl_2$, and 1 mM DTT). EVH2 proteins were stored on ice and used within 2 weeks of purification. Recombinant murine CP ($\alpha1\beta2$) was a gift from Dorothy Schafer (University of Virginia). Actin was prepared from rabbit muscle as described (Spudich and Watt, 1971) and gel filtered on Superdex 200 equilibrated in 2 mM Tris/HCl, pH 8.0, 0.2 mM ATP, 0.1 mM DTT, and 0.2 mM $CaCl_2$. Pyrenyl-actin was prepared as described in Bryan and Coluccio, 1985. For TIRF experiments, gel-filtered rabbit skeletal muscle actin was labeled with Alexa-488 succinimidyl ester (Molecular Probes). All proteins except actin were quantified from absorbance at 280 nm using extinction coefficients predicted from the amino acid sequence (PROTEIN CALCULATOR v3.3; http://www.scripps.edu/~cdputnam/protcalc.html): His-EVH2-VASP 5690 M^{-1} cm^{-1}, His-EVH2-Mena 6970 M^{-1} cm^{-1}; His-EVH2-Mena11a 8250 M^{-1} cm^{-1} (considered a tetramer). Actin was quantified from absorbance at 290 nm and the extinction coefficient of 26.600 M^{-1} cm^{-1}.

Other Proteins

Spectrin F-actin seeds (SAS) were prepared from human erythrocytes as described in DiNubile et al., 1995. The concentration of SAS was determined from the initial rate of actin polymerization using *k*on for actin = 11.6 M^{-1} cm^{-1}, assuming no pointed end growth.

Actin pelletting assays

Dialyzed G-actin o/n against G-buffer (2 mM Tris Cl ph8, 0.2 mM DTT, 0.2 mM ATP, 0.2mM $MgCl_2$) and EVH2 Ena/VASP in MKEI-200 buffer were spinned at 250000 X g for 30 minutes before the assay. 4 μM G-actin were polymerized for 2h at RT in F-actin buffer (500 mM NaCl, 10 mM MgCl2, 10mM EGTA, 100mM Imidazole pH7). 0.5μM of BSA or Ena/VASP proteins in a final volume of 40 μl were incubated with 4 μM F-actin for 15 minutes at RT (actin binding) or 1h at RT (for actin bundling). Samples were spun for 20 minutes at 250000 X g (actin binding) or 15000 X g (actin bundling) at 4°C. Pellet from actin binding assays were washed once in F-actin buffer and resuspended in SDS sample buffer. Pellet from actin bundling assays were resuspended in SDS sample buffer. Pellet and supernatants were separate on SDS PAGE and the gel stained with Coomassie brilliant blue.

Actin polymerization assays

Seeded polymerization reactions contained 1 μM actin (5% pyrene-labeled), 0.2 nM SAS, 10 nM CP, Ena/VASP proteins, in 20 mM imidazole, pH 7.0, 100 mM KCl, 2 mM $MgCl_g$, 1mM EGTA, 0.2 mM ATP, and 0.1 mM DTT (MKEI-

100 buffer). SAS were omitted from reactions monitoring spontaneous actin polymerization. Fluorescence of pyrenyl-actin (excitation at 365 nm, emission at 386 nm) was monitored for 600 s at 25 °C. All components except actin and SAS were mixed in MKEI-100 buffer; reactions were initiated by the simultaneous addition of actin (primed with 1 mM EGTA and 0.1 mM $MgCl_2$ for 90 s) and SAS. The delay between mixing reactants and recording fluorescence was <16 s. Initial rates of actin assembly were determined from linear fits of data collected during the initial 60 seconds. In control experiments, Ena/VASP did not alter the fluorescence of either pyrenyl-G-actin or pyrenyl-F-actin.

Total Internal Reflection Fluorescence Microscopy

Glass coverslips were cleaned and assembled into sample chambers on glass slides as described in Kuhn and Pollard, 2005. Chambers were coated for 1 min with Ena/VASP, or control protein (Casein, 5mg/ml or BSA 1%) followed by two washes with 1% BSA-containing buffer and once with MKEI-100 buffer (20 mM imidazole, pH 7.0, 100 mM KCl, 1 mM EGTA, 2 mM $MgCl_2$). TIRF microscopy was performed using an Olympus X71 inverted microscope equipped for through-the-lens total internal reflection illumination by an Argon laser; a 60x, 1.45 NA objective lens in combination with a ×1.5 auxiliary lens was used. Image acquisition began 30-60 s after flowing the sample into the chamber. Images (0.5-s exposure) were collected 1 frame/3 s for 200 frames by a Cool-Snap ES CCD camera (Photometrics) controlled by Isee imaging software (Innovision).

Filament capture assay

Flow chambers were coated for 1 min with 50 nM Ena/VASP, followed by blocking twice with 1% BSA and washing once with MKEI-100. Actin filaments were assembled from 0.8 μM actin (10% Alexa 488-actin) in imaging buffer containing 0.24% methylcellulose for 2-3 min. An aliquot was flowed into the chamber, and data were collected at 1 frame/3 s for 200 frames. Interactions of all filaments in the field with the surface were scored for the number of barbed end (BE) captures, pointed end captures, side interactions, and number of filaments not captured.

Filament bundling assay

Flow chambers were coated for 1 min with 1% BSA and washed once with MKEI-100. Actin filaments were assembled from 0.8 μM actin (10% Alexa 488-actin) in imaging buffer containing 0.24% methylcellulose for 2 min together with 100nM Ena/VASP proteins. An aliquot was flowed into the chamber, and data were collected at 1 frame/3 s for 200 frames.

Spreading assay

Spreading assays were performed as described in Applewhite, et al. 2007, with modifications. MV^{D7} EGFP and EGFP-Mena isoforms derivates cells were trypsinized and replated on laminin (20 μg/ml) coated coverslips. Cells were allowed to spread for 30 min and then fixed with cold methanol for 15 min at -20°C. Coverslips were washed 2 times with PBS. Afterwards cells were permeabilized 3 min at RT with 0.2% Triton-X 100 in PBS, washed 2 times with PBS and incubated with mouse monoclonal fascin antibody (1:50; Dako) to stain

filopodia. Cells phenotype were analyzed and categorized in cell with filopodia o cells without filopodia.

Electron microscopy

Tissues were fixed with 2.5% glutaraldehyde and 2.5% formaldehyde in 0.1 M sodium cacodylate-HCl, pH 7.2, for 60–90 min at 4°C, postfixed with 2% osmium tetroxide for 60 min at 4°C, dehydrated in up to 70% graded alcohol, and stained with 0.2% uranyl acetate in 70% alcohol for 60 min at 4°C. The samples were then processed for epon embedding. Thin epon sections (400 nm) were cut with a diamond knife, poststained with uranyl acetate and Reynold's lead citrate, and viewed with an electron microscope (G2 Spirit BioTWIN; Tecnai) operated at 80 kV. Digital images were taken with a camera (2k CCD; Advanced Microscopy Techniques; provided by the Harvard Medical School Electron Microscopy Facility).

Statistical analysis

Statistical differences between two conditions were determined using t test. For multiple conditions, means were compared by analysis of variance. All data found to be significant ($P < 0.05$) by analysis of variance were compared with Tukey's honestly significant difference post hoc test to reveal statistically different groups.

Chapter 3 - Results

Mena11a characterization in cancer cell lines

Human Mena11a was identified by RT-PCR performed on cDNAs isolated from a human luminal breast cancer cell line expressing high levels of an mRNA identified by SEREX technique (serological analysis of recombinant cDNA expression libraries) and encoding the human Mena gene (Di Modugno et al., 2004). Later analyses have shown that Mena11a is a splicing isoform of Mena, containing an insertion of 63 base pairs (21 aminoacids). This insertion falls in between the F-actin and the tetramerization domain of the EVH2 domain of Mena (Figure 5). To gain insight into the distribution and function of Mena11a in cells and tissues, we developed a rabbit polyclonal antibody against the first 20 amino acid of the human 11a exon (RDSPRKNQIVFDNRSYDSLH) sequence, modified with a C-terminal cysteine, needed for the binding of the peptide to a Iodoacetyl-based resin for the subsequent affinity purification. As shown in Figure 6-A, the polyclonal antibody specifically recognizes Mena11a, as determined by Western blot analysis on lysates from Ena/VASP deficient cells (MV^{D7}) reconstituted with EGFP, EGFP-Mena or EGFP-Mena11a. In cells, Mena11a localizes to the sites of active actin remodeling. In facts, it is enriched to the cell-cell junctions of MCF7 cell, where it colocalizes with adherents junctions markers (E-cadherin) (Figure 6-B), and in the neo-forming junctions of mouse primary keratinocytes (Figure 6-C) after Ca^{++} switch in the culture media. It also colocalizes with vinculin, a focal adhesions marker (Figure 6-D). Moreover, Mena11a is recruited to the leading edge of lamellipodia in EGF-stimulated (60 seconds, 0.5 nM EGF) MTLn3 cells (Figure 6-E). The localization of Mena11a in the hot-spots of actin polymerization suggests a role for Mena11a in the Mena-dependent actin cytoskeleton dynamics.

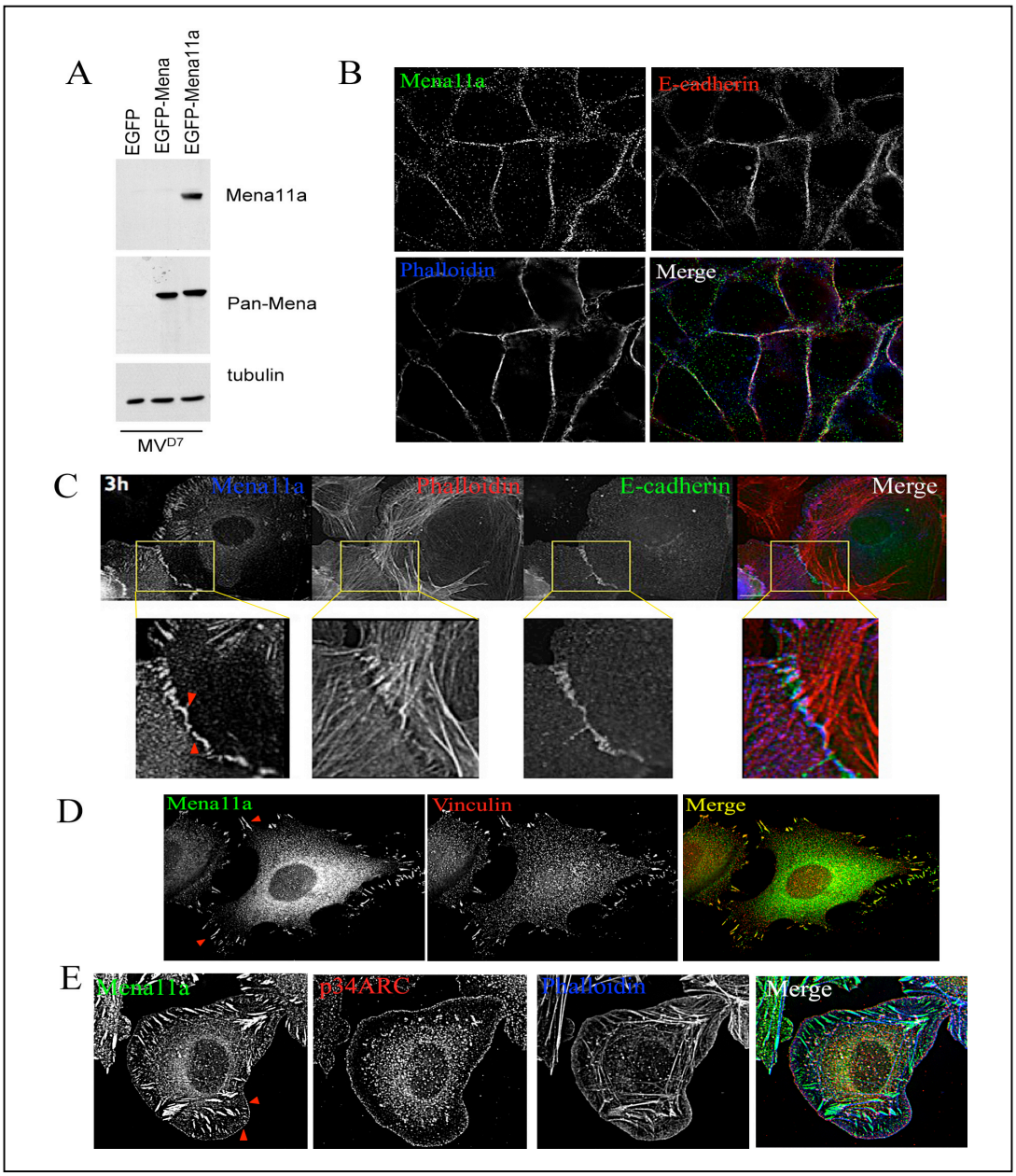

Figure 6. Mena11a distribution in epithelial cells. A) Mena11a antibody recognizes specifically Mena11a and not Mena in lysates from Ena/VASP deficient cells reconstituted with EGFP-tagged Mena isoforms. B) Mena11a localizes to the cell-cell junctions of MCF7 cells and neo-forming junctions of normal primary mouse keratinocytes, 3h after calcium switch in the culturing media (C). D) Mena11a colocalizes with vinculin to focal adhesions in MCF7 cells. E) Mena11a is recruited to the leading edge of MTLn3 cells during EGF treatment (60 seconds, 0.5 nM EGF). p34ARC is a subunit of the Arp 2/3 complex, used as leading edge marker. Color code as indicated in the Figure. Magnification 60x.

Mena11a is a marker of epithelia

To gain further insights into the fisiological role of Mena11a *in vivo*, we conducted immunofluorescence analysis on mouse tissues harvested from E10.5

(embryonic days post coitum), E13.5 and adult. We found striking differences in Mena11a and Pan-Mena localization. In the developing gut of E10.5 mouse embryos, Mena11a is exclusively expressed in the epithelium while Pan-Mena is also enriched in the surrounding mesenchyme (Figure 7-A). In the developing epidermis of E13.5 embryos (Figure 7-B) Mena11a is enriched in the keratinocytes while pan-Mena is also expressed in the underlying mesenchyme. In adult tissues Mena11a is expressed and localized to the basal layer of keratinocytes in the mouse skin (Figure 7-C) and in the bronchiole epithelium in the lungs (Figure 7-D). The broad expression of Mena11a in different epithelia strongly supports Mena11a as a marker of the epithelia.

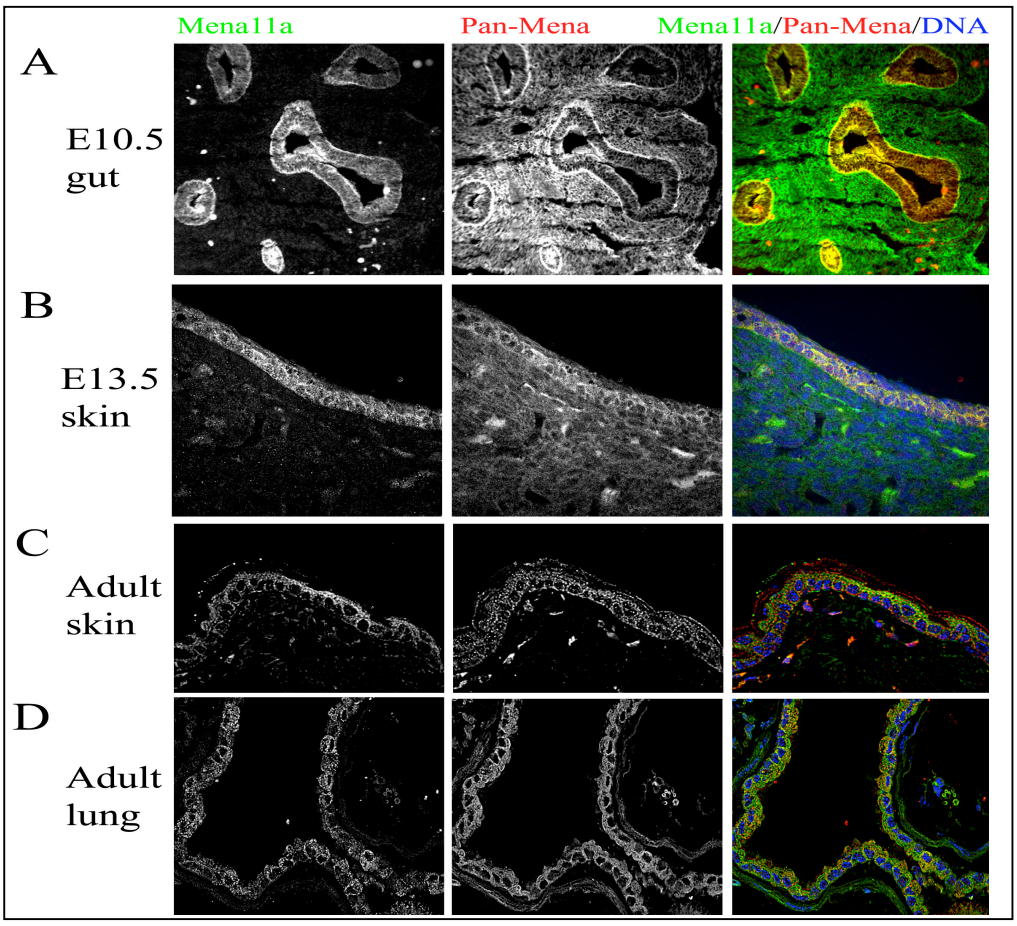

Figure. 7. Mena11a is enriched in epithelial tissues. A) Mena11a (green) is expressed and localizes in the developing gut of E10.5 mouse tissue while Pan-Mena (red) in also enriched in the surrounding mesenchyme. B) Mena11a is enriched in the developing epidermis and in the adult epidermis (C); D) Mena11a is abundant in the lung bronchiole epithelium of adult mice. Magnification 40x.

Mena11a is downregulated during the Epithelial to Mesenchymal Transition (EMT)

EMT is a process believed to be involved in the metastatization of epithelial cancers. We screened a large panel of cancer cell lines, epithelial (mammary and pancreatic cancers) and non epithelial (glioma and melanoma), for Mena11a expression together with epithelial (E-cadherin) or mesenchymal (N-cadherin and vimentin) markers. Mena11a is expressed in breast (Figure 8-A) and pancreatic (Figure 8-B) cancer cell lines with an epithelial phenotype (E-cadherin expression and "low invasive and metastatic potential" as referred in the literature) and is downregulated in the breast and pancreatic cells that concomitantly downregulate E-cadherin and upregulate N-cadherin and vimentin. Of note, non-epithelial cancers such as melanoma (Figure 8-C) and glioma (Figure 8-D), while expressing Mena, don't express Mena11a. In order to confirm that Mena11a is indeed downregulated during EMT we adopted an established EMT model of immortalized human mammary epithelial cells overexpressing the transcription factor Twist, that drives the transition from an epithelial-like to a mesenchymal-like phenotype (Yang et al., 2004). Mena11a is downregulated at the mRNA and protein levels in HMLE-pBP-TWIST, compared to the HMLE-pBP control cell line (Figure 8-E). To look at the kinetics of Mena11a downregulation, we used a modified HMLE EMT system. In this model, EMT is induced by treatment with 4-hydroxy tamoxifen (4-OHT, final concentration 20nM) of HMLE cells expressing a fusion protein Twist-ER. Following 4-OHT treatments, HMLE-Twist-ER cells develop a mesenchymal morphology similar to HMLE cells stably expressing Twist (not shown). HMLE-Twist-ER cells were treated with 4-OHT up to 17 days and total cell lysates were collected every 2 days. Upregulation of

N-cadherin is observed around day 7 with a progressive increase until day 17. E-cadherin protein level is drastically downregulated after day 11, showing undetectable levels at day 17, confirming the classical "cadherin switch". Of interest, while Pan-Mena protein level did not change, progressive downregulation of Mena11a is observed after day 11 until day 17, strongly suggesting a contribution for this Mena isoform in the regulation of the epithelial phenotype in mammary cells. DMSO treatment of the HMLE-Twist-ER cells doesn't affect protein expression levels of N-cadherin, E-cadherin and Mena isoforms (data not shown).

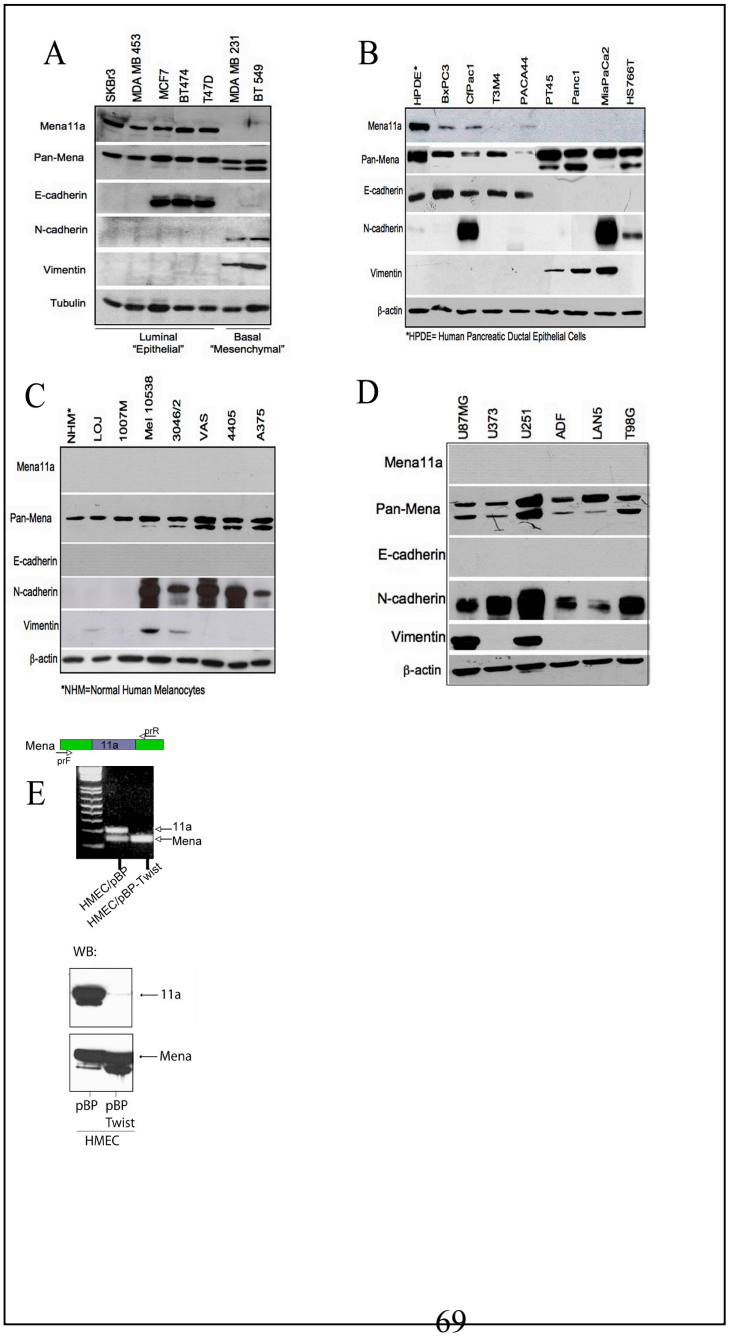

Figure 8. Mena11a is downregulated during EMT. Mena11a is downregulated in human breast cancer (A) and human pancreatic cancer cell lines (B) that express mesenchymal markers. Mena11a is not expressed in human melanoma (C) and glioma (D) cell lines. E) Mena11a is downregulated in HMLE-Twist cells, both at mRNA (upper) and protein (lower) level.

Mena11a is expressed in mammary cancer-derived metastases

In view of the finding that Mena11a is downregulated during the EMT process, we next asked whether Mena11a could be expressed in metastases from mammary cancers. We adopted the MMTV-PyMT mouse model to analyze Mena isoform expression in the primary tumor and in the lung metastases. MMTV-PyMT transgenic mice express the mouse polyomavirus middle-T antigen (PyMT) under the control of the mouse mammary tumor virus (MMTV) long terminal repeat. These transgenic animals uniformly develop multifocal mammary tumors with a high incidence of pulmonary metastases (Guy et al., 1992). Comparative studies have shown that the PyMT mouse model is an excellent model to understand the biology of mammary tumor progression, resembling in many aspects the human pathology (Lin et al., 2003).

Immunofluorescence analysis on paraffin-embedded primary tumors and lung metastases reveals a broad overlap in localization of Mena and Mena11a in the primary tumor (Figure 9-A), while the localization in the lung metastases was not completely overlapping. As shown in Figure 9-B, smaller is the metastasis less defined is the Mena11a localization to the cell-cell junctions of the metastatic cells. Mena11a localization to the cell-cell contacts is more pronounced in bigger metastases. Of note, Pan-Mena already localizes to the cell-cell junctions of the micrometastasis. It is tempting to speculate that Mena11a is down-regulated in the invasive cells that intravasate from the primary tumor to the systemic circulation and needs to be re-expressed gradually, once the metastatic cells extravasate from the capillary bead and infiltrate in the lung parenchyma. We are quantitatively correlating Mena11a and Mena localization to the cell junctions in metastasis of different sizes.

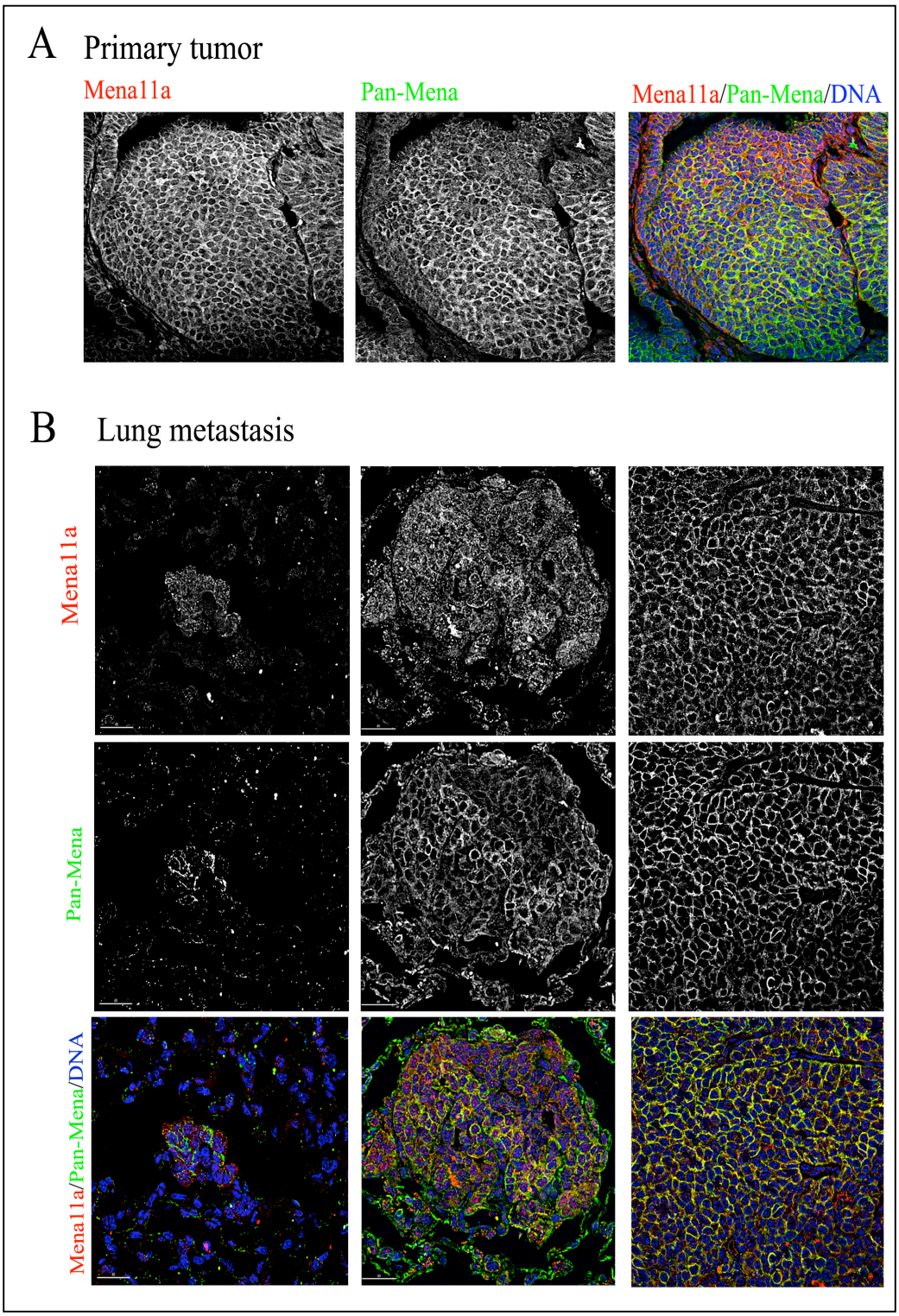

Figure 9. Mena11a expression in primary tumor and metastases of MMTV-PyMT mouse. A) Immunofluorescence analysis of mammary tumor and lung metastases (B) of MMTV-PyMT mouse. Note the difference in localization to the cell-cell junctions in the micrometastasis, between Pan-Mena (green) and Mena11a (red). Samples were harvested 4 months after birth. Magnification 40x.

Mena11a is downregulated specifically in invasive carcinoma cells

Previous data have shown that Mena isoforms are expressed differently in cells collected after an *in vivo* invasion assay performed in MMTV-PyMT mice (Goswami et al., 2009). In this assay, a micro needle filled with collagen and EGF is inserted in the mammary tumor of MMTV-PyMT mice. Invasive cells chemoactratted by a stable gradient of EGF are collected and plated on a coverslip for immunofluorescence analysis, using Pan-Mena, Mena11a, E-cadherin and vimentin antibodies. Invasive cells up-regulate Pan-Mena protein almost 3 fold ($P<0.0002$) compared to the average primary tumor cells (APTC), while downregulating Mena11a almost 3.75 folds ($P<0.005$). Interestingly, concomitant with the changes in Pan-Mena and Mena11a is the upregulation of the mesenchymal marker vimentin (almost 2 folds). No significant changes in E-cadherin levels were observed. Together these data suggest a temporally-defined expression of Mena11a during primary tumor formation, extravasation and metastatic dissemination and subsequent re-epithelialization during the colonization of secondary sites by metastatic cells. The latter process is often called Mesenchymal to Epithelial Transition (MET), but this is a phenomenon that is not yet fully investigated and understood.

Mena11a dampens the EGF-mediated cell protrusion in carcinoma cells

Recent data from Frank Gertler laboratory have shown a role for Mena in potentiating the EGF-mediated carcinoma cells protrusion, invasion and metastasis (Philippar et al., 2008). Mammary carcinoma cells respond to EGF treatment by the increasing actin polymerization that drives circumferential lamellipodia extension (Figure 10-A). This a pathway starts from EGFR and propagates through the release of cofilin from the cell membrane by hydrolysis of PIP2 mediated by PLC-γ. Activated cofilin severs actin mother filaments to produce free barbed ends leading to the elongation of newly polymerized actin filaments that are preferred for dendritic nucleation by the Arp 2/3 complex. We stably overexpressed EGFP, EGFP-Mena and EGFP-Mena11a in MTLn3 mammary carcinoma cells (Figure 10-B) and followed the EGF-mediated membrane protrusion of individual cells by time-lapse microscopy for 10 minutes, using sub-saturating concentrations of EGF (0.5 nM). A striking phenotype in the Mena11a-overexpressing cells was observed: while Mena overexpression induced a potent membrane protrusion with a flat lamellipodium, Mena11a overexpressing cells didn't spread as well being the protrusions similar to the ones observed in the EGFP control cells. Moreover, several unproductive protrusions were observed in the Mena11a overexpressing cells (Figure 10-C). The quantification of the cell area shows that Mena 11a dampens the EGF-mediated lamellipodia protrusion in MTLn3 cells (Figure 10-D). This observation was confirmed at different EGF concentrations, ranging from 1 to 0.06 nM (Figure 10-E).

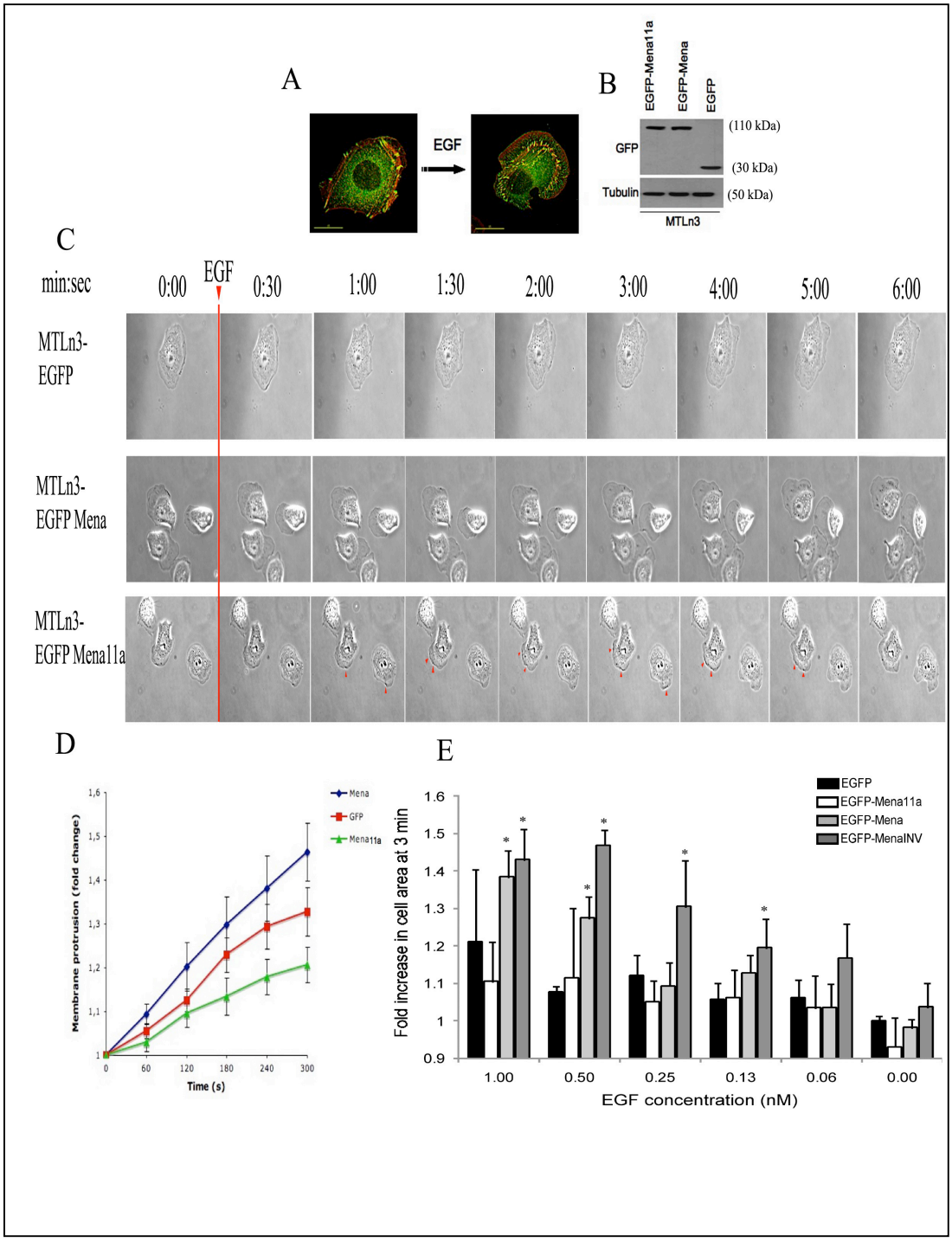

Figure 10. Mena11a dampens the EGF-mediated membrane protrusion in carcinoma cells. A) Effect of EGF stimulation (0.5 nM, 60 seconds) on MTLn3 cells (red, phalloidin,; green, EGFP-Mena). B) Levels of stable overexpression of EGFP-Mena11a, EGFP-Mena and EGFP in MTLn3 cells. C) Time lapse of MTLn3 cells, stimulated with 0.5 nM EGF. D) Time course quantification of the membrane protrusions. E) EGF dose-response curve quantification of the membrane protrusions at 3 minutes post stimulation. Asterisks indicate $p < 0.05$ versus EGFP-MTLn3 at each EGF concentration as determined by a Kruskal-Wallis non-parametric test, followed by post-processing with a Scheffe test. Data are shown as mean ± standard deviation and from three independent experiments. More that 120 cells were quantified per each experiments in panel D and E.

Mena11a-mediated lamellipodia extension doesn't results in productive protrusions

A detailed kinetic analysis of lamellipodia protrusions was performed by kymography. A kymograph is a montage created by extracting intensity values along a defined line region in each image of a time-lapse series and pasting them side-by-side to generate a composite image of object movement over time. In our analysis, we used a 1-pixel-wide line drawn in the direction of cell protrusion. The resulting kymographs reveal the dynamics of membrane activity at a single point along the cell perimeter. Analysis of such kymographs permits quantification of membrane extension rates and determination of the average time the membrane is engaged in individual protrusions. EGF treatment in control cells causes cycles of protrusion and withdrawal that generate a net extension of the membrane protrusion. Forced overexpression of Mena confers fewer cycles of membrane protrusion and withdrawal, and a potent membrane extension. Overexpression of Mena11a almost inhibits the effect of EGF treatment on the membrane protrusion in these carcinoma cells (Figure 11-A). Quantification of membrane velocity and persistency show a reduction in the mean velocity (8.7 um/sec vs. 4.7 um/sec in Mena and Mena11a, respectively; $P<0.001$) and mean persistency (7.6 sec vs. 4 sec in Mena and Mena11a, respectively; $P <0.01$) (Figure 11-B). Thus, Mena11a has a role in the regulation of the actin cytoskeleton dynamics during cell protrusions.

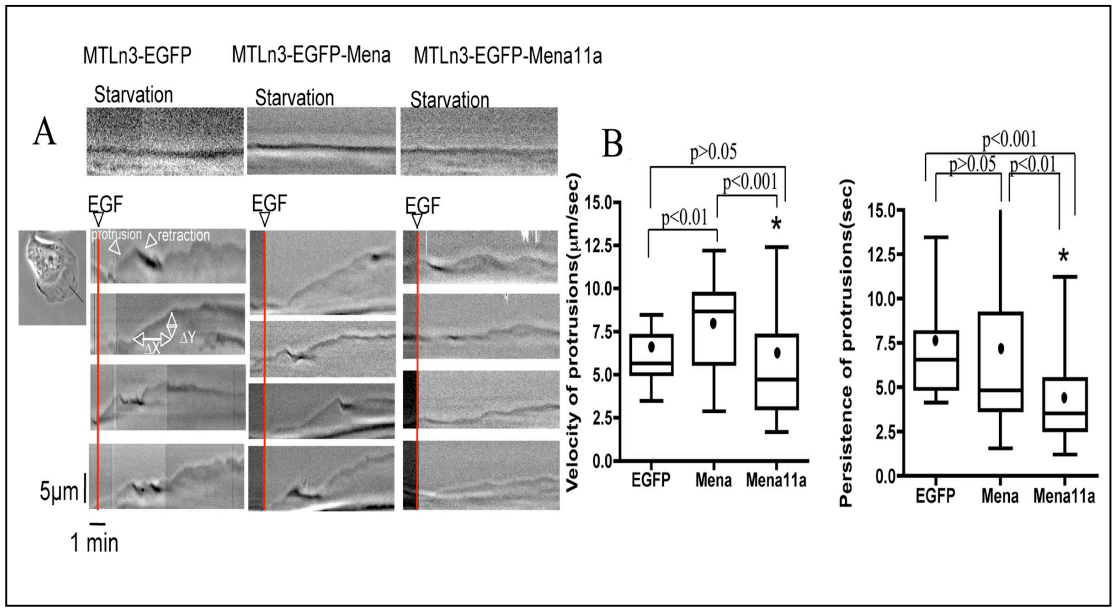

Figure 11. Kymography of EGF stimulated carcinoma cells. A)Representative kymographs of MTLn3 cells stably overexpressing EGFP, EGFP-Mena and EGFP-Mena11a. Kymographs show lamellipodia activity along the lines in phase contrast images. The red vertical line indicates the time when EGF (5 nM for 10 minutes) was added. B) Box and whisker plots for velocity (ΔY/ΔX) and persistance (ΔX) of individual events of protrusion for the different cell lines. Dot indicates mean, middle line of box indicates median, top box indicates 75th quartile, bottom box indicates 25th quartile, and whiskers indicate extent of 10th and 90th percentile, respectively. Data in panel B come from 103 events of protrusion in 80 cells per each cell line. ANOVA values, followed by post-processing with Tukey post test are indicated in the Figure.

Mena11a is in a complex with Mena

The fact that Mena11a overexpression impairs while Mena overexpression potentiates membrane protrusions can be due to a different compositions of the tetramers formed, acting on the actin cytoskeleton remodeling. In fact, endogenous Mena11a is found in complex with EGFP-Mena in MTLn3 EGFP-Mena cells. As shown in Figure 12-A, EGFP-Mena co-immunoprecipitates with Mena11a antibodies but not with rabbit control antibodies, Furthermore, endogenous Mena11a co-immunoprecipitatates with EGFP-Mena upon immunoprecipitation with EGFP antibodies. This interaction is between Mena and Mena11a and is not dependent upon binding of the EGFP tag with endogenous

Mena11a, since Mena11a is not immunoprecipitated by EGFP antibodies in protein lysates from MTLn3-EGFP cells (Figure 12-B).

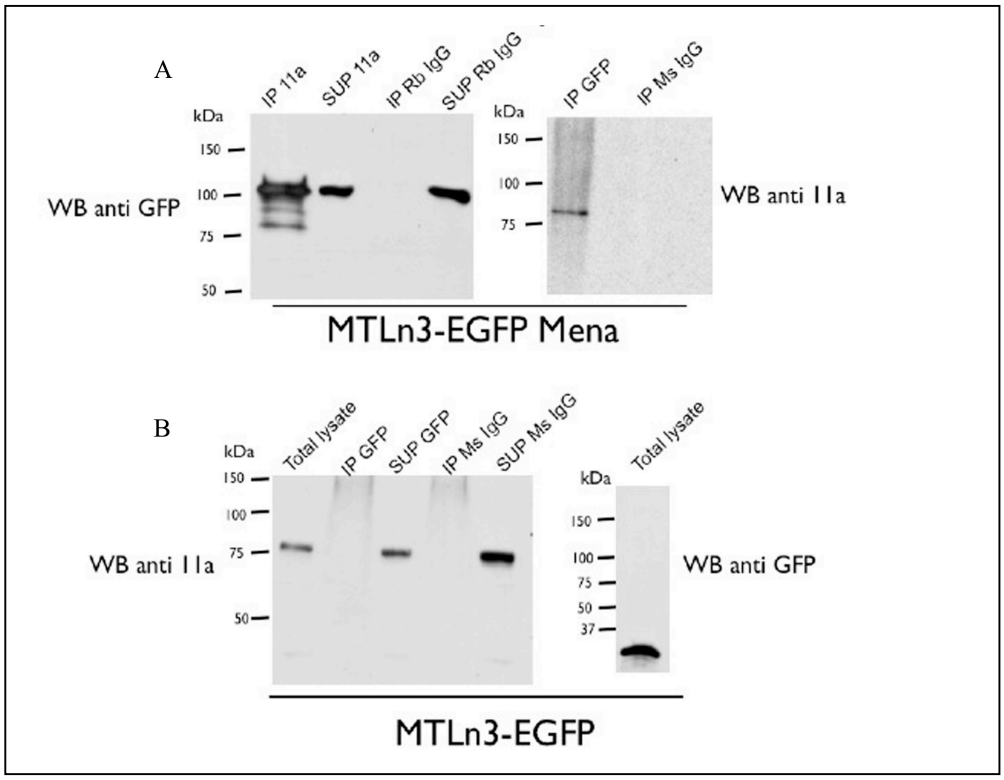

Figure 12. Endogenous Mena11a is in complex with EGFP-Mena. Cell lysates from either MTLn3 EGFP-Mena (A) or MTLn3 EGFP (B) were incubated with anti GFP, anti Mena11a and rabbit or mouse control antibodies and immunoprecipitated. Samples were then analyzed via SDS-PAGE and Western blotting with the antibodies indicated in the Figure.

Mena11a overexpression decreases carcinoma cells invasion *in vivo*

Cancer cell motility and invasion in response to chemotactic stimuli is the first step in the metastatic process. To mimic the *in vivo* invasion step, John Condeelis laboratory developed an *in vivo* invasion assay, in which cells with invasive potential within a tumor are chemoattracted by a gradient of EGF and collected in microneedles filled with EGF-collagen. In the *in vivo* invasion assay cells can only enter the needles by active migration since a block is used to prevent passive collection of cells and tissue during insertion of the needle into

the tissue. The block is removed and cell migration can be observed using multiphoton microscopy. Active migration has been demonstrated to be required for cell collection (Wang et al., 2004). MTLn3 cells stably overexpressing EGFP-control and different EGFP-tagged Mena isoforms were injected in the mammary fat pad of NOD/SCID mice. When the tumor reached 1.2-1.5 mm in diameter (around 4 weeks post-injection), the *in vivo* invasion assay was performed. The number of MTLn3-Mena11a cells collected in the needle at different concentration of EGF is statistically lower compared to Mena and MenaINV (a Mena Invasive isoform) overexpressing cells and, when concentrations of EGF higher than 1 nM were used, the difference was significant also compared to the EGFP control cells (Figure 13). Thus Mena11a can block the *in vivo* invasion of carcinoma cells. The analysis of metastases in these mice is still an on-going experiment.

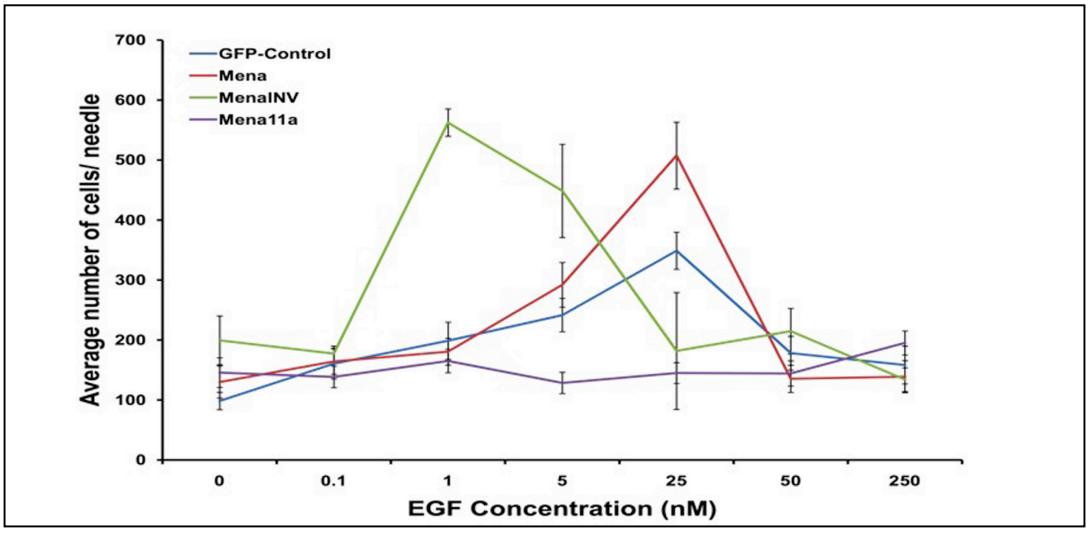

Figure 13. Mena11a overexpression decreases carcinoma cell invasion *in vivo*. *In vivo* invasion assay: EGF dose response curve of invasive cells collected from the MTLn3 cell tumors (indicated in the figure). Data normalized to average number of cells per needles containing 0.0 nM EGF for each type of xenograft. Errors bar indicates SEM. (Thank to E. Roussos, Condeelis lab).

The EVH2 domain of Mena11a has an F-actin binding and bundling activity

Ena/VASP are actin cytoskeleton regulatory proteins and several modes of actin remodeling have been shown. The EVH2 domain has been found to be the essential domain for actin remodeling and in cells, and EVH2 domain itself is able and sufficient to rescue all the different phenotypes of an Ena/VASP loss, suggesting an essential role of this domain for Ena/VASP function (Applewhite et al., 2007; Bachmann et al., 1999; Barzik et al., 2005; Bear et al., 2002; Loureiro et al., 2002). The site of insertion of the 11a exon in the EVH2 domain, between the F-actin binding site and the tetramerization domain, inspired us to perform experiments to investigate the involvement of Mena11a in the actin dynamics. First we cloned the full length of Mena, Mena11a and VASP in vectors containing a tandem of two C-terminal tags needed for the purification of the recombinant protein in affinity chromatography columns, a poly-histidine tag (HIS tag) and a strept-tag, a tag that can bind an engineered streptavidin. The functionality of these vectors were tested in filopodia-formation assays, showing the rescue of the loss of filopodia-spreading phenotype in MV^{D7} cells (not shown). Next we performed affinity purification chromatography with lysates of HEK-293 cells transfected with VASP-His, Mena-His and Mena11a-His vectors. We were able to purify the full-length of VASP, Mena and Mena11a from these cells but unfortunately not in sufficient amounts needed to perform biochemistry experiments (not shown). Therefore, we cloned the EVH2 of VASP, Mena and Mena11a in plasmids to express N-terminal his-tagged proteins in *E. Coli* and we purified actin from rabbit muscles. The late-shoulder of actin and recombinant proteins were collected by gel filtration chromatography on a SD-200 column. The quality of the purified actin was tested in F-actin polymerization assays (not

shown). Next we tested the recombinant proteins in actin pelletting assays, testing the ability of the recombinant proteins to bind (high speed centrifugation) F-actin and to bundle (low speed centrifugation) F-actin, as described in the materials and methods. The EVH2 domain of Mena11a binds (upper panel) and bundles (lower panel) F-actin in solution (Figure 14-A). Moreover, the bundling formation of Mena and Mena11a has been observed directly by Total Interference Reflection Fluorescence (TIRF) microscopy experiments, where 10% of the total actin was labeled with Alexa 488 (Figure 14-B). As negative control, bovine serum albumin was used and infact no effects on actin were observed, confirming that the pelletting of the Ena/VASP recombinant protein is not an aspecific binding to actin. Thus, the 11a insertion doesn't seem to affect the actin binding and bundling activity of Mena11a.

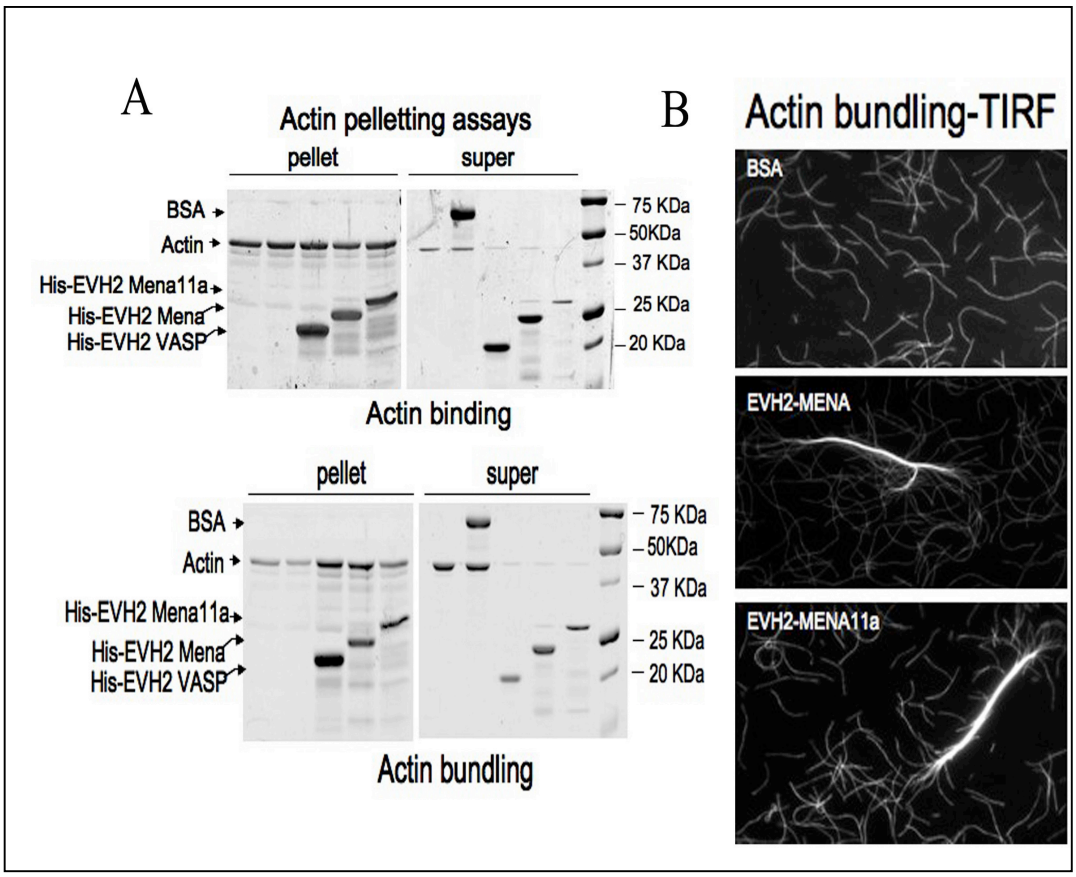

Figure 14. Mena11a has binding and bundling activity. A) Actin pelletting assays: BSA and the EVH2 domain of Mena11a, Mena and VASP were incubated with F-actin filament and subjected to high speed (binding assays, upper panel) or low speed (bundling assays) centrifugation. Pellets and supernatants are loaded on an SDS-PAGE and visualized by Coomassie brilliant blue staining. B) BSA and EVH2 domain of Mena11a, Mena and VASP were incubated with F-actin (10% Alexa488 labeled) and analyzed by TIRF microscopy. Magnification 60X.

EVH2-Mena11a has an anti capping activity as potent as EVH2-Mena in pyrene actin assays

The most accepted function of Ena/VASP is the so called "anti capping" activity, which allows actin-filaments elongation, even in presence of high levels of capping proteins (Barzik et al., 2005; Bear et al., 2002). *In vitro*, the anti capping activity of Ena/VASP has been tested using purified proteins and actin labeled with pyrene, a polycyclic aromatic hydrocarbon that increases its fluorescence once incorporated in actin filaments. We purified Spectrin-Actin Seeds (SAS) from human eritrocytes, which are needed to "prime" the initial polymerization. The anti capping activity of Mena11a was tested by this assay. As shown in Figure 15-A the EVH2 domain of Mena11a, similar to Mena, protects actin filaments barbed ends from capping in a dose-dependent manner (in a fisiological nanomolar range of Ena/VASP). In control assays, the elongation of actin filaments (no capping proteins added) was negligible (Figure 15-B). Moreover, the spontaneous nucleation of actin by Mena and Mena11a was also negligible under the conditions used in the assay (not shown). These data needs further confirmation addressing the question of the anti capping activity of Mena11a by TIRF microscopy. Indeed, one drawback of these otherwise highly effective pyrene-actin assays is the difficulty to discriminate between an increased nucleation and elongation rate of filaments during polymerization. In other words, many nucleating filaments that elongate slowly may give the same fluorescence signal as a few rapidly elongating filaments.

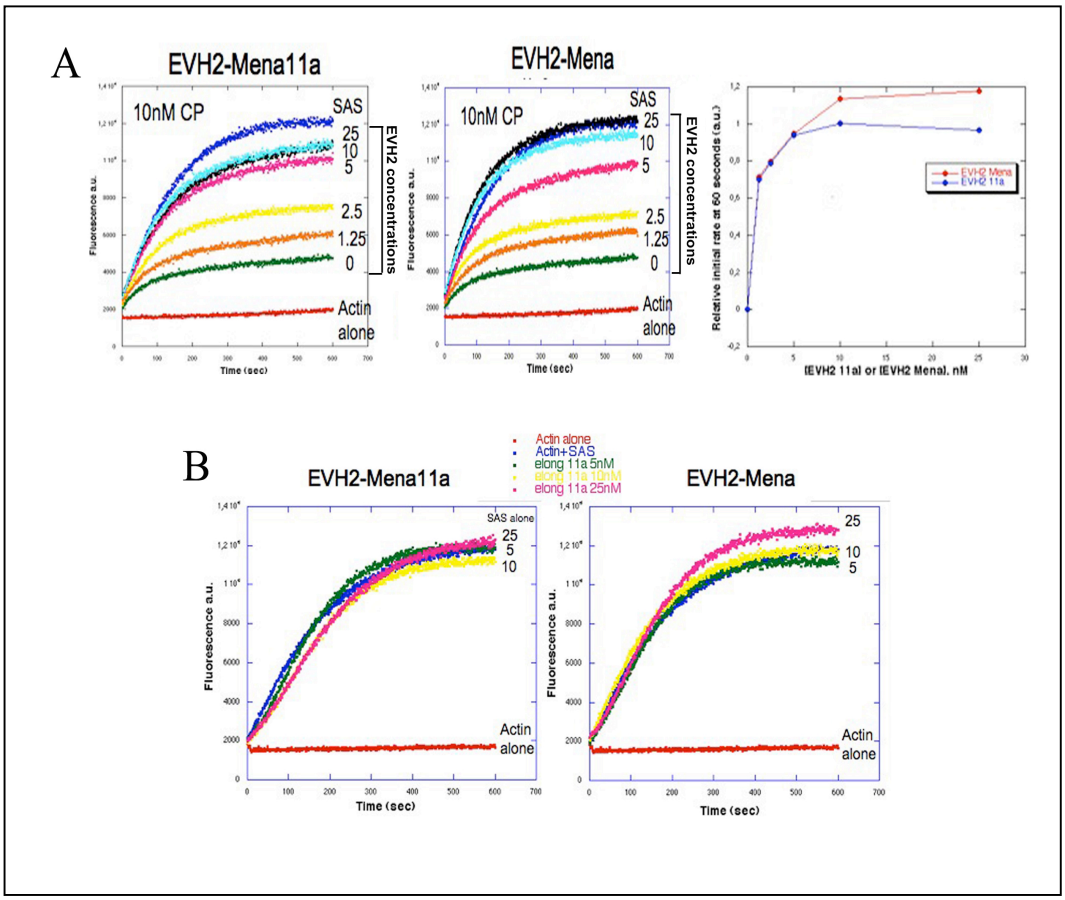

Figure 15. EVH2-Mena11a inhibits barbed end capping by capping proteins. A) EVH2 domain of Mena 11a (upper left) and Mena (upper center) increase the rate of actin polymerization in the presence of capping proteins (CP) in a dose dependent manner. Plotted is the fluorescence of pyrenyl-actin versus time in the reactions containing 1μM actin (5% pyrene labeled), 0.2 nM Spectrin Actin Seeds (SAS) (blue line), 10 nM CP and various amounts of EVH2-Mena and EVH2-Mena11a. Initial rates (upper right) were calculated from a linear fit to the first 60 seconds of each time course and normalized to the initial rate in the reaction containing SAS alone. B) EVH2 domain of Mena 11a (bottom left) and Mena (bottom right) don't increase the rate of actin polymerization. Plotted is the fluorescence of pyrenyl-actin versus time in the reactions containing 1μM actin (5% pyrene labeled), 0.2 nM Spectrin Actin Seeds (SAS), and various amounts of EVH2-Mena and EVH2-Mena11a (no CP is added in these assays).

Mena11a has an impaired barbed ends capture activity

We examined how the EVH2 domains of Mena and Mena11a influence the capture of the barbed ends of growing actin filaments by TIRF microscopy. Figure 16-A shows the schematic of the assay. We coated coverslips with 50 nM of the EVH2 of Mena or Mena11a, using as positive control coverslips coated with the same concentration of EVH2-VASP and as negative control 5 mg/ml of casein. Alexa488-actin (10% labeled) was primed for 1 minute and then flowed in the imaging chamber. Filaments initially diffused freely within the evanescent field. Gradually, filaments stopped diffusing freely and became tethered at the surface via attachment by their barbed ends (Figure 16-B). Once captured, end-attached filaments paused briefly before resuming their grow within 12 seconds. Captured filaments remained bound to the surface via an interaction along the side of the filament at the initial side where the barbed end capture had occurred. For VASP and Mena, the captured filaments was frequently captured again at the other sites on the surface as the filament continued to elongate, while Mena11a and casein didn't bind the barbed end that efficiently (Figure 16-C). On average, filaments experienced 1.43±0.30 BE capture/filament for VASP-coated coverslips; 1.78±0.34 BE capture/filament for Mena; 0.95±0.39 BE capture/filament for Mena11a and 0.58±0.46 for casein-coated coverslips. Of importance, as reported in table1, the percentage of non-attached filament was 10.3 fold less in Mena11a coated-coverslips compared to the Mena-coated ones. Moreover, the interaction of the actin filaments with the coated surfaces was prevalently through the barbed end and not through the pointed end or a side capture (Table1).

Collectively these data suggest a precise function for the 11a insertion in the EVH2 domain in the regulation of the initial capture of the barbed end in growing actin filaments and ultimately in the dynamics of actin polymerization mediated by Ena/VASP.

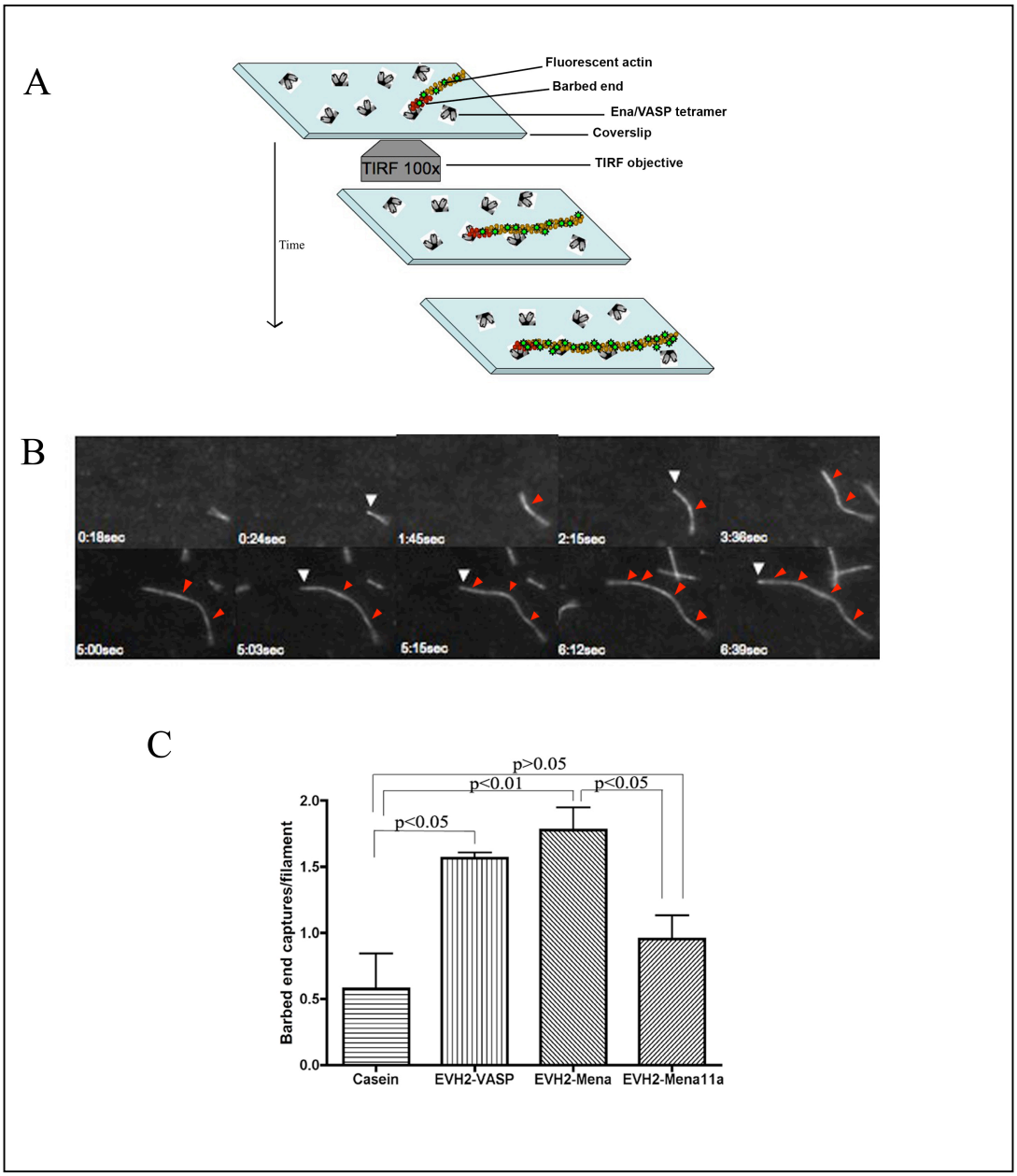

Figure 16. EVH2-Mena11a doesn't capture actin filament barbed ends. A) Schematic of the barbed end capture assay. B) Time lapse series showing capture of filaments by a EVH2-Mena coated surface using TIRF microscopy. White arrowheads mark the initial barbed end capture event, red arrowheads mark the old captured ends, now bounded by the side of the EVH2 molecule. B) Number of barbed end captures per filament efficiency by 5mg/ml casein or 50 nM EVH2-Mena11a, Mena or VASP. Error bars indicate standard deviation. ANOVA values, followed by post-processing with Tukey post-test are indicated in the Figure. The number of filaments scored and the different events are indicated in Table 1.

Table 1. Interactions of actin filaments with casein, EVH2-VASP, Mena and Mena11a-coated surfaces.

BE, barbed end; PE, pointed end. Data compiled from 3 independent experiments.

Surface coating	Total filaments	BE capture/filament	Side capture/filament	PE capture/filament	% non attached
Casein 5mg/ml	128	0.58±0.46	0.12±0.05	0.05±0.02	34
EVH2-VASP 50nM	124	1.43±0.30	0.22±0.06	0.10±0.01	5.9
EVH2-Mena 50nM	193	1.78±0.34	0.16±0.03	0.08±0.07	2.1
EVH2-11a 50nM	228	0.95±0.39	0.19±0.04	0.05±0.03	21.7

Mena11a expressing cells have an impaired filopodia formation

Ena/VASP exerts an important role for filopodia formation both in cultured cells and *in vivo* (Applewhite et al., 2007; Dent et al., 2007; Kwiatkowski et al., 2007; Lebrand et al., 2004). To study protrusion and filopodia formation, we used cell spreading as model system. Spreading cells are particularly protrusive and have many characteristics in common with migrating cells. We used Ena/VASP deficient cells to generate cells stably expressing EGFP, EGFP-Mena or EGFP-Mena11a. Ena/VASP deficient cells (MV^{D7}) spread on laminin-coated coverslips with three different modes: smooth-edged, filopodial and ruffling (Figure 17-A). We focused our attention to the percentage of cells that spread with a filopodia phenotype, and scored the filopodia-making cells using a specific marker for genuine filopodia (fascin). As reported by others (Applewhite et al., 2007), Mena expression in MV^{D7} rescues the loss of filopodia spreading-mode phenotype of the null cells. Infact, the population of cells with filopodia raises from 12% to 38%, when Mena is expressed ($P<0.001$ between EGFP and EGFP-Mena cells). Interestingly, the percentage of Mena11a-expressing cells making filopodia was

statistically lower (P<0.01 between Mena and Mena11a expressing cells), dropping from 38% to 20% (Figure 17-B).

This observation is important since filopodia initiation and formation needs both barbed ends capture and anti capping activity of Ena/VASP (Svitkina et al., 2003). Therefore the lack of barbed end capture activity can influence the overall activity of tetramers of Ena/VASP containing Mena11a.

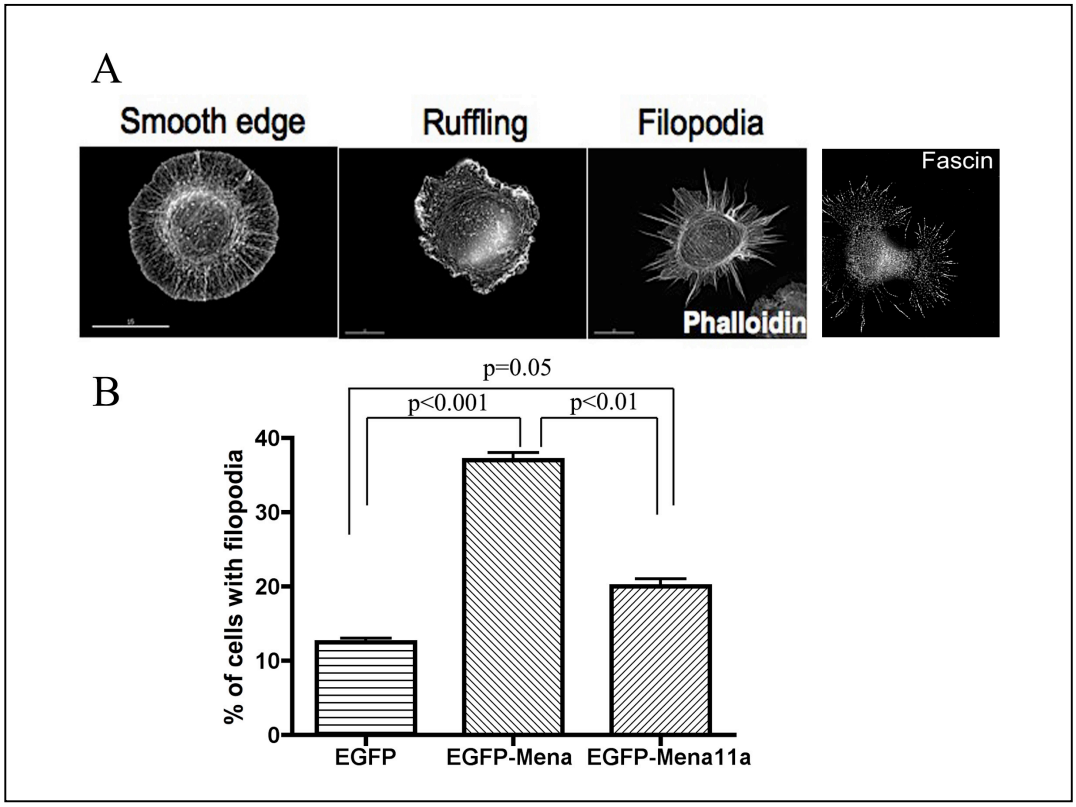

Figure 17. Mena11a expressing cells have an impaired filopodia formation. A) Three characteristic spreading phenotypes of Ena/VASP deficient mouse embryonic fibroblasts, 20 minutes after spreading on laminin coated coverslips (20 μg/ml). Cells are fixed and stained with phalloidin or fascin antibodies. B) Quantification of the percentage of cells spreading with filopodia, per each MV^{D7} cell line. ANOVA values, followed by post-processing with Tukey post-test, are indicated in the Figure. 390 cells per each cell line, over 3 independent experiments, were analyzed.

Chapter 4 - Discussion

This PhD work is aimed to understand the role of Mena11a, an alternatively spliced isoform of Mena, in cancer cell motility and epithelial morphogenesis. Mena is a member of the Ena/VASP family of actin cytoskeleton regulatory proteins, and is involved in several actin-based processes that are often deregulated in cancer and lead to metastatic disease.

Mena11a is a marker of the epithelial phenotype and is downregulated during EMT

Mena is upregulated in human breast cancer patients and in invasive rodents cells *in vivo* (Di Modugno et al., 2006; Wang et al., 2004; Yang et al., 2004). Moreover, Mena gene has been found to be alternatively spliced and recent observations are shedding the light on the role of these alternatively spliced isoforms. Alternative splicing of genes has been analyzed in great detail in the past years, but the specific function of these alternative transcripts is still a black box for most of the genes. By a deep sequencing of cDNA fragments from 15 human tissues and breast cancer cell lines, Chris Burge laboratory has found that 92-94% of human genes undergo alternative splicing (Wang et al., 2008), meaning that splicing events are a nearly universal mechanism of gene regulation. Several isoforms has been identified for Mena (Di Modugno et al., 2007; Gertler et al., 1996) (Figure 5), some of them like Mena+, seem to be a nervous system-specific isoforms even if may be also enriched in invasive and metastatic cancer cells (F. Gertler, personal communication). Another interesting isoform of Mena (MenaINV) has been described to be specifically upregulated in invasive cancer cells (Goswami et al., 2009) (Philippar et al., 2008). MenaINV overexpression enhances the metastatic potential of mammary carcinoma cells, and enhances the

invasion in 3D collagen matrices. Moreover MenaINV sensitizes carcinoma cells to EGF, enabling cellular responses, such as lamellipodia protrusion and invasion. Much lower EGF concentrations are required for there effects in MenaINV cells as compared to the parental cell line. The INV insertion (initially refered as +++) is right after the EVH1 domain, and is a small 13 aminoacids sequence. The molecular mechanisms of the EGF-mediated potentiation of cell protrusion and invasion by MenaINV are still unknown. It is curious that in the original paper from Frank Gertler (Gertler et al., 1996), the +++ exon was always found together with the + exon and never alone. Further studies on the role of the +++/+ isoform are ongoing in the Gertler laboratory and this isoform could be the real INV isoform identified by the Condeelis lab in invasive cells. Conversely, our major contribution in the understanding of the role of Mena11a is that this isoform maintains a "low invasive" phenotype in cancer cells. We identified Mena11a from an epithelial-like breast cancer cell line and further characterized this Mena isoform (Di Modugno et al., 2007). Mena11a overexpression in breast cancer cell lines conferred an increased proliferation rate and induced MAPK activation, suggesting a role for this isoform in the proliferation of mammary cancer cells. However, the functional mechanism of this increase in proliferation by Mena11a, and whether this could be a new function of Ena/VASP proteins in cancer, is still under investigation. Of major interest for pancreatic cancer, we identified Mena11a as a marker of sensitivity to EGFR inhibition by tyrosine kinase inhibitors (Pino et al., 2008). We also found that Mena11a expression correlates with the epithelial phenotype of breast and ductal pancreatic adenocarcinoma cells, while it is downregulated in cell lines that express mesenchymal markers, like vimentin and N-cadherin. Therefore, since Mena11a appears as a new marker for the Epithelial to Mesenchymal Transition status of cancer cells, we

investigated more in details the contribution of Mena11a in the EMT proces. We adopted an EMT model developed by Robert Weinberg's group, in which the transcription factor Twist drives the upregulation of mesenchymal genes that are important to confer metastatic behavior of mammary cells (Yang et al., 2004). Of interest, Mena is in the top 10 genes upregulated in the metastatic cells compared to the non-metastatic one. In the immortalized human mammary epithelial cells overexpressing Twist, Mena11a is downregulated together with E-cadherin, while at the same time N-cadherin and vimentin are upregulated. Hence, the downregulation of Mena11a and E-cadherin are both involved in the acquisition of a more spindle-like morphology and a more invasive and metastatic behavior. We think that Mena11a is necessary in order to keep an epithelial phenotype in normal and epithelial cancer cells, probably acting on the regulation of the Ena/VASP-dependent actin cytoskeleton dynamics. Infact, Mena11a is highly expressed in normal mouse epithelial tissue during the development and through the adult life (Figure 7). For example, Mena11a decors the layer of keratinocytes in the developing skin, while pan-Mena is expressed all over the skin epithelium and the underlying mesenchyme, suggesting an important role for this Mena isoform in the normal development of epithelia.

Mena expression was found to be progressively upregulated, from benign lesions to metastatic tumors, in breast cancer patients. A significant direct correlation with tumor size, proliferation index, and HER-2 overexpression and an inverse relationship with estrogen and progesterone receptors has been found in invasive carcinomas (Di Modugno et al., 2006). This study was conducted using an antibody recognizing all Mena isoforms, so the question regarding the dynamic expression of different Mena isoforms and the relative contribution of each isoform during cancer progression is still unresolved and will need further studies.

We wondered if Mena11a is also overexpressed in the primary tumor of transgenic mouse model for mammary cancer. We adopted the MMTV-PyMMT transgenic mice model, that express the mouse polyomavirus middle-T antigen (PyMT) under the control of the mouse mammary tumor virus (MMTV) long terminal repeat. These transgenic animals uniformly develop multifocal mammary tumors with a high incidence of pulmonary metastasis (Guy et al., 1992), histologically recapitulating the key steps of the human mammary disease, from adenoma to carcinoma and metastasis (Lin et al., 2003). In needs to be highlighted here that the initial steps of carcinogenesis may be different between the human tumors and this mouse model, and the PyMT is not expressed in human breast tumor cells. However PyMT acts as a potent oncogene activating several signal transduction pathways, including those of the Src family and the Ras and PI3 kinase pathways, which are also altered in human breast cancers, making this model suitable for our study. In addition, in PyMT mice mammary glands the expression of PyMT is found to be associated with an increased c-myc level and this gene is located in one of the three chromosomal regions amplified in human primary breast cancers. Remarkably, in the PyMT model the loss of estrogen and progesterone receptors (ERs and PgRs), and overexpression of ErbB2/Neu and cyclin D1 are observed, similarities to what is observed in human breast cancer with poor prognosis. Immunofluorescence analysis shows that Mena11a is highly expressed in the primary tumor and colocalizes with Pan-Mena (Figure 10). Conversely, Pan-Mena is expressed also in the tumor stroma rich in fibroblasts, myoepithelial cells and endothelial cells, confirming one more time that Mena11a expression is restricted to the epithelial tumor and not to the stroma. Since Mena11a is highly expressed in the primary tumor and is downregulated in cancer cell lines that underwent EMT, we asked next if Mena11a was also expressed in

the mammary cancer lung metastases in the same mouse model. Interestingly, we found a more defined Mena11a expression at the cell-cell junctions of the macrometastases compared to the little micrometastases, while Pan-Mena expression remained unchanged (Figure 10). It is tempting to speculate that little metastases are formed by "newly arrived" cancer cells colonizers of the lung parenchyma, while bigger metastasis are formed by "older" colonizers. Thus, we can imagine that Mena11a, being downregulated in order to allow the migration and invasion of cancer cells from the primary tumor to the metastatic sites (EMT), gets upregulated once the metastatic cells need to reform an epithelium in the host tissue (MET). A further consideration needs to be done here: even if the mouse model system that we used is a transgenic model of overexpression of an oncogene, and several multifocal tumors arise in the different mammary fat pads, no heterogeneity among cells in terms of up or down regulation of the signaling pathways necessary for the primary tumor formation has been shown and confounding variations across individual cancer cells and individual mice are minimal in MMTV-PyMT mouse model (Herschkowitz et al., 2007). The finding that Mena11a is expressed in metastases is in contrast with previously published data regarding Mena isoforms mRNA in the primary tumor, invasive cells and metastasis in the MMTV-PyMT mouse model (Goswami et al., 2009). The authors could not identify any Mena11a transcript in the lung metastases and they suggest that Mena11a is downregulated in the metastases. However, the lung samples for the mRNA extraction was collected not capturing or isolating the metastatic nodules but shedding the lung tissues with a needle and filtering twice through nylon filters to obtain single cells. At the contrary, we careful microdissected the metastases from the lung parenchyma and we were able to detect Mena11a expression by RT-PCR. Data suupporting the hypothesis of a

temporally defined Mena11a expression during primary tumor formation, invasion and metastasis come from the *in vivo* invasion experiment, performed on the MMTV-PyMT tumors. It was shown already by Goswami and colleagues that invasive cells chemoactratted by EGF-filled microneedles downregulate Mena11a and upregulate MenaINV isoforms at the mRNA level. We confirm these findings in this thesis also at the protein level (Figure 11). Infact we find a 3 fold upregulation of Pan-Mena and a 3.75 fold downregulation of Mena11a in the invasive cells compared to the primary tumor cells. Interestingly, we also found that the downregulation of Mena11a is associated with the upregulation of vimentin, a marker of EMT, confirming that invasive cells gain mesenchymal features compared to non-invasive cells. About the splicing regulations of Mena isoforms, recently Russ Carstens laboratory identified two splice factor proteins ESRP1 and ESRP2 as regulators of the epithelial splicing. Among several other genes analyzed the splicing of Mena11a seems to be regulated by these two splicing factors (Warzecha et al., 2009a; Warzecha et al., 2009b). Interestingly, any other exon of Mena doesn't seem to be regulated by ESRPs. Two other investigators have found splicing factors that may regulate Mena11a splicing. Kalsotra and colleagues have found that during mouse and chicken heart development, the exon11a is gradually included from E14 to adult and the splicing may be regulated by CUGBP and ETR-3-like factors (CELF), muscleblind-like (MBNL) and Fox proteins, even if the direct splicing of 11a inclusion has not been shown (Kalsotra et al., 2008). Yeo and colleagues have identified Fox2 as splicing factor in human embryonic stem cells (hESC) that, if depleted, resulted in the exon 11a skipping. Interestingly, at mRNA level, about 80% of total Mena transcript in hESC is Mena11a (Yeo et al., 2009). To gain insight into the splicing regulation of Mena11a and to monitor the splicing event

in vivo, we engineered a bichromatic splice reporter for Mena11a. If 11a is inserted the cells will be red and green, if 11a is excluded the cells will be only green. Intravital microscopy experiments on xenografted splice reporter mammary cancer cells will allow us to follow the splicing of the intravasating cells and we can predict a lack of "11a splicing in" in the these cells.

Mena11a affects the actin cytoskeleton dynamics

Ena/VASP regulates the dynamics of the actin cytoskeleton acting in proximity of the barbed end, the growing end of the actin filament. Although there is considerable evidence that Ena/VASP proteins act as actin anti capping proteins, some controversy remains over their mechanism of action. The general idea of anti capping by Ena/VASP proteins is that the proteins permit actin-filament elongation, even in the presence of high levels of capping proteins. This activity is necessary to allow the formation of the long filaments within cells that contribute to structures such as filopodia. Ena/VASP supports filopodium formation by antagonizing actin filament capping activity (Barzik et al., 2005; Bear et al., 2002) and by promoting clustering of filaments at their polymerizing ends (Applewhite et al., 2007). However, there is considerable controversy in this field, some of which arises from confusion over the definition of anti capping activity. The anti capping hypothesis of Ena/VASP function specifically states that Ena/VASP proteins associate with elongating actin filaments at or near their rapidly growing (barbed) end in such a way as to block the action of capping proteins that terminate elongation. It is important to note that this hypothesis does not state that Ena/VASP proteins can remove capping proteins that have become stably associated with filaments (uncapping) nor does it state that Ena/VASP

proteins have any effect on the depolymerization of actin filaments from their barbed end (weak capping) nor that Ena/VASP associates processively with the growing actin filaments. One final point about this hypothesis is that anti capping is not mutually exclusive with other established Ena/VASP functions such as filament clustering, bundling or anti-branching. Several types of evidence support an anti capping function for Ena/VASP, including *in vitro* assays with purified proteins, structural analysis, cell biological experiments and genetics. Ena/VASP anti capping activity has been observed indirectly in pyrene actin polymerization assays (Barzik et al., 2005; Bear et al., 2002) and directly in total internal reflection fluorescence microscopy (TIRF) assays (Pasic et al., 2008).

Mena was found overexpressed in invasive cells chemoactratted by EGF in *in vivo* invasion assays (Wang et al., 2004). Forced overexpression of Mena, and in particular MenaINV, increases the capacity of cancer cells to migrate in response to chemotactic stimuli, invade the surrounding stroma, enter blood and lymphatic vessels and metastasize, all actin-dependent properties (Philippar et al., 2008). We asked whether Mena11a could influence the actin cytoskeleton dynamics in carcinoma cells. We overexpressed Mena11a in MTLn3, a mammary carcinoma cell line that responds to EGF stimulation protruding with a lamellipodia (Chan et al., 1998). This response is mediated by the cofilin pathway that leads to the formation of free barbed ends and dendritic network nucleation by the Arp2/3 complex. Interestingly, Mena11a damped the EGF-mediated lamellipodia protrusion in these cells, while same levels of overexpression of Mena significantly potentiated the lamellipodia protrusion. A detailed analysis of the lamellipodia leading edge showed that the protrusion of the Mena11a cells are often unproductive, while the ones stimulated by Mena are faster and persistent. Moreover, the number of Mena11a overexpressing cells collected by *in vivo*

invasion assay was sensibly low compared to the Mena, MenaINV overexpressing and control cells, suggesting that a forced expression of Mena11a can suppress the invasive potential of these metastatic cancer cells. Importantly, endogenous Mena11a is in complex with EGFP-Mena in MTLn3 carcinoma cells. This can explain, at least in part, why the overexpression of Mena11a dampens the protrusion of these cells. We can hypothesize that the natural compositions of the tetramers formed by Mena and Mena11a is unbalanced when Mena11a is overexpressed, so that too much Mena11a can deregulate the Mena-dependent actin cytoskeleton remodeling, bringing to a suppression of the actin polymerization in the cell. Another mechanism that we are currently investigating is the suppression of the Arp2/3-mediated branching. Infact, Mena overexpression leads to a cytoskeleton with filaments longer and less branched compared to control cells in fibroblasts (Bear et al., 2002) and carcinoma cells (Balsamo, not shown). The mechanism of this direct effect on branching remains unknown, although it is tempting to speculate that Ena/VASP proteins compete with the Arp2/3 complex for actin monomers, which are necessary cofactors for branching. Alternatively, Ena/VASP proteins might act directly to inhibit branching by preventing the docking of the Arp2/3 complex onto the side of a mother actin filament. Another possible explanation for the observed anti-branching activity of Ena/VASP proteins is through an indirect effect on capping proteins. Dyche Mullins laboratory recently described a striking mechanism for controlling the frequency of Arp2/3 branching through the capping of barbed ends (Akin and Mullins, 2008). They demonstrated that increasing capping activity actually increases branching because the levels of actin monomers are locally elevated. Anti capping factors such as Ena/VASP proteins could decrease branching by reducing of barbed-end capping, which would lead to the increased consumption

of monomers through their addition to barbed ends. In this context, different Mena isoforms could exert different roles affecting different kinetics of actin polymerization.

Another mechanisms that we found to be potentially important to explain the phenotype of the Mena11a overexpressing cells comes from the biochemistry of Ena/VASP. The insertion of the 11a exon between the F-actin binding and the tetramerization domain inspired us to test whether the insertion could influence directly the actin remodeling functions of Mena11a. Using purified proteins, biochemical and microscopy based approaches, we have found that the EVH2 domain of Mena11a, while conserving an actin binding and bundling activity (Figure 16), has an impaired barbed ends capture activity compared to the EVH2 of Mena and VASP (Figure 18). The ability of recombinant VASP to bind the barbed end of growing actin filaments has been shown recently by Dorothy Schafer laboratory (Pasic et al., 2008). The barbed end capture is a transient property since once captured the filaments stop growing for few seconds but then get captured by the side and re-start growing. This finding supports the hypothesis that transient interactions of Ena/VASP proteins with actin filament barbed ends allow this family of proteins to regulate the rate of actin filament elongation, barbed end capping and provide a mechanism to recruit filaments barbed ends during assembly of specialized actin filaments structures. Of note, the mutation of the G-actin binding and the F-actin binding domains in VASP, while affecting the F-actin binding, doesn't affect the barbed end capture activity of the molecule and the region between the F-actin and the tetramerization domain was found to be sufficient for the barbed end capture (Pasic et al., 2008). Hence, the region between the F-actin binding and the tetramerization domain can be a novel site for the specific function of binding to the barbed end. The 11a insertion in that region

can impair the barbed end capture, and may work as an additional site of regulation for Mena-Mena11a tetramers interaction with the barbed end of growing filaments. Importantly EVH2-Mena coated surfaces captured the barbed ends 10 times more efficiently then EVH2-Mena11a (table 1). Interestingly, the barbed end capturing region and the coiled coil domain fold in an unusual right handed coiled coil (Kuhnel et al., 2004), similarly of the ends of actin, which also folds in a right-handed coil. What can be the fisiological function of the barbed end capture? Barbed end capture can be important for filopodia formation and initiation, since drugs like cytochalasin D that bind the barbed end of growing actin filaments completely abolish the filopodia formation in cells, so the free barbed end is needed for the formation of filopodia. We have found that Mena11a doesn't support filopodia formation during cell spreading on laminin, while Mena strongly enhances this activity (Applewhite et al., 2007), supporting the biochemical data regarding the impaired barbed end capture activity of purified Mena11a.

We also tested the possibility of an impaired anti capping activity by Mena11a compared to Mena. The currently data suggest that Mena11a has an anti capping activity as strong as Mena by pyrene actin polymerization assays. In these assays the actin polymerization is measured by the increase of fluorescence in a bulk format such as a cuvette, so the assay doesn't give information about the length or architecture of the actin filaments that are formed. This means that several informations regarding the actual actin remodeling cannot be acquired. TIRF experiment are ongoing in order to visualize the anti capping property of Mena11a compared to Mena, so that we can have more kinetic parameters to quantify and compare.

In conclusion, my research project focused on the role of a splice isoforms of Mena in cancer and epithelial morphogenesis. In particular my findings are important to understand why cancer cells need to modify their motility machinery during invasion and metastasis. The loss of regulators of epithelial morphology can be important for the initial steps of intravasation and subsequent extravasation. Mena11a can be considered an important player for these steps in the metastatic cascade.

Chapter 5 - References

Ahern-Djamali, S. M., Bachmann, C., Hua, P., Reddy, S. K., Kastenmeier, A. S., Walter, U., and Hoffmann, F. M. (1999). Identification of profilin and src homology 3 domains as binding partners for Drosophila enabled. Proc Natl Acad Sci U S A *96*, 4977-4982.

Akin, O., and Mullins, R. D. (2008). Capping protein increases the rate of actin-based motility by promoting filament nucleation by the Arp2/3 complex. Cell *133*, 841-851.

Ansieau, S., Bastid, J., Doreau, A., Morel, A. P., Bouchet, B. P., Thomas, C., Fauvet, F., Puisieux, I., Doglioni, C., Piccinin, S.*, et al.* (2008). Induction of EMT by twist proteins as a

collateral effect of tumor-promoting inactivation of premature senescence. Cancer Cell *14*, 79-89.

Applewhite, D. A., Barzik, M., Kojima, S., Svitkina, T. M., Gertler, F. B., and Borisy, G. G. (2007). Ena/VASP proteins have an anti-capping independent function in filopodia formation. Mol Biol Cell *18*, 2579-2591.

Aszodi, A., Pfeifer, A., Ahmad, M., Glauner, M., Zhou, X. H., Ny, L., Andersson, K. E., Kehrel, B., Offermanns, S., and Fassler, R. (1999). The vasodilator-stimulated phosphoprotein (VASP) is involved in cGMP- and cAMP-mediated inhibition of agonist-induced platelet aggregation, but is dispensable for smooth muscle function. Embo J *18*, 37-48.

Ayala, R., Shu, T., and Tsai, L. (2007). Trekking across the Brain: The Journey of Neuronal Migration Cell *128*, 29-43.

Bachmann, C., Fischer, L., Walter, U., and Reinhard, M. (1999). The EVH2 domain of the vasodilator-stimulated phosphoprotein mediates tetramerization, F-actin binding, and actin bundle formation. J Biol Chem *274*, 23549-23557.

Bamburg, J. R. (1999). PROTEINS OF THE ADF/COFILIN FAMILY: Essential Regulators of Actin Dynamics. Annual Review of Cell and Developmental Biology *15*, 185-230.

Barzik, M., Kotova, T. I., Higgs, H. N., Hazelwood, L., Hanein, D., Gertler, F. B., and Schafer, D. A. (2005). Ena/VASP proteins enhance actin polymerization in the presence of barbed end capping proteins. J Biol Chem *280*, 28653-28662.

Bashaw, G. J., Kidd, T., Murray, D., Pawson, T., and Goodman, C. S. (2000). Repulsive axon guidance: Abelson and Enabled play opposing roles downstream of the roundabout receptor. Cell *101*, 703-715.

Bear, J. E., Loureiro, J. J., Libova, I., Fassler, R., Wehland, J., and Gertler, F. B. (2000). Negative regulation of fibroblast motility by Ena/VASP proteins. Cell *101*, 717-728.

Bear, J. E., Svitkina, T. M., Krause, M., Schafer, D. A., Loureiro, J. J., Strasser, G. A., Maly, I. V., Chaga, O. Y., Cooper, J. A., Borisy, G. G., and Gertler, F. B. (2002). Antagonism between Ena/VASP proteins and actin filament capping regulates fibroblast motility. Cell *109*, 509-521.

Bentley, D., and Toroian-Raymond, A. (1986). Disoriented pathfinding by pioneer neurone growth cones deprived of filopodia by cytochalasin treatment. Nature *323*, 712-715.

Bhowmick, N. A., Ghiassi, M., Bakin, A., Aakre, M., Lundquist, C. A., Engel, M. E., Arteaga, C. L., and Moses, H. L. (2001). Transforming Growth Factor-{beta}1 Mediates Epithelial to Mesenchymal Transdifferentiation through a RhoA-dependent Mechanism. Mol Biol Cell *12*, 27-36.

Bingle, L., Brown, N. J., and Lewis, C. E. (2002). The role of tumour-associated macrophages in tumour progression: implications for new anticancer therapies. J Pathol *196*, 254-265.

Birgit, W.-H., Sofia, Y. K., Horst, H., Brigitte, M. J., and Susanne, I. (2002). The vasodilator-stimulated phosphoprotein promotes actin polymerisation through direct binding to monomeric actin. FEBS letters *529*, 275-280.

Bissell, M. J., and Radisky, D. (2001). Putting tumours in context. Nat Rev Cancer *1*, 46-54.
Boeda, B., Briggs, D. C., Higgins, T., Garvalov, B. K., Fadden, A. J., McDonald, N. Q., and Way, M. (2007). Tes, a specific Mena interacting partner, breaks the rules for EVH1 binding. Mol Cell *28*, 1071-1082.

Bolender, D. L., and Markwald, R. R. (1979). Epithelial-mesenchymal transformation in chick atrioventricular cushion morphogenesis. Scan Electron Microsc, 313-321.

Breitsprecher, D., Kiesewetter, A. K., Linkner, J., Urbanke, C., Resch, G. P., Small, J. V., and Faix, J. (2008). Clustering of VASP actively drives processive, WH2 domain-mediated actin filament elongation. Embo J *27*, 2943-2954.

Brindle, N. P., Holt, M. R., Davies, J. E., Price, C. J., and Critchley, D. R. (1996). The focal-adhesion vasodilator-stimulated phosphoprotein (VASP) binds to the proline-rich domain in vinculin. Biochem J *318*, 753-757.

Bryan, J., and Coluccio, L. M. (1985). Kinetic analysis of F-actin depolymerization in the presence of platelet gelsolin and gelsolin-actin complexes. J Cell Biol *101*, 1236-1244.

Bukholm, I. K., Nesland, J. M., and Borresen-Dale, A. L. (2000). Re-expression of E-cadherin, alpha-catenin and beta-catenin, but not of gamma-catenin, in metastatic tissue from breast cancer patients [seecomments]. J Pathol *190*, 15-19.

Bukholm, I. K., Nesland, J. M., Karesen, R., Jacobsen, U., and Borresen-Dale, A. L. (1998). E-cadherin and alpha-, beta-, and gamma-catenin protein expression in relation to metastasis in human breast carcinoma. J Pathol *185*, 262-266.

Butt, E., Abel, K., Krieger, M., Palm, D., Hoppe, V., Hoppe, J., and Walter, U. (1994). cAMP- and cGMP-dependent protein kinase phosphorylation sites of the focal adhesion vasodilator-stimulated phosphoprotein (VASP) in vitro and in intact human platelets. J Biol Chem *269*, 14509-14517.

Carlier, M. F., Laurent, V., Santolini, J., Melki, R., Didry, D., Xia, G. X., Hong, Y., Chua, N. H., and Pantaloni, D. (1997). Actin depolymerizing factor (ADF/cofilin) enhances the rate of filament turnover: implication in actin-based motility. J Cell Biol *136*, 1307-1322.

Chakraborty, T., Ebel, F., Domann, E., Niebuhr, K., Gerstel, B., Pistor, S., Temm-Grove, C. J., Jockusch, B. M., Reinhard, M., Walter, U., and et al. (1995). A focal adhesion factor directly linking intracellularly motile Listeria monocytogenes and Listeria ivanovii to the actin-based cytoskeleton of mammalian cells. Embo J *14*, 1314-1321.

Chambers, A., Groom, A., and MacDonald, I. (2002). Metastasis: Dissemination and growth of cancer cells in metastatic sites. Nat Rev Cancer *2*, 563-572.

Chan, A. Y., Raft, S., Bailly, M., Wyckoff, J. B., Segall, J. E., and Condeelis, J. S. (1998). EGF stimulates an increase in actin nucleation and filament number at the leading edge of the lamellipod in mammary adenocarcinoma cells. J Cell Sci *111 (Pt 2)*, 199-211.

Chereau, D., and Dominguez, R. (2006). Understanding the role of the G-actin-binding domain of Ena/VASP in actin assembly. J Struct Biol *155*, 195-201.

Colavita, A., and Culotti, J. G. (1998). Suppressors of ectopic UNC-5 growth cone steering identify eight genes involved in axon guidance in Caenorhabditis elegans. Dev Biol *194*, 72-85.

Condeelis, J. (1993). Life at the leading edge: the formation of cell protrusions. Annu Rev Cell Biol *9*, 411-444.

Condeelis, J. (2001). How is actin polymerization nucleated in vivo? Trends Cell Biol *11*, 288-293.

Condeelis, J., and Segall, J. E. (2003). Intravital imaging of cell movement in tumours. Nat Rev Cancer *3*, 921-930.

Coppolino, M. G., Krause, M., Hagendorff, P., Monner, D. A., Trimble, W., Grinstein, S., Wehland, J., and Sechi, A. S. (2001). Evidence for a molecular complex consisting of Fyb/SLAP, SLP-76, Nck, VASP and WASP that links the actin cytoskeleton to Fcgamma receptor signalling during phagocytosis. J Cell Sci *114*, 4307-4318.

Davenport, R. W., Dou, P., Rehder, V., and Kater, S. B. (1993). A sensory role for neuronal growth cone filopodia. Nature *361*, 721-724.

de Visser, K. E., Eichten, A., and Coussens, L. M. (2006). Paradoxical roles of the immune system during cancer development. Nat Rev Cancer *6*, 24-37.

DeNardo, D. G., Barreto, J. B., Andreu, P., Vasquez, L., Tawfik, D., Kolhatkar, N., and Coussens, L. M. (2009). CD4(+) T cells regulate pulmonary metastasis of mammary carcinomas by enhancing protumor properties of macrophages. Cancer Cell *16*, 91-102.

Dent, E. W., Kwiatkowski, A. V., Mebane, L. M., Philippar, U., Barzik, M., Rubinson, D. A., Gupton, S., Van Veen, J. E., Furman, C., Zhang, J.*, et al.* (2007). Filopodia are required for cortical neurite initiation. Nat Cell Biol *9*, 1347-1359.

Di Modugno, F., Bronzi, G., Scanlan, M. J., Del Bello, D., Cascioli, S., Venturo, I., Botti, C., Nicotra, M. R., Mottolese, M., Natali, P. G.*, et al.* (2004). Human Mena protein, a serex-defined antigen overexpressed in breast cancer eliciting both humoral and CD8+ T-cell immune response. Int J Cancer *109*, 909-918.

Di Modugno, F., DeMonte, L., Balsamo, M., Bronzi, G., Nicotra, M. R., Alessio, M., Jager, E., Condeelis, J. S., Santoni, A., Natali, P. G., and Nistico, P. (2007). Molecular cloning of hMena (ENAH) and its splice variant hMena+11a: epidermal growth factor increases their expression and stimulates hMena+11a phosphorylation in breast cancer cell lines. Cancer Res *67*, 2657-2665.

Di Modugno, F., Mottolese, M., Di Benedetto, A., Conidi, A., Novelli, F., Perracchio, L., Venturo, I., Botti, C., Jager, E., Santoni, A.*, et al.* (2006). The cytoskeleton regulatory protein hMena (ENAH) is overexpressed in human benign breast lesions with high risk of transformation and human epidermal growth factor receptor-2-positive/hormonal receptor-negative tumors. Clin Cancer Res *12*, 1470-1478.

DiNubile, M. J., Cassimeris, L., Joyce, M., and Zigmond, S. H. (1995). Actin filament barbed-end capping activity in neutrophil lysates: the role of capping protein-beta 2. Mol Biol Cell *6*, 1659-1671.

Drees, B., Friederich, E., Fradelizi, J., Louvard, D., Beckerle, M. C., and Golsteyn, R. M. (2000). Characterization of the interaction between zyxin and members of the Ena/vasodilator-stimulated phosphoprotein family of proteins. J Biol Chem *275*, 22503-22511.

Egeblad, M., Littlepage, L. E., and Werb, Z. (2005). The fibroblastic coconspirator in cancer progression. Cold Spring Harb Symp Quant Biol *70*, 383-388.

Ermekova, K. S., Zambrano, N., Linn, H., Minopoli, G., Gertler, F., Russo, T., and Sudol, M. (1997). The WW domain of neural protein FE65 interacts with proline-rich motifs in Mena, the mammalian homolog of Drosophila enabled. J Biol Chem *272*, 32869-32877.

Etienne-Manneville, S., and Hall, A. (2002). Rho GTPases in cell biology. Nature *420*, 629-635.

Ewald, A., Brenot, A., Duong, M., Chan, D., and Werb, Z. (2008). Collective Epithelial Migration and Cell Rearrangements Drive Mammary Branching Morphogenesis Dev Cell *14*, 570-581.

Ferron, F., Rebowski, G., Lee, S. H., and Dominguez, R. (2007). Structural basis for the recruitment of profilin-actin complexes during filament elongation by Ena/VASP. Embo J *26*, 4597-4606.

Fidler, I. (2003). The pathogenesis of cancer metastasis: the 'seed and soil' hypothesis revisited. Nat Rev Cancer *3*, 453-445.

Findlater, G., McDougall, R., and Kaufman, M. (1993). Eyelid development, fusion and subsequent reopening in the mouse. J Anat *183* 121-129.

Fitchett, J. E., and Hay, E. D. (1989). Medial edge epithelium transforms to mesenchyme after embryonic palatal shelves fuse. Dev Biol *131*, 455-474.

Fodde, R., and Brabletz, T. (2007). Wnt/beta-catenin signaling in cancer stemness and malignant behavior. Curr Opin Cell Biol *19*, 150-158.

Friedl, P., and Wolf, K. (2003). Tumour-cell invasion and migration: diversity and escape mechanisms. Nat Rev Cancer *3*, 362-374.

Fujita, Y., Krause, G., Scheffner, M., Zechner, D., Leddy, H. E., Behrens, J., Sommer, T., and Birchmeier, W. (2002). Hakai, a c-Cbl-like protein, ubiquitinates and induces endocytosis of the E-cadherin complex. Nat Cell Biol *4*, 222-231.

Furman, C., Sieminski, A. L., Kwiatkowski, A. V., Rubinson, D. A., Vasile, E., Bronson, R. T., Fassler, R., and Gertler, F. B. (2007). Ena/VASP is required for endothelial barrier function in vivo. J Cell Biol *179*, 761-775.

Gabbiani, G., Chaponnier, C., and Huttner, I. (1978). Cytoplasmic filaments and gap junctions in epithelial cells and myofibroblasts during wound healing. J Cell Biol *76*, 561-568.

Gaggioli, C., Hooper, S., Hidalgo-Carcedo, C., Grosse, R., Marshall, J. F., Harrington, K., and Sahai, E. (2007). Fibroblast-led collective invasion of carcinoma cells with differing roles for RhoGTPases in leading and following cells. Nat Cell Biol *9*, 1392-1400.

Galbraith, C. G., Yamada, K. M., and Sheetz, M. P. (2002). The relationship between force and focal complex development. J Cell Biol *159*, 695-705.

Gates, J., Mahaffey, J. P., Rogers, S. L., Emerson, M., Rogers, E. M., Sottile, S. L., Van Vactor, D., Gertler, F. B., and Peifer, M. (2007). Enabled plays key roles in embryonic epithelial morphogenesis in Drosophila. Development *134*, 2027-2039.

Geese, M., Loureiro, J. J., Bear, J. E., Wehland, J., Gertler, F. B., and Sechi, A. S. (2002). Contribution of Ena/VASP proteins to intracellular motility of listeria requires phosphorylation and proline-rich core but not F-actin binding or multimerization. Mol Biol Cell *13*, 2383-2396.

Geiger, B., Bershadsky, A., Pankov, R., and Yamada, K. M. (2001). Transmembrane crosstalk between the extracellular matrix--cytoskeleton crosstalk. Nat Rev Mol Cell Biol *2*, 793-805.

Gertler, F. B., Comer, A. R., Juang, J. L., Ahern, S. M., Clark, M. J., Liebl, E. C., and Hoffmann, F. M. (1995). enabled, a dosage-sensitive suppressor of mutations in the Drosophila Abl tyrosine kinase, encodes an Abl substrate with SH3 domain-binding properties. Genes Dev *9*, 521-533.

Gertler, F. B., Doctor, J. S., and Hoffmann, F. M. (1990). Genetic suppression of mutations in the Drosophila abl proto-oncogene homolog. Science *248*, 857-860.

Gertler, F. B., Niebuhr, K., Reinhard, M., Wehland, J. r., and Soriano, P. (1996). Mena, a Relative of VASP and Drosophila Enabled, Is Implicated in the Control of Microfilament Dynamics. Cell *87*, 227-239.

Gitai, Z., Yu, T. W., Lundquist, E. A., Tessier-Lavigne, M., and Bargmann, C. I. (2003). The netrin receptor UNC-40/DCC stimulates axon attraction and outgrowth through enabled and, in parallel, Rac and UNC-115/AbLIM. Neuron *37*, 53-65.

Goh, K. L., Cai, L., Cepko, C. L., and Gertler, F. B. (2002). Ena/VASP proteins regulate cortical neuronal positioning. Curr Biol *12*, 565-569.

Goliger, J. A., and Paul, D. L. (1995). Wounding alters epidermal connexin expression and gap junction-mediated intercellular communication. Mol Biol Cell *6*, 1491-1501.

Goswami, S., Philippar, U., Sun, D., Patsialou, A., Avraham, J., Wang, W., Di Modugno, F., Nistico, P., Gertler, F. B., and Condeelis, J. S. (2009). Identification of invasion specific splice variants of the cytoskeletal protein Mena present in mammary tumor cells during invasion in vivo. Clin Exp Metastasis *26*, 153-159.

Goswami, S., Sahai, E., Wyckoff, J. B., Cammer, M., Cox, D., Pixley, F. J., Stanley, E. R., Segall, J. E., and Condeelis, J. S. (2005). Macrophages promote the invasion of breast carcinoma cells via a colony-stimulating factor-1/epidermal growth factor paracrine loop. Cancer Res *65*, 5278-5283.

Grady, W. M., Parkin, R. K., Mitchell, P. S., Lee, J. H., Kim, Y. H., Tsuchiya, K. D., Washington, M. K., Paraskeva, C., Willson, J. K., Kaz, A. M.*, et al.* (2008). Epigenetic silencing of the intronic microRNA hsa-miR-342 and its host gene EVL in colorectal cancer. Oncogene *27*, 3880-3888.

Gregory, P. A., Bert, A. G., Paterson, E. L., Barry, S. C., Tsykin, A., Farshid, G., Vadas, M. A., Khew-Goodall, Y., and Goodall, G. J. (2008). The miR-200 family and miR-205 regulate epithelial to mesenchymal transition by targeting ZEB1 and SIP1. Nat Cell Biol *10*, 593-601.

Grevengoed, E. E., Loureiro, J. J., Jesse, T. L., and Peifer, M. (2001). Abelson kinase regulates epithelial morphogenesis in Drosophila. J Cell Biol *155*, 1185-1198.

Guilford, P., Hopkins, J., Harraway, J., McLeod, M., McLeod, N., Harawira, P., Taite, H., Scoular, R., Miller, A., and Reeve, A. E. (1998). E-cadherin germline mutations in familial gastric cancer. Nature *392*, 402-405.

Gurzu, S., Jung, I., Prantner, I., Chira, L., and Ember, I. (2009). The immunohistochemical aspects of protein Mena in cervical lesions. Rom J Morphol Embryol *50*, 213-216.

Gurzu, S., Jung, I., Prantner, I., Ember, I., Pavai, Z., and Mezei, T. (2008). The expression of cytoskeleton regulatory protein Mena in colorectal lesions. Rom J Morphol Embryol *49*, 345-349.

Guy, C. T., Cardiff, R. D., and Muller, W. J. (1992). Induction of mammary tumors by expression of polyomavirus middle T oncogene: a transgenic mouse model for metastatic disease. Mol Cell Biol *12*, 954-961.

Haffner, C., Jarchau, T., Reinhard, M., Hoppe, J., Lohmann, S. M., and Walter, U. (1995). Molecular cloning, structural analysis and functional expression of the proline-rich focal adhesion and microfilament-associated protein VASP. Embo J *14*, 19-27.

Han, G., Lu, S. L., Li, A. G., He, W., Corless, C. L., Kulesz-Martin, M., and Wang, X. J. (2005). Distinct mechanisms of TGF-beta1-mediated epithelial-to-mesenchymal transition and metastasis during skin carcinogenesis. J Clin Invest *115*, 1714-1723.

Hartwell, K. A., Muir, B., Reinhardt, F., Carpenter, A. E., Sgroi, D. C., and Weinberg, R. A. (2006). The Spemann organizer gene, Goosecoid, promotes tumor metastasis. Proc Natl Acad Sci U S A *103*, 18969-18974.

Hartwig, J. H., Bokoch, G. M., Carpenter, C. L., Janmey, P. A., Taylor, L. A., Toker, A., and Stossel, T. P. (1995). Thrombin receptor ligation and activated rac uncap actin filament

barbed ends through phosphoinositide synthesis in permeabilized human platelets. Cell *82*, 643-653.

Hay, E. D. (1995). An overview of epithelio-mesenchymal transformation. Acta Anat (Basel) *154*, 8-20.

Heasman, S. J., and Ridley, A. J. (2008). Mammalian Rho GTPases: new insights into their functions from in vivo studies. Nat Rev Mol Cell Biol *9*, 690-701.

Herschkowitz, J., Simin, K., Weigman, V., Mikaelian, I., Usary, J., Hu, Z., Rasmussen, K., Jones, L., Assefnia, S., Chandrasekharan, S.*, et al.* (2007). Identification of conserved gene expression features between murine mammary carcinoma models and human breast tumors. Genome Biology *8*, R76.

Horwitz, A., Duggan, K., Buck, C., Beckerle, M. C., and Burridge, K. (1986). Interaction of plasma membrane fibronectin receptor with talin--a transmembrane linkage. Nature *320*, 531-533.

Hu, L. D., Zou, H. F., Zhan, S. X., and Cao, K. M. (2008). EVL (Ena/VASP-like) expression is up-regulated in human breast cancer and its relative expression level is correlated with clinical stages. Oncol Rep *19*, 1015-1020.

Huttelmaier, S., Harbeck, B., Steffens, O., Messerschmidt, T., Illenberger, S., and Jockusch, B. M. (1999). Characterization of the actin binding properties of the vasodilator-stimulated phosphoprotein VASP. FEBS Lett *451*, 68-74.

Jacinto, A., Wood, W., Balayo, T., Turmaine, M., Martinez-Arias, A., and Martin, P. (2000). Dynamic actin-based epithelial adhesion and cell matching during Drosophila dorsal closure. Curr Biol *10*, 1420-1426.

Janda, E., Lehmann, K., Killisch, I., Jechlinger, M., Herzig, M., Downward, J., Beug, H., and Grunert, S. (2002). Ras and TGF{beta} cooperatively regulate epithelial cell plasticity and metastasis: dissection of Ras signaling pathways. J Cell Biol *156*, 299-314.

Janssens, K., De Kimpe, L., Balsamo, M., Vandoninck, S., Vandenheede, J. R., Gertler, F., and Van Lint, J. (2009). Characterization of EVL-I as a protein kinase D substrate. Cell Signal *21*, 282-292.

Jean-FranÁois, C., and Gary, C. S. (2001). Towards a cellular and molecular understanding of neurulation. Developmental Dynamics *221*, 117-145.

Joyce, C. T., and Raghu, K. (2007). Mechanisms of metastasis: Epithelial-to-mesenchymal transition and contribution of tumor microenvironment. Journal of Cellular Biochemistry *101*, 816-829.

Joyce, J., and Pollard, J. (2009a). Microenvironmental regulation of metastasis. Nat Rev Cancer *9*, 239-252.

Joyce, J. A., and Pollard, J. W. (2009b). Microenvironmental regulation of metastasis. Nat Rev Cancer *9*, 239-252.

Kalluri, R., and Weinberg, R. A. (2009). The basics of epithelial-mesenchymal transition. J Clin Invest *119*, 1420-1428.

Kalluri, R., and Zeisberg, M. (2006). Fibroblasts in cancer. Nat Rev Cancer *6*, 392-401.
Kalsotra, A., Xiao, X., Ward, A. J., Castle, J. C., Johnson, J. M., Burge, C. B., and Cooper, T. A. (2008). A postnatal switch of CELF and MBNL proteins reprograms alternative splicing in the developing heart. Proc Natl Acad Sci U S A *105*, 20333-20338.

Kim, K. K., Kugler, M. C., Wolters, P. J., Robillard, L., Galvez, M. G., Brumwell, A. N., Sheppard, D., and Chapman, H. A. (2006). Alveolar epithelial cell mesenchymal transition develops in vivo during pulmonary fibrosis and is regulated by the extracellular matrix. Proc Natl Acad Sci U S A *103*, 13180-13185.

Kiosses, W. B., Shattil, S. J., Pampori, N., and Schwartz, M. A. (2001). Rac recruits high-affinity integrin alphavbeta3 to lamellipodia in endothelial cell migration. Nat Cell Biol *3*, 316-320.

Kolsch, V., Charest, P. G., and Firtel, R. A. (2008). The regulation of cell motility and chemotaxis by phospholipid signaling. J Cell Sci *121*, 551-559.

Korpal, M., Lee, E. S., Hu, G., and Kang, Y. (2008). The miR-200 family inhibits epithelial-mesenchymal transition and cancer cell migration by direct targeting of E-cadherin transcriptional repressors ZEB1 and ZEB2. J Biol Chem *283*, 14910-14914.

Krause, M., Leslie, J. D., Stewart, M., Lafuente, E. M., Valderrama, F., Jagannathan, R., Strasser, G. A., Rubinson, D. A., Liu, H., Way, M.*, et al.* (2004). Lamellipodin, an Ena/VASP ligand, is implicated in the regulation of lamellipodial dynamics. Dev Cell *7*, 571-583.

Krause, M., Sechi, A. S., Konradt, M., Monner, D., Gertler, F. B., and Wehland, J. (2000).

Fyn-binding protein (Fyb)/SLP-76-associated protein (SLAP), Ena/vasodilator-stimulated phosphoprotein (VASP) proteins and the Arp2/3 complex link T cell receptor (TCR) signaling to the actin cytoskeleton. J Cell Biol *149*, 181-194.

Krugmann, S., Jordens, I., Gevaert, K., Driessens, M., Vandekerckhove, J., and Hall, A. (2001). Cdc42 induces filopodia by promoting the formation of an IRSp53:Mena complex. Curr Biol *11*, 1645-1655.

Kuhn, J. R., and Pollard, T. D. (2005). Real-time measurements of actin filament polymerization by total internal reflection fluorescence microscopy. Biophys J *88*, 1387-1402.

Kuhnel, K., Jarchau, T., Wolf, E., Schlichting, I., Walter, U., Wittinghofer, A., and Strelkov, S. V. (2004). The VASP tetramerization domain is a right-handed coiled coil based on a 15-residue repeat. Proc Natl Acad Sci U S A *101*, 17027-17032.

Kwiatkowski, A. V., Rubinson, D. A., Dent, E. W., Edward van Veen, J., Leslie, J. D., Zhang, J., Mebane, L. M., Philippar, U., Pinheiro, E. M., Burds, A. A.*, et al.* (2007). Ena/VASP Is Required for neuritogenesis in the developing cortex. Neuron *56*, 441-455.

Lafuente, E. M., van Puijenbroek, A. A., Krause, M., Carman, C. V., Freeman, G. J., Berezovskaya, A., Constantine, E., Springer, T. A., Gertler, F. B., and Boussiotis, V. A.

(2004). RIAM, an Ena/VASP and Profilin ligand, interacts with Rap1-GTP and mediates Rap1-induced adhesion. Dev Cell *7*, 585-595.

Lambrechts, A., Kwiatkowski, A. V., Lanier, L. M., Bear, J. E., Vandekerckhove, J., Ampe, C., and Gertler, F. B. (2000). cAMP-dependent protein kinase phosphorylation of EVL, a Mena/VASP relative, regulates its interaction with actin and SH3 domains. J Biol Chem *275*, 36143-36151.

Lanier, L. M., Gates, M. A., Witke, W., Menzies, A. S., Wehman, A. M., Macklis, J. D., Kwiatkowski, D., Soriano, P., and Gertler, F. B. (1999). Mena is required for neurulation and commissure formation. Neuron *22*, 313-325.

Larjava H, Salo T, Haapasalmi K, Kramer RH, and J., H. (1993). Expression of integrins and basement membrane components by wound keratinoctyes. J Clin Invest *92*, 1425-1435.

Lauffenburger, D. A., and Horwitz, A. F. (1996). Cell migration: a physically integrated molecular process. Cell *84*, 359-369.

Laurent, V., Loisel, T. P., Harbeck, B., Wehman, A., Grobe, L., Jockusch, B. M., Wehland, J., Gertler, F. B., and Carlier, M.-F. (1999). Role of Proteins of the Ena/VASP Family in Actin-based Motility of Listeria monocytogenes. J Cell Biol *144*, 1245-1258.

Lawrence, D. W., Comerford, K. M., and Colgan, S. P. (2002). Role of VASP in reestablishment of epithelial tight junction assembly after Ca2+ switch. Am J Physiol Cell Physiol *282*, C1235-1245.

Lebrand, C., Dent, E. W., Strasser, G. A., Lanier, L. M., Krause, M., Svitkina, T. M., Borisy, G. G., and Gertler, F. B. (2004). Critical role of Ena/VASP proteins for filopodia formation in neurons and in function downstream of netrin-1. Neuron *42*, 37-49.

Lidke, D. S., Lidke, K. A., Rieger, B., Jovin, T. M., and Arndt-Jovin, D. J. (2005). Reaching out for signals: filopodia sense EGF and respond by directed retrograde transport of activated receptors. J Cell Biol *170*, 619-626.

Lin, E. Y., Jones, J. G., Li, P., Zhu, L., Whitney, K. D., Muller, W. J., and Pollard, J. W. (2003). Progression to malignancy in the polyoma middle T oncoprotein mouse breast cancer model provides a reliable model for human diseases. Am J Pathol *163*, 2113-2126.

Loureiro, J. J., Rubinson, D. A., Bear, J. E., Baltus, G. A., Kwiatkowski, A. V., and Gertler, F. B. (2002). Critical roles of phosphorylation and actin binding motifs, but not the central proline-rich region, for Ena/vasodilator-stimulated phosphoprotein (VASP) function during cell migration. Mol Biol Cell *13*, 2533-2546.

Mani, S. A., Guo, W., Liao, M. J., Eaton, E. N., Ayyanan, A., Zhou, A. Y., Brooks, M., Reinhard, F., Zhang, C. C., Shipitsin, M.*, et al.* (2008). The epithelial-mesenchymal transition generates cells with properties of stem cells. Cell *133*, 704-715.

Mani, S. A., Yang, J., Brooks, M., Schwaninger, G., Zhou, A., Miura, N., Kutok, J. L., Hartwell, K., Richardson, A. L., and Weinberg, R. A. (2007). Mesenchyme Forkhead 1 (FOXC2) plays a key role in metastasis and is associated with aggressive basal-like breast cancers. Proc Natl Acad Sci U S A *104*, 10069-10074.

Martín-Blanco, E., Pastor-Pareja, J., and A, G.-B. (2000). JNK and decapentaplegic signaling control adhesiveness and cytoskeleton dynamics during thorax closure in Drosophila. PNAS *97*, 7888-7893.

Massague, J. (2008). TGFbeta in Cancer. Cell *134*, 215-230.

May, R. C., Caron, E., Hall, A., and Machesky, L. M. (2000). Involvement of the Arp2/3 complex in phagocytosis mediated by FcgammaR or CR3. Nat Cell Biol *2*, 246-248.

Moeller, M. J., Soofi, A., Braun, G. S., Li, X., Watzl, C., Kriz, W., and Holzman, L. B. (2004). Protocadherin FAT1 binds Ena/VASP proteins and is necessary for actin dynamics and cell polarization. Embo J *23*, 3769-3779.

Mykkanen, O. M., Gronholm, M., Ronty, M., Lalowski, M., Salmikangas, P., Suila, H., and Carpen, O. (2001). Characterization of human palladin, a microfilament-associated protein. Mol Biol Cell *12*, 3060-3073.

Nanney, L., and King, L. (1996). Epidermal growth factor and transforming growth factor. . in: Clark RAF, ed The molecular and cellular biology of wound repair, New York: Plenum Press *2nd ed.*, 171-194.

Niebuhr, K., Ebel, F., Frank, R., Reinhard, M., Domann, E., Carl, U. D., Walter, U., Gertler, F. B., Wehland, J., and Chakraborty, T. (1997). A novel proline-rich motif present in ActA of Listeria monocytogenes and cytoskeletal proteins is the ligand for the EVH1 domain, a protein module present in the Ena/VASP family. Embo J *16*, 5433-5444.

Orengo, J. P., Bundman, D., and Cooper, T. A. (2006). A bichromatic fluorescent reporter for cell-based screens of alternative splicing. Nucleic Acids Res *34*, e148.

Paladini, R. D., Takahashi, K., Bravo, N. S., and Coulombe, P. A. (1996). Onset of re-epithelialization after skin injury correlates with a reorganization of keratin filaments in wound edge keratinocytes: defining a potential role for keratin 16. J Cell Biol *132*, 381-397.

Pasic, L., Kotova, T., and Schafer, D. A. (2008). Ena/VASP proteins capture actin filament barbed ends. J Biol Chem *283*, 9814-9819.

Pellegrin, S., and Mellor, H. (2005). The Rho family GTPase Rif induces filopodia through mDia2. Curr Biol *15*, 129-133.

Philippar, U., Roussos, E. T., Oser, M., Yamaguchi, H., Kim, H. D., Giampieri, S., Wang, Y., Goswami, S., Wyckoff, J. B., Lauffenburger, D. A.*, et al.* (2008). A Mena invasion isoform potentiates EGF-induced carcinoma cell invasion and metastasis. Dev Cell *15*, 813-828.
Pilcher, B. K., Dumin, J. A., Sudbeck, B. D., Krane, S. M., Welgus, H. G., and Parks, W. C. (1997). The Activity of Collagenase-1 Is Required for Keratinocyte Migration on a Type I Collagen Matrix. J Cell Biol *137*, 1445-1457.

Pino, M. S., Balsamo, M., Di Modugno, F., Mottolese, M., Alessio, M., Melucci, E., Milella, M., McConkey, D. J., Philippar, U., Gertler, F. B.*, et al.* (2008). Human Mena+11a isoform serves as a marker of epithelial phenotype and sensitivity to epidermal growth factor receptor inhibition in human pancreatic cancer cell lines. Clin Cancer Res *14*, 4943-4950.

Pistor, S., Chakraborty, T., Walter, U., and Wehland, J. (1995). The bacterial actin nucleator protein ActA of Listeria monocytogenes contains multiple binding sites for host microfilament proteins. Curr Biol *5*, 517-525.

Pollard, T. D., and Borisy, G. G. (2003). Cellular motility driven by assembly and disassembly of actin filaments. Cell *112*, 453-465.

Prehoda, K. E., Lee, D. J., and Lim, W. A. (1999). Structure of the enabled/VASP homology 1 domain-peptide complex: a key component in the spatial control of actin assembly. Cell *97*, 471-480.

Radisky, D. C., Levy, D. D., Littlepage, L. E., Liu, H., Nelson, C. M., Fata, J. E., Leake, D., Godden, E. L., Albertson, D. G., Nieto, M. A.*, et al.* (2005). Rac1b and reactive oxygen species mediate MMP-3-induced EMT and genomic instability. Nature *436*, 123-127.

Raich, W. B., Agbunag, C., and Hardin, J. (1999). Rapid epithelial-sheet sealing in the Caenorhabditis elegans embryo requires cadherin-dependent filopodial priming. Current Biology *9*, 1139-1146, S1131.

Riento, K., and Ridley, A. J. (2003). Rocks: multifunctional kinases in cell behaviour. Nat Rev Mol Cell Biol *4*, 446-456.

Robinson, B. D., Sica, G. L., Liu, Y. F., Rohan, T. E., Gertler, F. B., Condeelis, J. S., and Jones, J. G. (2009). Tumor microenvironment of metastasis in human breast carcinoma: a potential prognostic marker linked to hematogenous dissemination. Clin Cancer Res *15*, 2433-2441.

Rodriguez, O. C., Schaefer, A. W., Mandato, C. A., Forscher, P., Bement, W. M., and Waterman-Storer, C. M. (2003). Conserved microtubule-actin interactions in cell movement and morphogenesis. Nat Cell Biol *5*, 599-609.

Rottner, K., Behrendt, B., Small, J. V., and Wehland, J. (1999). VASP dynamics during lamellipodia protrusion. Nat Cell Biol *1*, 321-322.

Sahai, E., Garcia-Medina, R., Pouyssegur, J., and Vial, E. (2007). Smurf1 regulates tumor cell plasticity and motility through degradation of RhoA leading to localized inhibition of contractility. J Cell Biol *176*, 35-42.

Samarin, S., Romero, S., Kocks, C., Didry, D., Pantaloni, D., and Carlier, M. F. (2003). How VASP enhances actin-based motility. J Cell Biol *163*, 131-142.

Simpson, K. J., Selfors, L. M., Bui, J., Reynolds, A., Leake, D., Khvorova, A., and Brugge, J. S. (2008). Identification of genes that regulate epithelial cell migration using an siRNA screening approach. Nat Cell Biol *10*, 1027-1038.

Skoble, J., Portnoy, D. A., and Welch, M. D. (2000). Three regions within ActA promote Arp2/3 complex-mediated actin nucleation and Listeria monocytogenes motility. J Cell Biol *150*, 527-538.

Smith, C. L. (1994). The initiation of neurite outgrowth by sympathetic neurons grown in vitro does not depend on assembly of microtubules [published erratum appears in J Cell Biol 1995 Feb;128(3):443]. J Cell Biol *127*, 1407-1418.

Spudich, J. A., and Watt, S. (1971). The regulation of rabbit skeletal muscle contraction. I. Biochemical studies of the interaction of the tropomyosin-troponin complex with actin and the proteolytic fragments of myosin. J Biol Chem *246*, 4866-4871.

Srinivasan, S., Wang, F., Glavas, S., Ott, A., Hofmann, F., Aktories, K., Kalman, D., and Bourne, H. R. (2003). Rac and Cdc42 play distinct roles in regulating PI(3,4,5)P3 and polarity during neutrophil chemotaxis. J Cell Biol *160*, 375-385.

Svitkina, T. M., Bulanova, E. A., Chaga, O. Y., Vignjevic, D. M., Kojima, S.-i., Vasiliev, J. M., and Borisy, G. G. (2003). Mechanism of filopodia initiation by reorganization of a dendritic network. J Cell Biol *160*, 409-421.

Takaku, M., Machida, S., Hosoya, N., Nakayama, S., Takizawa, Y., Sakane, I., Shibata, T., Miyagawa, K., and Kurumizaka, H. (2009a). Recombination activator function of the novel RAD51- and RAD51B-binding protein, human EVL. J Biol Chem *284*, 14326-14336.

Takaku, M., Machida, S., Nakayama, S., Takahashi, D., and Kurumizaka, H. (2009b). Biochemical analysis of the human EVL domains in homologous recombination. Febs J *276*, 5841-5848.

Tani, K., Sato, S., Sukezane, T., Kojima, H., Hirose, H., Hanafusa, H., and Shishido, T. (2003). Abl interactor 1 promotes tyrosine 296 phosphorylation of mammalian enabled (Mena) by c-Abl kinase. J Biol Chem *278*, 21685-21692.

Tarin, D., Thompson, E. W., and Newgreen, D. F. (2005). The fallacy of epithelial mesenchymal transition in neoplasia. Cancer Res *65*, 5996-6000; discussion 6000-5991.

Theriot, J. A., Rosenblatt, J., Portnoy, D. A., Goldschmidt-Clermont, P. J., and Mitchison, T. J. (1994). Involvement of profilin in the actin-based motility of L. monocytogenes in cells and in cell-free extracts. Cell *76*, 505-517.

Thiery, J. P. (2002). Epithelial-mesenchymal transitions in tumour progression. Nat Rev Cancer *2*, 442-454.

Thiery, J. P., and Sleeman, J. P. (2006). Complex networks orchestrate epithelial-mesenchymal transitions. Nat Rev Mol Cell Biol *7*, 131-142.

Tobias, E. S., Hurlstone, A. F., MacKenzie, E., McFarlane, R., and Black, D. M. (2001). The TES gene at 7q31.1 is methylated in tumours and encodes a novel growth-suppressing LIM domain protein. Oncogene *20*, 2844-2853.

Toyoda, A., Kawana, H., Azuhata, K., Yu, J., Omata, A., Kishi, H., Higashi, M., and Harigaya, K. (2009). Aberrant expression of human ortholog of mammalian enabled (hMena) in human colorectal carcinomas: implications for its role in tumor progression. Int J Oncol *34*, 53-60.

Tu, Y., Wu, S., Shi, X., Chen, K., and Wu, C. (2003). Migfilin and Mig-2 link focal adhesions to filamin and the actin cytoskeleton and function in cell shape modulation. Cell *113*, 37-47.

Vasioukhin, V., Bauer, C., Yin, M., and Fuchs, E. (2000). Directed actin polymerization is the driving force for epithelial cell-cell adhesion. Cell *100*, 209-219.

Vicovac, L., and Aplin, J. D. (1996). Epithelial-mesenchymal transition during trophoblast differentiation. Acta Anat (Basel) *156*, 202-216.

Vincent, T., Neve, E. P., Johnson, J. R., Kukalev, A., Rojo, F., Albanell, J., Pietras, K., Virtanen, I., Philipson, L., Leopold, P. L.*, et al.* (2009). A SNAIL1-SMAD3/4 transcriptional repressor complex promotes TGF-beta mediated epithelial-mesenchymal transition. Nat Cell Biol *11*, 943-950.

Vincent-Salomon, A., and Thiery, J. P. (2003). Host microenvironment in breast cancer development: epithelial-mesenchymal transition in breast cancer development. Breast Cancer Res *5*, 101-106.

Wang, E. T., Sandberg, R., Luo, S., Khrebtukova, I., Zhang, L., Mayr, C., Kingsmore, S. F., Schroth, G. P., and Burge, C. B. (2008). Alternative isoform regulation in human tissue transcriptomes. Nature *456*, 470-476.

Wang, W., Goswami, S., Lapidus, K., Wells, A. L., Wyckoff, J. B., Sahai, E., Singer, R. H., Segall, J. E., and Condeelis, J. S. (2004). Identification and testing of a gene expression signature of invasive carcinoma cells within primary mammary tumors. Cancer Res *64*, 8585-8594.

Wang, W., Mouneimne, G., Sidani, M., Wyckoff, J., Chen, X., Makris, A., Goswami, S., Bresnick, A. R., and Condeelis, J. S. (2006). The activity status of cofilin is directly related to invasion, intravasation, and metastasis of mammary tumors. J Cell Biol *173*, 395-404.

Wang, W., Wyckoff, J. B., Goswami, S., Wang, Y., Sidani, M., Segall, J. E., and Condeelis, J. S. (2007). Coordinated regulation of pathways for enhanced cell motility and chemotaxis is conserved in rat and mouse mammary tumors. Cancer Res *67*, 3505-3511.

Warzecha, C. C., Sato, T. K., Nabet, B., Hogenesch, J. B., and Carstens, R. P. (2009a). ESRP1 and ESRP2 are epithelial cell-type-specific regulators of FGFR2 splicing. Mol Cell *33*, 591-601.

Warzecha, C. C., Shen, S., Xing, Y., and Carstens, R. P. (2009b). The epithelial splicing factors ESRP1 and ESRP2 positively and negatively regulate diverse types of alternative splicing events. RNA Biol *6*.

Welch, M. D., and Mullins, R. D. (2002a). Cellular control of actin nucleation. Annu Rev Cell Dev Biol *18*, 247-288.

Welch, M. D., and Mullins, R. D. (2002b). CELLULAR CONTROL OF ACTIN NUCLEATION. Annual Review of Cell and Developmental Biology *18*, 247-288.

Werner, S., Smola, H., Liao, X., Longaker, M. T., Krieg, T., Hofschneider, P. H., and Williams, L. T. (1994). The function of KGF in morphogenesis of epithelium and reepithelialization of wounds. Science *266*, 819-822.

Wicki, A., Lehembre, F., Wick, N., Hantusch, B., Kerjaschki, D., and Christofori, G. (2006). Tumor invasion in the absence of epithelial-mesenchymal transition: podoplanin-mediated remodeling of the actin cytoskeleton. Cancer Cell *9*, 261-272.

Williams-Masson, E., Malik, A., and Hardin, J. (1997). An actin-mediated two-step mechanism is required for ventral enclosure of the C. elegans hypodermis. Development *124*.

Winograd-Katz, S. E., Itzkovitz, S., Kam, Z., and Geiger, B. (2009). Multiparametric analysis of focal adhesion formation by RNAi-mediated gene knockdown. J Cell Biol *186*, 423-436.

Wolf, K., Mazo, I., Leung, H., Engelke, K., von Andrian, U. H., Deryugina, E. I., Strongin, A. Y., Brocker, E. B., and Friedl, P. (2003). Compensation mechanism in tumor cell migration: mesenchymal-amoeboid transition after blocking of pericellular proteolysis. J Cell Biol *160*, 267-277.

Wyckoff, J., Wang, W., Lin, E. Y., Wang, Y., Pixley, F., Stanley, E. R., Graf, T., Pollard, J. W., Segall, J., and Condeelis, J. (2004). A paracrine loop between tumor cells and macrophages is required for tumor cell migration in mammary tumors. Cancer Res *64*, 7022-7029.

Wyckoff, J. B., Jones, J. G., Condeelis, J. S., and Segall, J. E. (2000). A critical step in metastasis: in vivo analysis of intravasation at the primary tumor. Cancer Res *60*, 2504-2511.

Wyckoff, J. B., Pinner, S. E., Gschmeissner, S., Condeelis, J. S., and Sahai, E. (2006). ROCK- and myosin-dependent matrix deformation enables protease-independent tumor-cell invasion in vivo. Curr Biol *16*, 1515-1523.

Xia, Y., and Kao, W. W. Y. (2004). The signaling pathways in tissue morphogenesis: a lesson from mice with eye-open at birth phenotype. Biochemical Pharmacology *68*, 997-1001.

Yang, J., Mani, S. A., Donaher, J. L., Ramaswamy, S., Itzykson, R. A., Come, C., Savagner, P., Gitelman, I., Richardson, A., and Weinberg, R. A. (2004). Twist, a master regulator of morphogenesis, plays an essential role in tumor metastasis. Cell *117*, 927-939.

Yeo, G. W., Coufal, N. G., Liang, T. Y., Peng, G. E., Fu, X. D., and Gage, F. H. (2009). An RNA code for the FOX2 splicing regulator revealed by mapping RNA-protein interactions in stem cells. Nat Struct Mol Biol *16*, 130-137.

Zavadil, J., Narasimhan, M., Blumenberg, M., and Schneider, R. J. (2007). Transforming growth factor-beta and microRNA:mRNA regulatory networks in epithelial plasticity. Cells Tissues Organs *185*, 157-161.

Zeisberg, E. M., Tarnavski, O., Zeisberg, M., Dorfman, A. L., McMullen, J. R., Gustafsson, E., Chandraker, A., Yuan, X., Pu, W. T., Roberts, A. B.*, et al.* (2007a). Endothelial-to-mesenchymal transition contributes to cardiac fibrosis. Nat Med *13*, 952-961.

Zeisberg, M., Yang, C., Martino, M., Duncan, M. B., Rieder, F., Tanjore, H., and Kalluri, R. (2007b). Fibroblasts derive from hepatocytes in liver fibrosis via epithelial to mesenchymal transition. J Biol Chem *282*, 23337-23347.

Zimmermann, J., Labudde, D., Jarchau, T., Walter, U., Oschkinat, H., and Ball, L. J. (2002). Relaxation, Equilibrium Oligomerization, and Molecular Symmetry of the VASP (336,àí380) EVH2 Tetramer,Ä†. Biochemistry *41*, 11143-11151.

Chapter 6 - Index